

CCT Key Comparison 9 Final Report

ITS-90 SPRT Calibration from the Ar TP to the Zn FP

Tobias Herman¹ Michal Chojnacky¹ Ken Hill² Steffen Rudtsch³
Inseok Yang⁴ Petrus Paulus Maria Steur⁵ Roberto Dematteis⁵
Giuseppina Lopardo⁵ Fernando Sparasci⁶ Catherine Martin⁶ Lara Risegari⁶
Januarius Widiatmo⁷ Tohru Nakano⁷ Ikuhiko Saito⁷ Klaus Natorf Quelhas⁸
Patricia Giorgio⁹ Jianping Sun¹⁰ Jintao Zhang¹⁰ Jonathan Pearce¹¹
Jayne Gray¹¹

¹ National Institute of Standards and Technology, Gaithersburg, MD 20871 USA

² National Research Council of Canada, Ottawa, ON, Canada

³ Physikalisch-Technische Bundesanstalt (PTB), Abbestra e, 2-12, 10587 Berlin, Germany

⁴ Korea Research Institute of Standards and Science (KRISS), Daejeon 34113, Korea

⁵ Istituto Nazionale di Ricerca Metrologica – INRIM, Strada Delle Cacce, 91, 10135 Turin, Italy

⁶ LNE-Cnam, 61 rue du Landy, 93210 La Plaine Saint-Denis, FRANCE

⁷ National Metrology Institute of Japan, National Institute of Advanced Industrial Science and Technology (NMIJ, AIST), Umezono 1-1-1, Tsukuba, Ibaraki 305-8563 Japan

⁸ Instituto Nacional de Metrologia, Qualidade e Tecnologia - Inmetro

⁹ Instituto Nacional de Tecnología Industrial, Departamento de Termodinámica - INTI - SOMCEI, Av. Gral. Paz 5445 - Edificios 3 y 44. B1650KNA, San Martín - Prov. Buenos

Aires - República Argentina

¹⁰ National Institute of Metrology, Beijing, China
Physical Laboratory, Hampton Road, Teddington, TW10 4AB, UK

¹¹ National Physical Laboratory, Hampton Road, Teddington, TW11 0LW, United Kingdom

Contents

1	Introduction	3
1.1	Participating laboratories	3
2	Protocol used in the comparison	6
2.1	Protocol	6
2.2	Calculating $\Delta T_{\text{NMI-KCRV}}$	6
2.3	Calculating uncertainties	8
2.4	Calculating the uncertainty of the key comparison reference value	9
2.5	Alternative $\overline{\Delta T}$ calculations	10
3	Devices used and measurement results	11
3.1	Devices used	11
3.2	Stabilization of SPRTs	11
3.3	Data collection at NIST	11
3.4	SPRT data collection	15
3.5	Evaluation of transfer uncertainty cutoff criteria	15
3.5.1	Criterion 1	16
3.5.2	Criterion 2	16
3.5.3	Role of “failed” measurements	16
3.6	Additional transfer standard uncertainty	19
3.7	Exclusion of Batch 4 and Batch 9 Hg measurements	19
4	Additional error during repeated calibration cycles	20
4.1	Distribution of shifts in SPRT measurements	20
4.2	Comparison of shifts during transfer to uncertainty budgets – visualizing cutoff criterion 1	24
4.3	Scatter in NIST proxy measurements contrasted with uncertainty budget	31
5	Key comparison reference value	32
5.1	Calculation of key comparison reference value	32
5.2	NMI results with respect to $\overline{\Delta T}$, organized by fixed point	33
5.2.1	Zinc	34
5.2.2	Tin	35
5.2.3	Indium	36
5.2.4	Gallium	37
5.2.5	Mercury	38
5.2.6	Argon	39
5.3	NMI results with respect to $\overline{\Delta T}$, organized by lab	40

5.3.1	BIPM	40
5.3.2	INMETRO	41
5.3.3	INRIM	42
5.3.4	INTI	43
5.3.5	KRISS	44
5.3.6	LNE-CNAM	45
5.3.7	NIM	46
5.3.8	NIST	47
5.3.9	NMIA	48
5.3.10	NMIJ/AIST	49
5.3.11	NPL	50
5.3.12	NRC	51
5.3.13	PTB	52
5.3.14	VSL	53
Appendix A	Original protocol	54
Appendix B	Raw Data tables	64
B.1	<i>W</i> values and uncertainty	64
Appendix C	Uncertainty budgets	80
Appendix D	Temperature shifts during SPRT transfer, by NMI	126
Appendix E	Variations on the calculation of $\bar{\Delta T}$	132
E.1	$\bar{\Delta T}$ as a weighted average	132
E.1.1	Weighted by SPRT failures	132
E.1.2	Weighted by uncertainty budget	132
E.2	Ignoring the additional variation seen in the at-NIST measurements	133
E.2.1	Average of ante-NIST and post-NIST data used	133
E.2.2	Only ante-NIST data used	136
E.2.3	Only post-NIST data used	136
Appendix F	Bilateral comparisons	137
F.1	Bilateral comparisons organized by fixed point	137
F.2	Bilateral comparisons organized by NMI	144

Chapter 1

Introduction

This is a report to the Consultative Committee for Thermometry (CCT) on the key comparison 9 of Standard Platinum Resistance Thermometer (SPRT) calibration on the International Temperature Scale of 1990 (ITS-90) [1] from 83.8058 K (the Ar triple point) to 692.677 K (the Zn freezing point). The comparison followed a collapsed star protocol, with each of the fourteen participating laboratories shipping two standard platinum resistance thermometers (SPRTs) as transfer standards to the pilot laboratory (National Institute of Standards and Technology, NIST) for a direct comparison of SPRT calibration at the National Metrology Institute (NMI) of origin to calibration at NIST. Measurements were taken at the participating laboratories before and after measurement at NIST to assess the effect of transportation on the transfer standards. The pooled results from all laboratories were combined to calculate a key comparison reference value (KCRV).

This report includes the calculation of, and comparisons to, the KCRV as well as bilateral comparisons between labs. In addition, there is space devoted to analysis of the shifts in SPRT values following travel.

1.1 Participating laboratories

The laboratories that participated in this key comparison represent four distinct regional metrology organizations:

- APMP: Asia Pacific Metrology Programme
- COOMET: Euro-Asian Cooperation of National Metrological Institutions
- EUROMET: European Association of National Metrology Institutes
- SIM: Inter-American Metrology System

The laboratories are summarized in Table 1.1 and laboratory contacts listed in Table 1.2.

Fourteen NMI laboratories participated in this comparison, in addition to the pilot lab. One of those labs, VNIIM, noted instability in both their transfer standards and had to withdraw from the comparison after data collection had been completed. Originally a fifteenth participant (National Metrology Institute of South Africa, located in Pretoria, South Africa) was included, but equipment and personnel challenges forced them to withdraw from the comparison before measurements were complete.

Pilot (SIM)	NIST	National Institute of Standards and Technology	Gaithersburg, USA
APMP	KRISS	Korea Research Institute of Standards and Science	Daejeon, South Korea
APMP	NIM	National Institute of Metrology of the People's Republic of China	Beijing, China
APMP	NMLA	National Metrology Institute, Australia	West Lindfield, Australia
APMP	NMIJ/AIST	National Metrology Institute of Japan	Tsukuba, Japan
COOMET	VNIIM	D.I. Mendeleyev Institute for Metrology	St. Petersburg, Russia
EUROMET	BIPM	Bureau International des Poids et Mesures	Sèvres, France
EURAMET	INRIM	Istituto Nazionale di Ricerca Metrologica	Torino, Italy
EURAMET	LNE-Cnam	Laboratoire national de métrologie et d'essais	Paris, France
EURAMET	NPL	National Physical Laboratory	Teddington, UK
EURAMET	PTB	Physikalisch-Technische Bundesanstalt	Berlin, Germany
EURAMET	VSL	Van Swinden Laboratory	Deft, Netherlands
SIM	INMETRO	National Institute of Metrology, Standardization and Industrial Quality	Rio de Janeiro, Brazil
SIM	INTI	Instituto Nacional de Tecnología Industrial	Buenos Aires, Argentina
SIM	NRC	National Research Council	Ottawa, Canada

Table 1.1: Participating NMIs

Pilot (SIM)	NIST	
APMP	KRISS	Inseok Yang
APMP	NIM	Jianping Sun
APMP	NMIA	Mong-Kim Ho
APMP	NMIJ/AIST	Januarius Widiatmo
COOMET	VNIIM	<i>Withdrawn</i>
EUROMET	BIPM	Stephane Solve
EURAMET	INRIM	Giuseppina Lopardo
EURAMET	LNE-Cnam	Fernando Sparasci
EURAMET	NPL	Jonathon Pearce
EURAMET	PTB	Steffan Rudtsch
EURAMET	VSL	Conny de Bruin Barendrect
SIM	INMETRO	Klaus Quelhas
SIM	INTI	Javier Garcia Skabar
SIM	NRC	Sergey Dedyulin

Table 1.2: NMI contacts

Chapter 2

Protocol used in the comparison

2.1 Protocol

Each participating NMI selected two of their own SPRTs for use in the comparison. NMIs calibrated their SPRTs at every available ITS-90 fixed point within the range of this comparison. The initial calibration results were provided to the pilot laboratory (NIST), and the SPRTs were transported to NIST for calibration. Following the NIST calibration, the SPRTs were returned to their respective owners, and each NMI completed a final set of calibrations at their facility. All measurement results, corresponding uncertainties, and fixed-point cell uncertainty budgets were reported to NIST in a format suggested by Appendices A and C in the Key Comparison 9 (“K9”) Protocol (the original protocol is included here as Appendix A).

The key comparison reference value (KCRV) specified in the K9 Protocol is calculated as a simple mean of individual NMI values at each fixed point. However, a number of SPRTs were excluded from the KCRV calculation, as larger-than-expected shifts during transportation caused these SPRTs to fail the “cutoff criteria,” derived from the NMI measurements and NMI-reported uncertainty budgets (see Chapter 3). A detailed analysis of the larger-than-expected shifts observed during repeated calibration cycles is presented in Chapter 4. There was no clear source for the greater than expected shifts, and no attempt was made to adjust the protocol to reduce the number of “failures” when evaluating the cutoff criteria.

Furthermore, there was a greater-than-expected variation in the “at-NIST” measurements at certain fixed points. This additional variation is addressed by increasing the uncertainty of the relevant at-NIST measurements, as will be described in later chapters, but the calculations outlined in the original protocol and described below were still followed.

Some other interpretations of how to calculate the KCRV, $\overline{\Delta T}$, are discussed in Appendix E

2.2 Calculating $\Delta T_{\text{NMI-KCRV}}$

We begin with an explicit derivation of the calculations used in this comparison, reproduced from the original protocol but in greater detail. This section is not required to understand the comparison results presented in Chapter 3.

Resistance ratios, W , were measured at each of the six fixed points included in this comparison. Each participating NMI recorded initial values of W for their two SPRTs (W_1^{Ante} and W_2^{Ante}). The SPRTs were then transported to, and measured at, NIST (W_1^{NIST} and W_2^{NIST}), and finally returned to their respective NMIs for a third and final measurement (W_1^{Post} and W_2^{Post}). Here, the superscript refers to measurements taken before, at, or after NIST, and the subscript identifies

either SPRT #1 or SPRT #2. NMI measurements, (W_i^{Ante} and W_i^{Post}), may have included multiple realizations for each SPRT at each fixed point. NIST measurements (W_i^{NIST}) were generated from a single realization for each SPRT at each fixed point.

Average W values are calculated using:

$$\bar{W}_i = \frac{1}{2} (W_i^{\text{Ante}} + W_i^{\text{Post}}) \quad (2.1)$$

Some participants were concerned that measurements performed upon return from NIST should not appear in this calculation, meaning:

$$\bar{W}_i = W_i^{\text{Ante}} \quad (2.2)$$

Results using Eq. 2.2 are included as in Appendix E, along with the alternative interpretation: $\bar{W}_i = W_i^{\text{Post}}$; these alternative definitions of \bar{W}_i produced results that were very similar to those that used Eq. 2.1.

Each SPRT measurement set is used to calculate an independent temperature difference, ΔT_i , between the fixed-point realization performed at NIST and each participating NMI.

$$\Delta T_i = \left| \frac{\bar{W}_i - W_i^{\text{NIST}}}{(dW_r/dT)} \right| + C_i \quad (2.3)$$

W_r is the ITS-90 reference function and C_i is a term accounting for changes in resistance ratio associated with the travel, handling, and stability of each SPRT. Its value is assumed to be zero, with an associated uncertainty that will be discussed below.

The values of ΔT_i are combined (at a given fixed point) to give:

$$\Delta T_{\text{NMI}} = \frac{1}{2} (\Delta T_1 + \Delta T_2) \quad (2.4)$$

In cases where only one SPRT measurement was reported at a particular fixed point (for instance due to damage to, or instability of, the other SPRT) ΔT_{NMI} is set equal to the ΔT_i of that SPRT.

The KCRV is calculated from the $\Delta T_{\text{NMI}}^\dagger$ values of the participating NMIs, where $\Delta T_{\text{NMI}}^\dagger$ is calculated in the same way as ΔT_{NMI} , but excludes SPRT measurements that fail the cutoff criteria described in section 3.5.

The difference of the fixed-point realization temperature (at each fixed point, for each NMI) from the corresponding KCRV, $\bar{\Delta T}$, is calculated using:

$$\Delta T_{\text{NMI-KCRV}} = \Delta T_{\text{NMI}} - \bar{\Delta T} \quad (2.5)$$

based on a KCRV ($\bar{\Delta T}$) calculated independently for each fixed point:

$$\bar{\Delta T} = \frac{1}{n} \sum_{j=1}^n \Delta T_{\text{NMI},j}^\dagger \quad (2.6)$$

As mentioned above, $\Delta T_{\text{NMI}}^\dagger$ is calculated in the same way as ΔT_{NMI} , but excludes SPRT measurements that fail the cutoff criteria described in section 3.5. n represents the number of individual NMI laboratories (j) that reported a value for $\Delta T_{\text{NMI}}^\dagger$ at that fixed point; n varies by fixed point (between 10 and 12 in this comparison).

$\bar{\Delta T}$ is used to provide a common reference point from which to compare laboratory realizations of each fixed point, but does not have a physical meaning. $\bar{\Delta T}$ is not used in bilateral comparisons between NMIs (included as Appendix F) since any two labs may be connected through their respective values of ΔT_{NMI} , with lower uncertainty.

2.3 Calculating uncertainties

Uncertainty budgets provided by each NMI are used to evaluate the cutoff criteria for each SPRT and to calculate the uncertainty of each lab's final $\Delta T_{\text{NMI-KCRV}}$ value. NMIs classified each uncertainty contribution in their budgets according to the evaluation method used (Type A, evaluated statistically, or Type B, evaluated in any other fashion), and whether the contribution was strongly correlated between measurements (systematic) or fluctuated randomly between measurements (random). Some NMIs made multiple realizations of their SPRT measurements at each fixed point, reducing contributions from random uncertainty components to calculations in this report. In the discussion that follows, random and systematic uncertainty components are represented by u_R and u_S , respectively. Combined uncertainties have no subscript.

Each measurement (ante- or post-NIST) has an associated uncertainty, $u(W_i)$, such that:

$$u^2(W_i) = \frac{u_R^2(W_i)}{n} + u_S^2(W_i) \quad (2.7)$$

where n is the number of realizations measured by that particular SPRT at the indicated fixed point. While W is a unitless quantity, uncertainties in W are expressed in kelvin (after scaling each uncertainty by the value of $\frac{dW_r(\text{ITS-90})}{dT}$ at the given fixed point), as is customary.

The uncertainty in \bar{W}_i for each SPRT, arising from the combined ante- and post-NIST measurement sets, is calculated as follows. Random uncertainties are treated as completely uncorrelated and combined according to the Guide to the Expression of Uncertainty in Measurement (GUM)[2] section 5.1.2. Due to the large time separation between ante- and post-NIST measurements, we expect the correlation of systematic uncertainties to be less than one. Nevertheless, systematic uncertainties are treated as completely correlated and combined according to GUM section 5.2.2, the most conservative approach. The uncertainty in \bar{W}_i , $u(\bar{W}_i)$ satisfies:

$$u^2(\bar{W}_i) = \frac{1}{4} \left[\frac{u_R^2(W_i^{\text{Ante}})}{n^{\text{Ante}}} + \frac{u_R^2(W_i^{\text{Post}})}{n^{\text{Post}}} \right] + \left[\frac{u_S(W_i^{\text{Ante}})}{2} + \frac{u_S(W_i^{\text{Post}})}{2} \right]^2 \quad (2.8)$$

where the first group of terms corresponds to $u_R^2(\bar{W}_i)$, and the second group of terms corresponds to $u_S^2(\bar{W}_i)$. When an NMI's uncertainty budget was the same for ante- and post-NIST measurements, and the number of realizations was also the same ante- and post-NIST, this reduces to

$$u^2(\bar{W}_i) = \frac{1}{2} \left[\frac{u_R^2(W_i)}{n} \right] + [u_S(W_i)]^2 \quad (2.9)$$

which is equivalent to doubling the number of realizations during a single set of measurements.

Every SPRT used in the comparison is assigned a transfer uncertainty associated with its measurements at each fixed point. The transfer uncertainties ($u(C_i)$) are calculated from the shift in W measured at the NMI before and after transport to NIST.

$$u(C_i) = \frac{1}{2\sqrt{3}} \frac{|W_i^{\text{Post}}(\text{FP}) - W_i^{\text{Ante}}(\text{FP)}|}{(dW_r(\text{ITS-90})/dT)} \quad (2.10)$$

In other words, transfer of the SPRT to and from NIST introduces an uncertainty about the mean value (\bar{W}_i), which is bounded by the minimum and maximum measured value ($W_i^{\text{Ante}}, W_i^{\text{Post}}$), and is assumed to have a rectangular distribution.

The total uncertainty in ΔT_i , $u(\Delta T_i)$, can be found using:

$$u^2(\Delta T_i) = u_R^2(\bar{W}_i) + u_S^2(\bar{W}_i) + u_R^2(W_i^{\text{NIST}}) + u^2(C_i) \quad (2.11)$$

Since the NIST systematic uncertainties influence all ΔT_i measurements identically, only the random NIST uncertainty contributions are included in this total uncertainty calculation. NIST systematic uncertainty contributions appear exclusively in $\Delta T_{\text{NIST-KCRV}}$, not in any other $\Delta T_{\text{NMI-KCRV}}$ values.

Since measurements for this comparison were spread over a period of years, the assumption that systematic contributions to the uncertainty of NIST measurements remained constants requires justification. All systematic components in the uncertainty of NIST measurements originate from the resistance bridge or from the fixed-point cells. The bridge remained unchanged over the comparison, and for many years before and after the comparisons measurements; it showed no evidence of significant drift over this period. The individual fixed-point cells also remained unchanged over the period of these measurements; they also showed no signs of drift.

As will be discussed in Chapter 4, the variation in the at-NIST measurements was larger than expected from the random components of the NIST uncertainty budget at some fixed points. However, the origin of this variability is unknown, and there is no strong evidence that it is best accounted for by hypothesizing a long-term variation in the NIST systematic components.

Combining the SPRT #1 and SPRT #2 measurements, assuming that the systematic uncertainty contributions from each are completely correlated, the combined uncertainty in ΔT_{NMI} , $u(\Delta T_{\text{NMI}})$, is found from:

$$\begin{aligned} u^2(\Delta T_{\text{NMI}}) &= \frac{1}{4} [u_{\text{R}}^2(\Delta T_1) + u_{\text{R}}^2(\Delta T_2)] + \left[\frac{u_{\text{S}}(\Delta T_1) + u_{\text{S}}(\Delta T_2)}{2} \right]^2 \\ &= \frac{1}{4} \left[[u_{\text{R}}^2(\overline{W_1}) + u_{\text{R}}^2(\overline{W_2}) + 2u_{\text{R}}^2(W^{\text{NIST}}) + u^2(C_1) + u^2(C_2)] \right. \\ &\quad \left. + [u_{\text{S}}(\overline{W_1}) + u_{\text{S}}(\overline{W_2})]^2 \right] / (dW_{\text{r}}/dT) \end{aligned} \quad (2.12)$$

Since $\Delta T_{\text{NMI}}^\dagger$ has the same form as ΔT , its uncertainty is also given by Eq. 2.12, unless one of the SPRT's failed to meet the cutoff criteria at a given fixed point. In that case, $\Delta T_{\text{NMI}}^\dagger = \Delta T_i$ of the remaining measurement and the uncertainty $u(\Delta T_{\text{NMI}}^\dagger)$ is set equal to the uncertainty of the SPRT that did pass, as expressed in Eq. 2.11.

2.4 Calculating the uncertainty of the key comparison reference value

The uncertainty of $\overline{\Delta T}$, $u(\overline{\Delta T})$, is calculated by combining the uncertainties of all the $\Delta T_{\text{NMI}}^\dagger$ measurements at that fixed point using:

$$u^2(\overline{\Delta T}) = \frac{1}{n^2} \sum_{j=1}^n u^2(\Delta T_{\text{NMI}_j}^\dagger) \quad (2.13)$$

To calculate $u(\Delta T_{\text{NMI-KCRV}})$, the correlation between ΔT_{NMI} and $\overline{\Delta T}$ must be included. Following GUM section 5.2.2, we find $u(\Delta T_{\text{NMI-KCRV}})$ from:

$$\begin{aligned} u^2(\Delta T_{\text{NMI-KCRV}}) &= u^2(\Delta T_{\text{NMI}}) + u^2(\overline{\Delta T}) \\ &\quad + 2 \frac{\partial(\Delta T_{\text{NMI-KCRV}})}{\partial \overline{\Delta T}} \frac{\partial(\Delta T_{\text{NMI-KCRV}})}{\partial \Delta T_{\text{NMI}}} u(\Delta T_{\text{NMI}}, \overline{\Delta T}) \\ &= u^2(\Delta T_{\text{NMI}}) + u^2(\overline{\Delta T}) - 2u(\Delta T_{\text{NMI}}, \overline{\Delta T}) \end{aligned} \quad (2.14)$$

where $u(\Delta T_{\text{NMI}}, \overline{\Delta T})$ is the covariance associated with ΔT_{NMI} and $\overline{\Delta T}$. The covariance is calculated following GUM section F.1.2.3, treating both ΔT_{NMI} and $\overline{\Delta T}$ as functions of the individual values ($\Delta T_{\text{NMI},j}$) calculated for each NMI. By GUM Equation F.2 we have:

$$u(\Delta T_{\text{NMI}}, \overline{\Delta T}) = \sum_{j=1}^n \frac{\partial(\overline{\Delta T})}{\partial \Delta T_{\text{NMI},j}} \frac{\partial(\Delta T_{\text{NMI}})}{\partial \Delta T_{\text{NMI},j}} u^2(\Delta T_{\text{NMI},j}) \quad (2.15)$$

Since $\overline{\Delta T}$ is a simple mean of the individual values of $\Delta T_{\text{NMI},j}$, the first partial derivative is equal to $1/n$ for all j . The second derivative is zero except with respect to the NMI's own value, when it is unity. Thus Eq. 2.15 reduces to:

$$u(\Delta T_{\text{NMI}}, \overline{\Delta T}) = \frac{1}{n} u^2(\Delta T_{\text{NMI}}) \quad (2.16)$$

which leads to

$$u^2(\Delta T_{\text{NMI-KCRV}}) = \left(1 - \frac{2}{n}\right) u^2(\Delta T_{\text{NMI}}) + u^2(\overline{\Delta T}) \quad (2.17)$$

unless the value of $\Delta T_{\text{NMI}}^\dagger$ is not used in the calculation of $\overline{\Delta T}$ because of the cutoff criteria described in Section 3.5. In that case there is no correlation, and we have:

$$u^2(\Delta T_{\text{NMI-KCRV}}) = u^2(\Delta T_{\text{NMI}}) + u^2(\overline{\Delta T}) \quad (2.18)$$

2.5 Alternative $\overline{\Delta T}$ calculations

Two alternative approaches to calculating $\overline{\Delta T}$ were investigated. In one $\overline{\Delta T}$ was calculated as a weighted mean, with each NMI's contribution scaled according to the lab's stated uncertainty. In the other $\overline{\Delta T}$ was calculated from a modified simple mean, in which an individual SPRT's contribution to a lab's $\Delta T_{\text{NMI}}^\dagger$ was weighted based on the number of cutoff criteria tests passed. Details of these calculations, results, and implications are included in Appendix E.

Chapter 3

Devices used and measurement results

3.1 Devices used

Each NMI selected two of their own SPRTs for use in the comparison and coordinated SPRT transport to the pilot laboratory. In a small number of cases, an NMI-selected SPRT was damaged in transit to NIST, or was found to be incompatible with NIST fixed-point cells (e.g. sheath diameter too large). In these cases, the NMI could choose to supply a replacement SPRT, if available. The SPRTs used in the comparison are listed in Table 3.1.

3.2 Stabilization of SPRTs

Upon receipt, and before calibration, participant SPRTs underwent stabilization at NIST using the same procedure used for our calibration service[4]. The resistance of each SPRT at the triple point of water (TPW) was measured, followed by an eight hour anneal at 450 °C. The SPRT was removed swiftly to room temperature and remeasured at the triple point of water once cooled to room temperature. If the shift in TPW resistance during the anneal cycle was less than the equivalent of 0.2 mK the SPRT was considered stable and ready for calibration. If the shift exceeded 0.2 mK, the annealing process was repeated. Any SPRT that failed to pass the stabilization criterion after five anneal cycles was considered unstable. NIST alerted the associated NMI to give them an opportunity to replace it with another SPRT.

3.3 Data collection at NIST

Comparison measurements at NIST were performed from December 2011 through January 2015. A total of ten calibration batches were measured as part of the comparison. Each batch contained up to four SPRTs from different participating laboratories. In addition, a single NIST “proxy” SPRT was included in every batch but one; this SPRT was used to collect the NIST data for this comparison. Calibration batches were measured consecutively, from the Zn FP to the Ar TP (batch K9-BIPM was an exception, only including measurements at Ga MP and TPW). The same NIST fixed-point cells and maintenance systems were used throughout the comparison measurements, with the exception of TPW cells. Four TPW cells were used interchangeably at NIST throughout the comparison. A TPW cell interchangeability parameter is included in NIST’s uncertainty budget. Details of NIST’s realization of the ITS-90 in this range can be found in NIST SP250-81[4].

When practical, the two SPRTs belonging to a given NMI were split into different batches (batch K9-BIPM was an exception, only including SPRTs from BIPM). Batch K9-B9 consisted of

	SPRT #	Manufacturer	Model #	Serial #
BIPM	1	Hart	5683	4240
BIPM	2	L&N	8167	1857442
INMETRO	1	Hart	5681	1251
INMETRO	2	Rosemount	162CE	3713
INRIM	1	Hart	5681	1282
INRIM	2	Hart	5681	1283
INTI	1	Tinsley	5187SA	235996
INTI	2	Hart	5681	71089
KRISS	1	L&N	8163Q	1849612
KRISS	2	L&N	8167	1860931
LNE-CNAM	1	L&N	8167	1825320
LNE-CNAM	2	YSI	8167	B91280
NIM	1	Yunnan	Yunnan	4101
NIM	2	Yunnan	Yunnan	5128
NIST	1	Hart	5681	1030
NIST	2	Hart	5681	1030
NIST	3	Hart	5681	1030
NMIA	1	Hart	5681	1671
NMIA	2	Chino	R800-2	RS104-09
NMIJ/AIST	1	Chino	R800-2	RS994-13
NMIJ/AIST	2	Hart	5683	4315
NPL	1	Hart	5683	4275
NPL	2	Hart	5683	4276
NRC	1	Chino	R800-2	RS58A-1
NRC	2	Chino	R800-2	RS895-2
PTB	1	YSI	8167	4807
PTB	2	Hart	5698	95185
VNIIM	1	ETC-25	ETC-25	98-02
VNIIM	2	PTC-25	PTC-25	53
VSL	1	L&N	8167	1761951
VSL	2	L&N	8167	1867658

Table 3.1: SPRTs used in this intercomparison.[3]

Batch K9-A1	Dec. 2011 – Jan. 2012
NPL	4275
INMETRO	1251
NMIJ/AIST	1359
NIST proxy	1030
damaged in transit	
Batch K9-A2	Jun 2012 – Jul 2012
PTB	4807
VSL	1761951
NMIJ/AIST	RS994-13
NPL	4276
NIST proxy	1030
NIST database error affected Sn point	
Batch K9-A3	Jul 2013 – Aug 2013
PTB	95185
VSL	1867658
KRISS	1849612
INMETRO	3713
NIST proxy	1030
Batch K9-A4	Jan 2013 – Apr 2013
KRISS	1860931
LNE-CNAM	1825320
INRIM	1282
NIM	4101
NIST proxy	1030
damaged in transit	
Batch K9-BIPM	Mar 2013
BIPM	4240
BIPM	1857442
NIST proxy	1030

Table 3.2: Measurement matrix of SPRTs used in this intercomparison.

Batch K9-A5	May 2013	
LNE-CNAM	B91280	
INRIM	1283	
NIM	5128	
VNIIM	53	
NIST proxy	1030	
Batch K9-B6	Jun 2013 – Jul 2013	
INTI	235996	
INTI	4118	failed stabilization
VNIIM	52	platinum wire damaged in transit
NMIA	1671	
NIST proxy	1030	
Batch K9-B7	Sep 2013	
INTI	71089	
NMIA	RS104-09	
NIST proxy	1030	
Batch K9-B8	Dec 2013 – Jan 2014	
NRC	RS58A-1	
NIST proxy	1030	
Batch K9-B9	Mar 2014 – May 2014	
<i>other NMI</i>	data not used in K9	
<i>other NMI</i>	data not used in K9	
NIST proxy	1030	
Batch K9-replacement	Dec 2014 – Jan 2015	
NMIJ/AIST	4315	
NRC	RS895-2	
VNIIM	98-02	

Table 3.3: Measurement matrix of SPRTs used in this intercomparison, continued.

SPRTs belonging to an NMI that did not participate in K9 – these measurements are intended to form a bilateral comparison linked to K9 at some point in the future. This batch is included in the table because it provides the ninth set of NIST proxy SPRT data. The proxy SPRT was not included in the batch K9-replacement, as this batch was added after the core data collection was complete, and contained a mix of intercomparison SPRTs and SPRTs belonging to measurement service customers.

The NIST proxy SPRT (recalibrated with each batch) provides a mechanism to include NIST data in the comparison in the same format as the other NMI’s and also provides a measure of the repeatability of multiple calibrations in NIST fixed-point cells used throughout the comparison, without any transfer of the SPRT outside the lab space. Later in this report you will see references to NIST SPRT #1 through #3; these are all the same (“proxy”) SPRT, with measurements in batches 1 through 3 treated as the “ante-NIST,” “at-NIST” and “post-NIST” measurements for NIST “SPRT #1,” batches 4 through 6 as “SPRT #2” and batches 7 through 9 as “SPRT #3.”

The realization of the ITS-90 at NIST includes a triple-point realization of Ga rather than a melting point. A uniform 2.0 mK correction is applied to offset the difference between the temperature of these two transitions. As real SPRTs deviate slightly from the ITS-reference function, there will be some additional uncertainty from the assumption that the temperature dependence of each SPRT is identical, but this difference is insignificantly small over the 2.0 mK correction applied here.

3.4 SPRT data collection

NMIs reported their ante- and post-NIST W values in a tabular worksheet, as required by the comparison protocol. In some cases, NMI-reported measurement uncertainties in Appendix A differed from the NMI-supplied uncertainty budget in Appendix C. In these cases, the uncertainties in Appendix C were used in the comparison analysis. Any SPRT identified as unstable by its NMI owner was excluded from the analysis.

NMI data sets are compiled along with the corresponding NIST measurements for each SPRT in Appendix B. Each table includes values of W , the associated uncertainties u_c , and the number of realizations, as supplied by NMIs. The tables also show the magnitude of the random uncertainty component, u_r , identified with each W value, and its effective degrees of freedom. These parameters are integral to the cutoff criteria calculation used to select the measurements contributing to $\overline{\Delta T}$.

The NIST proxy SPRT measurements are treated similarly to the other NMI SPRT data sets. The nine measurement cycles are divided into three sets of three measurements each. Within each set, the three measurements are identified as “ante-NIST,” “at NIST,” and “post-NIST,” respectively. In this way, the nine measurements of the NIST proxy SPRT at each fixed point play the role of three independent SPRT data sets with the same form as the other NMI data. Importantly, since $\overline{\Delta T}$ is already formulated relative to the NIST realization of each fixed point, NIST proxy SPRT data processed in this manner are excluded from the calculation of $\overline{\Delta T}$.

3.5 Evaluation of transfer uncertainty cutoff criteria

As described in section 2.3, the shift in W from ante-NIST to post-NIST is used to calculate a transfer uncertainty for each SPRT. This shift is also used to evaluate “cutoff criteria” determining which SPRTs contribute to $\overline{\Delta T}$. The cutoff criteria compare the change in W_i to $u(W_i)$, and are used to minimize the effects of SPRT instability on $\overline{\Delta T}$. The two criteria test the following issues (which are related but not identical):

-
1. Did the shift occurring during travel to and from NIST exceed the variation expected from the measurement process itself?
 2. Was the magnitude of any observed shift significant when compared to the overall uncertainty budget?

Since these two tests only examine ante- and post-NIST data, measurements performed at NIST do not factor into the cutoff criteria, although the uncertainty of the at-NIST measurements does through ΔT_{NMI_j} . An affirmative answer in either case counts as “failing” that test. Failing both tests excludes an SPRT from $\overline{\Delta T}$. If only one test is failed, then the measurement is retained in $\overline{\Delta T}$. The cutoff criteria tests are performed at each of the six fixed points for each SPRT, such that twelve independent pairs of tests are used to evaluate the data from each NMI. As a result, each SPRT included in the comparison may contribute to the $\overline{\Delta T}$ at all fixed points, at some fixed points or at no fixed points. Results of these tests are summarized in Tables 3.4 and 3.5.

3.5.1 Criterion 1

The first criterion compares the observed change in W_i from ante- to post-NIST to the natural variation between measurements (i.e. the random component of the uncertainty). A shift outside the 95% confidence interval, where the effective degrees of freedom, ν_{eff} , are calculated using the Welch-Satterthwaite equation, indicates a failure of cutoff criterion 1:

$$\left| \frac{W_i^{\text{Post}} - W_i^{\text{Ante}}}{(dW_r/dT) \sqrt{u_r^2(W_i^{\text{Post}}) + u_r^2(W_i^{\text{Ante}})}} \right| > t_{0.975, \nu_{\text{eff}}} \quad (3.1)$$

3.5.2 Criterion 2

The second criterion compares the magnitude of the transfer uncertainty ($u(C_i)$) to the the combined uncertainty. A measurement with a transfer uncertainty greater than about one third of the total uncertainty represents a failure of cutoff criterion 2:

$$u(C_i) > \frac{\sqrt{u^2(\Delta T_i) - u^2(C_i)}}{3} \quad (3.2)$$

or, equivalently:

$$u^2(C_i) > \frac{u^2(\Delta T_i)}{10} \quad (3.3)$$

3.5.3 Role of “failed” measurements

SPRT measurements that fail both cutoff criteria are excluded from $\Delta T_{\text{NMI}}^\dagger$ and thus from $\overline{\Delta T}$. In cases where both SPRTs fail, an NMI’s contribution is excluded from $\overline{\Delta T}$ at that fixed point.

All measurements are included in the value of ΔT_{NMI} used to calculate inter-comparison results, regardless of cutoff criteria outcomes. The only measurements excluded from ΔT_{NMI} are those identified as unstable. Measurements of unstable SPRTs have been excluded from the raw data tables (App. B).

Since almost half of the measurements failed cutoff criterion 1, there appears to be an additional, unexpected source of error in the transfer standards used in this study.

NMI		Zn		Sn		In		Ga		Hg		Ar	
		I	II										
BIPM	SPRT1	–	–	–	–	–	–	✓	✓	–	–	–	–
	SPRT2	–	–	–	–	–	–	✓	✓	–	–	–	–
INMETRO	SPRT1	✓	✗	✓	✗	✓	✓	✓	✓	✓	✓	✓	✓
	SPRT2	✓	✗	✓	✗	✓	✓	✓	✓	✓	✓	✓	✓
INRIM	SPRT1	–	–	–	–	–	–	–	–	–	–	–	–
	SPRT2	✓	✓	✗	✓	✗	✓	✓	✓	✗	✗	✗	✗
INTI	SPRT1	–	–	–	–	–	–	–	–	✓	✗	✓	✓
	SPRT2	✗	✓	✓	✓	✗	✗	✓	✗	✗	✗	✓	✓
KRISS	SPRT1	✓	✓	✓	✓	✓	✓	✓	✓	✓	✓	✓	✓
	SPRT2	–	–	–	–	–	–	–	–	–	–	–	–
LNE-CNAM	SPRT1	✓	✓	✗	✗	✗	✗	✗	✗	✗	–	✓	✓
	SPRT2	✓	✓	✗	✗	✗	✗	✓	✗	✗	✗	✗	✓
NIM	SPRT1	✗	✓	✓	✓	✗	✓	✓	✗	✗	–	✗	✓
	SPRT2	✗	✓	✗	✓	✗	✓	✗	✓	✓	✓	✓	✓
NIST	SPRT1	–	–	–	–	–	–	–	–	–	–	–	–
	SPRT2	–	–	–	–	–	–	–	–	–	–	–	–
	SPRT3	–	–	–	–	–	–	–	–	–	–	–	–
NMIA	SPRT1	✗	✓	✗	✗	✗	✓	✓	✗	✓	✓	✗	✓
	SPRT2	✗	✓	✗	✓	✗	✓	✓	✓	✗	✓	✗	✓
NMIJ/AIST	SPRT1	✓	✓	✓	✓	✗	✓	✓	✗	✓	✓	✓	✓
	SPRT2	✓	✓	✗	✓	✗	✓	✓	✗	✓	✓	✓	✓
NPL	SPRT1	✓	✓	✗	✗	✓	✓	✓	✓	✓	✓	✓	✓
	SPRT2	✓	✓	✓	✓	–	✓	✓	✗	✓	✓	✓	✓
NRC	SPRT1	✗	✗	✗	✗	✓	✓	✓	✓	✓	✓	✓	✓
	SPRT2	✗	✓	✓	✓	✓	✓	✓	✓	✓	✓	✓	✓
PTB	SPRT1	–	–	✓	✓	✓	✓	✓	✓	✓	✓	✓	✓
	SPRT2	✗	✓	✗	✓	✓	✓	✓	✓	✓	✓	✗	✓
VSL	SPRT1	✗	✗	✗	✗	✗	✗	✗	✓	✓	✓	✓	✓
	SPRT2	✗	✓	✗	✓	✗	✓	✓	✗	✓	✓	✗	✓
# passes:		10	16	9	12	9	18	13	19	14	16	13	21
# fails:		10	4	12	8	12	3	10	4	8	4	9	1

Table 3.4: Results of cutoff criteria tests. As described in the text, two separate tests (1 and 2) are used to assess whether any significant change in a SPRT’s W value occurred. A checkmark (✓) indicates “pass,” an X (✗) represents “fail” and ‘–’ indicates a missing measurement, or one that was excluded from $\overline{\Delta T}$ for reasons other than failing the tests.

NMI	Zn	Sn	In	Ga	Hg	Ar
BIPM	SPRT1	–	–	–	✓	–
	SPRT2	–	–	–	✓	–
INMETRO	SPRT1	✓	✓	✓	✓	✓
	SPRT2	✓	✓	✓	✓	✓
INRIM	SPRT1	–	–	–	–	–
	SPRT2	✓	✓	✓	✓	✗
INTI	SPRT1	–	–	–	–	✓
	SPRT2	✓	✓	✗	✓	✓
KRISS	SPRT1	✓	✓	✓	✓	✓
	SPRT2	–	–	–	–	–
LNE-CNAM	SPRT1	✓	✗	✗	✗	–
	SPRT2	✓	✗	✓	✗	✓
NIM	SPRT1	✓	✓	✓	✗	–
	SPRT2	✓	✓	✓	✓	✓
NIST	SPRT1	–	–	–	–	–
	SPRT2	–	–	–	–	–
	SPRT3	–	–	–	–	–
NMIA	SPRT1	✓	✗	✓	✓	✓
	SPRT2	✓	✓	✓	✓	✓
NMIJ/AIST	SPRT1	✓	✓	✓	✓	✓
	SPRT2	✓	✓	✓	✓	✓
NPL	SPRT1	✓	✗	✓	✓	✓
	SPRT2	✓	–	✓	✓	✓
NRC	SPRT1	✗	✗	✓	✓	✓
	SPRT2	✓	✓	✓	✓	✓
PTB	SPRT1	–	✓	✓	✓	✓
	SPRT2	✓	✓	✓	✓	✓
VSL	SPRT1	✗	✗	✗	✓	✓
	SPRT2	✓	✓	✓	✓	✓

Table 3.5: SPRT inclusion in $\overline{\Delta T}$: if an SPRT passes at least one cutoff criterion test at a given fixed point, it is included in $\overline{\Delta T}$ as indicated by a checkmark (✓). An SPRT that fails both tests is indicated by an X (✗). A dash ‘–’ indicates a missing measurement, or one that was excluded from $\overline{\Delta T}$ for reasons other than failing the tests.

3.6 Additional transfer standard uncertainty

One of the following scenarios may explain the large number of cutoff criterion 1 failures:

1. Magnitude of random contributions to SPRT measurement error at each fixed point are severely underestimated (i.e. random uncertainty).
2. Realization and measurement system changes incurred during the prolonged measurement period are underestimated.
3. Uncertainty contributions introduced by SPRT transport are much larger than anticipated.
4. Repeated SPRT calibration cycling contributes an additional source of uncorrelated error, independent of transportation.

The first and second possibilities seem unlikely (but not impossible) given the depth of experience of participants in this comparison. To distinguish between the third and fourth, one needs two data sets: a set of repeat measurements on SPRTs that have traveled to and from NIST and a set of repeat measurements on an SPRT that remained at a single NMI for the entire comparison. In fact we have these data, and they favor the last option – when taking SPRTs through an entire calibration cycle we observe non-repeatability greater than the uncertainty in the realization of each fixed point. The next chapter will display this variability in a number of different ways.

Regardless of its origin, this larger-than-expected variation places limits on the effectiveness of SPRTs as transfer standards during laboratory inter-comparisons.

3.7 Exclusion of Batch 4 and Batch 9 Hg measurements

Participants identified a potentially anomalous realization of the Hg TP at NIST during Batch 4 measurements. NIM requested the removal of these measurements from the comparison and no objections were raised. As such, calculations of the KCRV at the Hg TP exclude data for Batch 4 SPRTs. The raw data for the Batch 4 NIST SPRT are included in the raw data tables in Appendix B, even though they are not used in any calculations.

During review it was suggested to remove the batch 9 NIST Hg measurement. This measurement was anomalously high, and no other participant SPRTs were included in this batch. Its elimination had no effect on any participant results except NIST, and dramatically reduced the scatter of the Hg measurements leading to tighter uncertainties for the comparison at that point.

Chapter 4

Additional error during repeated calibration cycles

The protocol assumes that the transfer uncertainty, $u(C_i)$, accounts for all W_i ante- and post-NIST variation in excess of the uncorrelated uncertainty at each fixed point, lumping together measurement shifts due to handling, transport, and instability. With evidence that there is a sizable natural variation in W_i values during recalibration of the same SPRT even without transportation, it may not be appropriate to treat C_i as a rectangular distribution bound by the difference. This chapter demonstrates that there appears to be an extra, random component to the error of an SPRT subject to repeated calibration.

To quantify the variability upon repeat calibrations, we examine the differences in all SPRT readings ($\Delta W = W^{\text{Post}} - W^{\text{Ante}}$). Shifts in the NIST proxy SPRT between successive cycles (e.g. $\Delta W = W^{\text{Cycle } 3} - W^{\text{Cycle } 2}$, etc) are examined in a similar fashion.

4.1 Distribution of shifts in SPRT measurements

The following figures (4.1 through 4.6) show the distribution of these shifts, ΔW , at each fixed point. NIST data are not included. Overlaid is a probability distribution function assuming a normal distribution with the same standard deviation as the measurements, excluding outliers (which are defined, for the purpose of this calculation, as any measurements showing a change of over 1 mK). These distributions of shifts should reflect, in some way, the distribution in random uncertainties for the realization of each fixed point at various NMIs as well as some random error from handling, etc. The near-constant value of the standard deviation of these shifts across fixed points, despite some points (e.g. gallium) having much smaller uncertainty at most labs, is strong evidence of an additional source of error. There was also no correlation between the shift magnitudes and the SPRT models.

The same data are summarized in tabular form in Table 4.1. NIST proxy SPRT data are included in the table as a separate column. Unlike the other-NMI data, the standard deviation for the NIST data is calculated using all data rather than applying a filter that removes shifts greater than 1 mK.

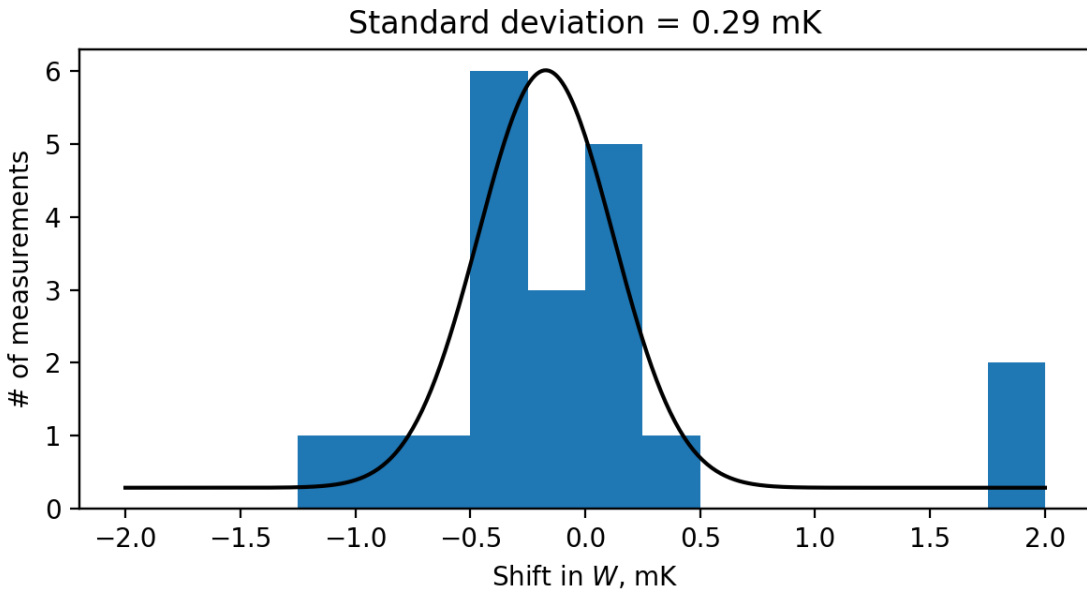


Figure 4.1: Results for the shift in measured W after repeated calibration cycles for non-NIST SPRTs used in this study, at the zinc point. These values are calculated by subtracting the value measured before sending the SPRT from the value measured upon return of the SPRT from NIST. Shifts of 1 mK and greater are excluded from the overlaid fit.

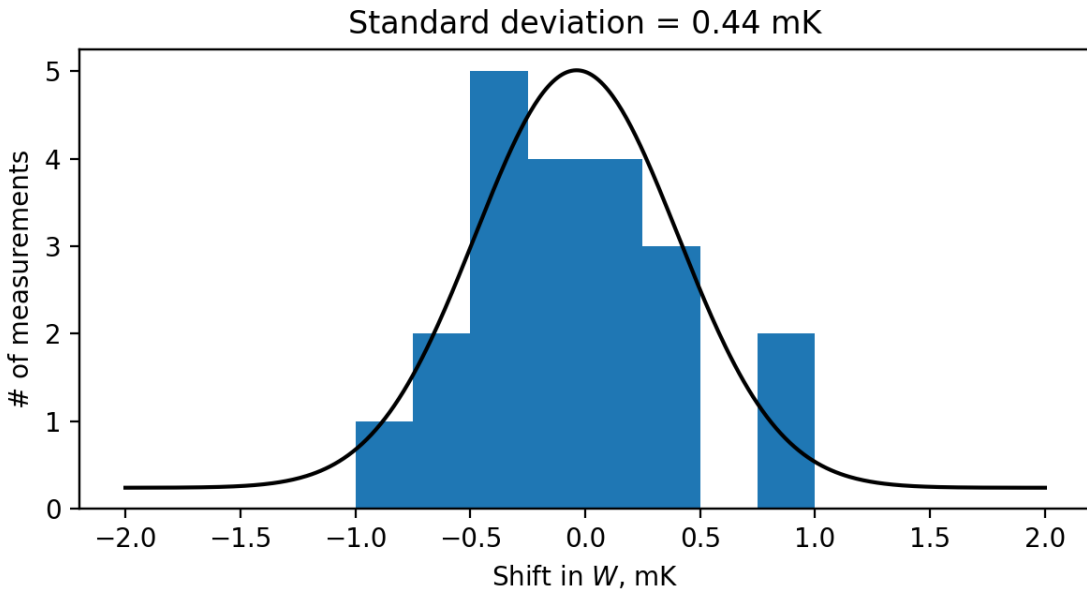


Figure 4.2: Results for the shift in measured W after repeated calibration cycles for non-NIST SPRTs used in this study, at the tin point. These values are calculated by subtracting the value measured before sending the SPRT from the value measured upon return of the SPRT from NIST. Shifts of 1 mK and greater are excluded from the overlaid fit.

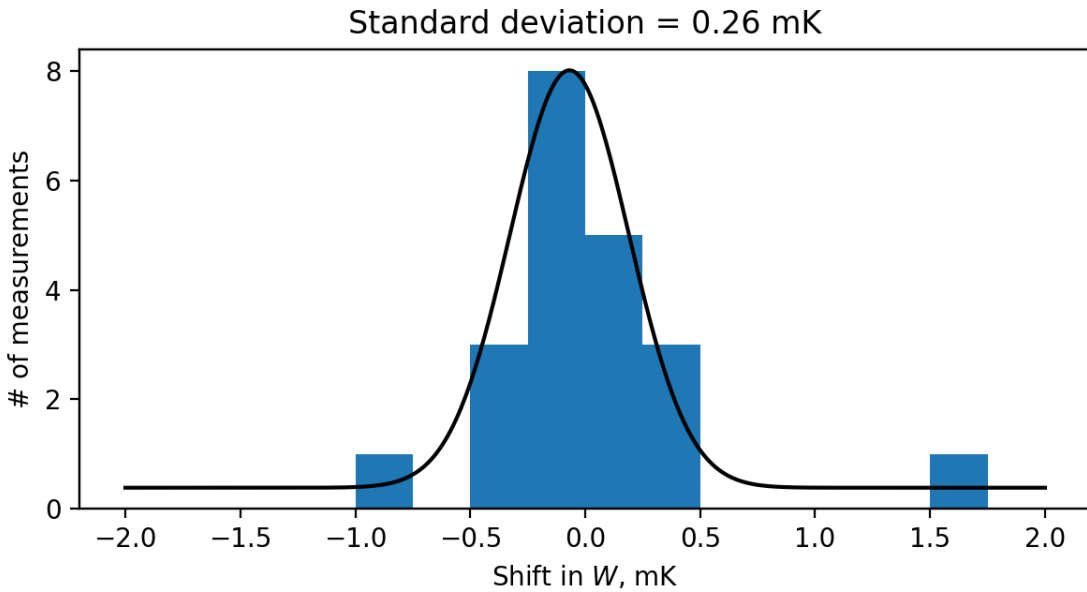


Figure 4.3: Results for the shift in measured W after repeated calibration cycles for non-NIST SPRTs used in this study, at the indium point. These values are calculated by subtracting the value measured before sending the SPRT from the value measured upon return of the SPRT from NIST. Shifts of 1 mK and greater are excluded from the overlaid fit.

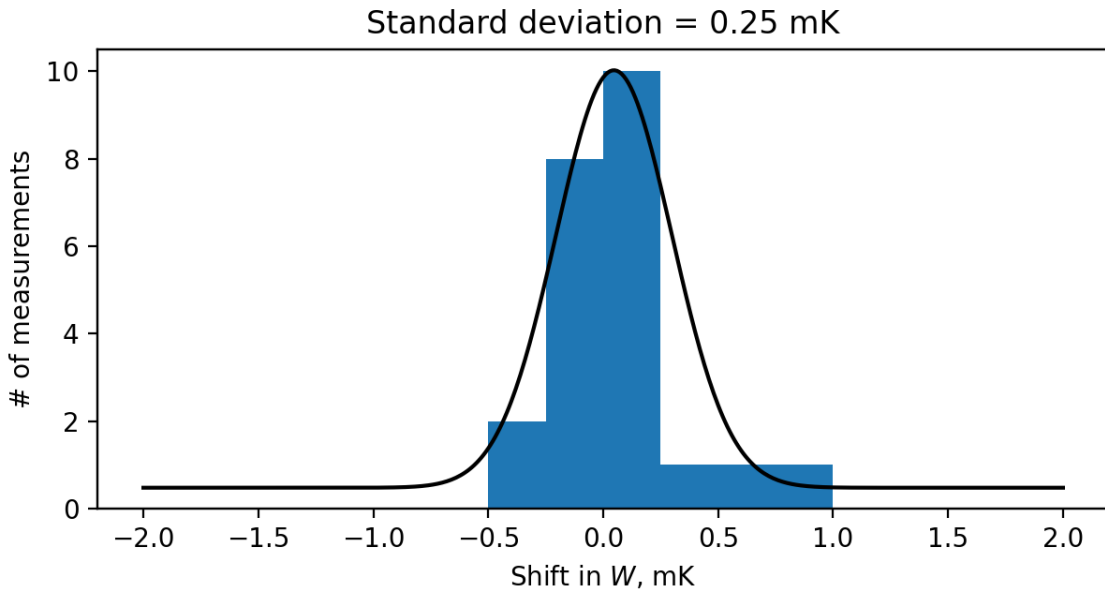


Figure 4.4: Results for the shift in measured W after repeated calibration cycles for non-NIST SPRTs used in this study, at the gallium point. These values are calculated by subtracting the value measured before sending the SPRT from the value measured upon return of the SPRT from NIST. Shifts of 1 mK and greater are excluded from the overlaid fit.

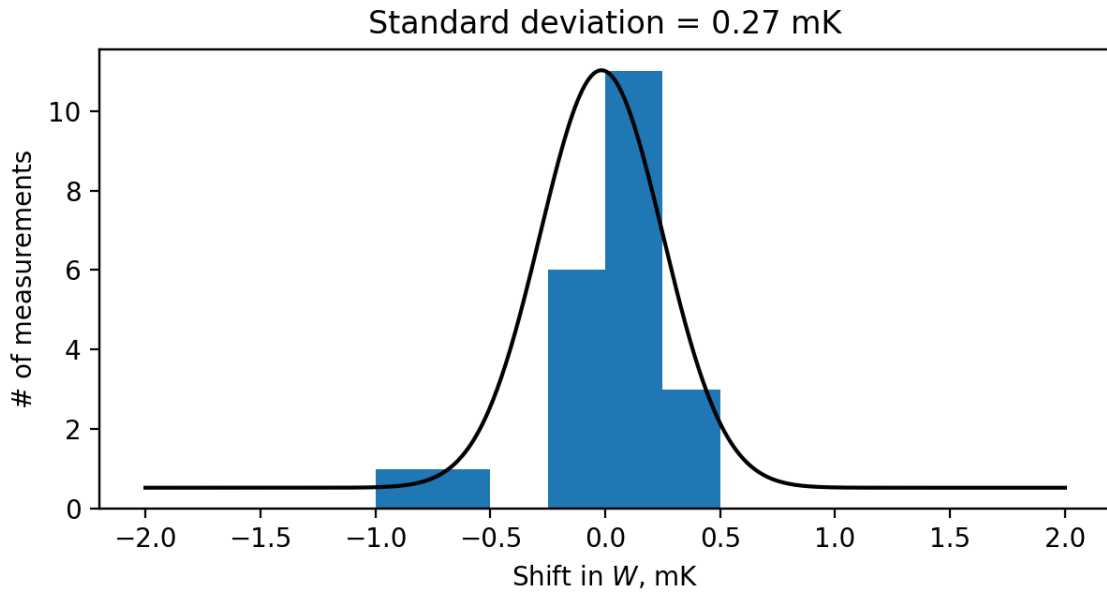


Figure 4.5: Results for the shift in measured W after repeated calibration cycles for non-NIST SPRTs used in this study, at the mercury point. These values are calculated by subtracting the value measured before sending the SPRT from the value measured upon return of the SPRT from NIST. Shifts of 1 mK and greater are excluded from the overlaid fit.

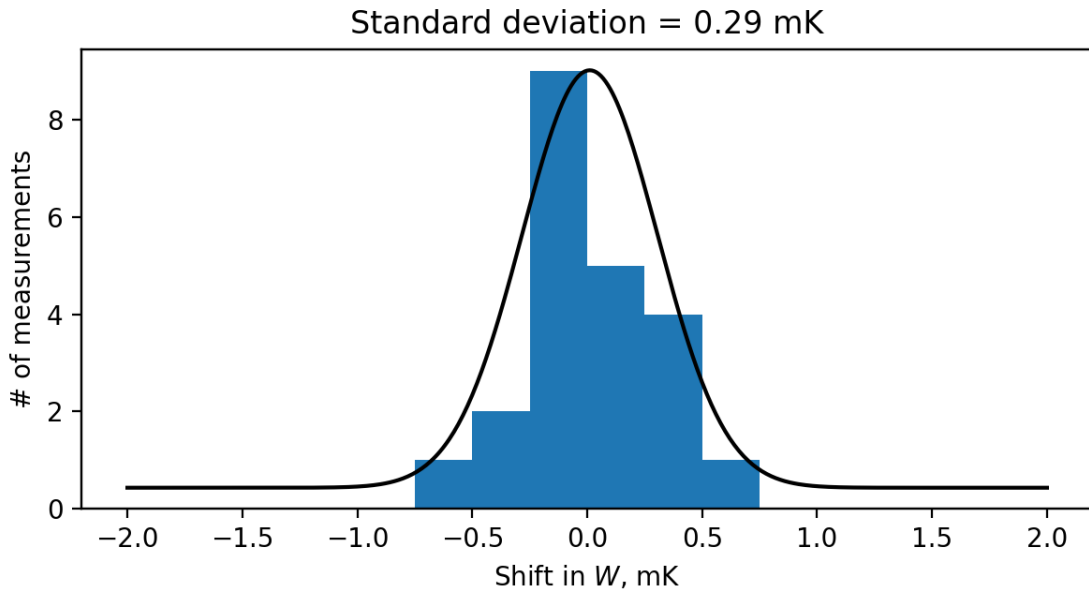


Figure 4.6: Results for the shift in measured W after repeated calibration cycles for non-NIST SPRTs used in this study, at the argon point. These values are calculated by subtracting the value measured before sending the SPRT from the value measured upon return of the SPRT from NIST. Shifts of 1 mK and greater are excluded from the overlaid fit.

	Other		Pilot	
	NMIs		NMI	
	n	St. Dev.	n	St. Dev.
Zn	17	0.29	8	0.21
Sn	21	0.44	8	0.13
In	20	0.26	8	0.12
Ga	23	0.25	8	0.19
Hg	22	0.27	6	0.16
Ar	22	0.29	8	0.52

Table 4.1: Distribution of measured shifts in SPRTs upon transfer to and from NIST and distribution of measured cycle-to-cycle shifts in the NIST proxy SPRT.

4.2 Comparison of shifts during transfer to uncertainty budgets – visualizing cutoff criterion 1

Here we compare the apparent temperature shift between measurements

$$\Delta W_{\text{transfer}} = W^{\text{Post}} - W^{\text{Ante}}$$

to the uncertainty of that shift, $U(\Delta W_{\text{transfer}})$. If the shifts are truly random one expects to find the points distributed about zero, with most points bound by the condition

$$|\Delta W_{\text{transfer}}| < U_R(\Delta W_{\text{transfer}})$$

– denoted in the following figures (e.g. Fig. 4.7) by dashed lines. These dashed lines are a graphical representation of cutoff criterion 1 (Eq. 3.1), albeit assuming infinite degrees of freedom rather than using the finite degrees of freedom (ν_{eff}) assigned by the individual laboratories.

Many points lie outside of the lines, and are thus incompatible with the uncertainty budget supplied, implying a significant error due to handling or some other (unaccounted for) contribution.

Some points in these figures are difficult to distinguish since they are clustered at low ΔW ; to highlight the magnitude of these shifts relative to the uncertainty budget the figures are also re-plotted after being scaled by the stated uncertainty at each NMI:

$$\frac{\Delta W_{\text{transfer}}}{U(\Delta W_{\text{transfer}})} \text{ vs } U(\Delta W_{\text{transfer}})$$

Such a plot (e.g. Fig. 4.8) should have most points distributed within the interval (-1, 1). That is clearly not the case, indicating an additional error is present.

A third set of figures is included in Appendix D, where the same data have been grouped by NMI rather than by fixed point.

The origin of this additional error is unclear. It may be an effect of transporting SPRTs to and from NIST. Perhaps it is more fundamental, and related to a limit on repeatability when calibrating an SPRT over a large temperature range. Whatever its source, this additional error places a limit on the power of laboratory comparisons based on traveling SPRTs. While the data from this comparison cannot shine light on the source of this unexpected variation, future work may tease out its origin.

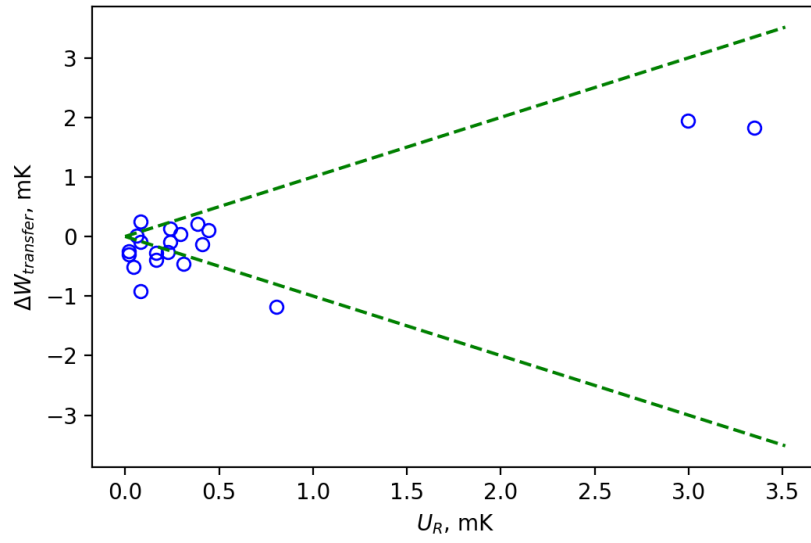


Figure 4.7: Shift in measured W upon recalibration for each SPRT used in this study, at the Zn point. Dashed lines represent the uncertainty of the shift (i.e. the random components of the budgeted uncertainty).

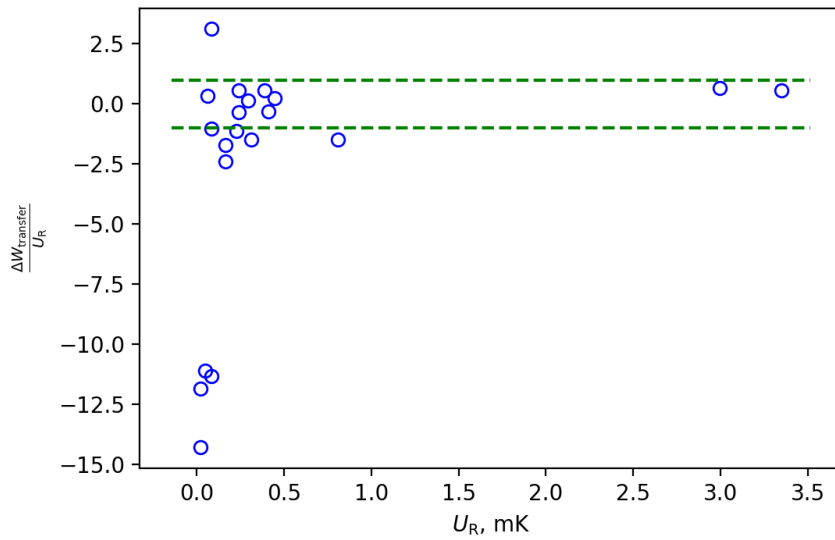


Figure 4.8: Shift in measured W upon recalibration for each SPRT used in this study, at the Zn point, scaled by the random uncertainty of that shift.

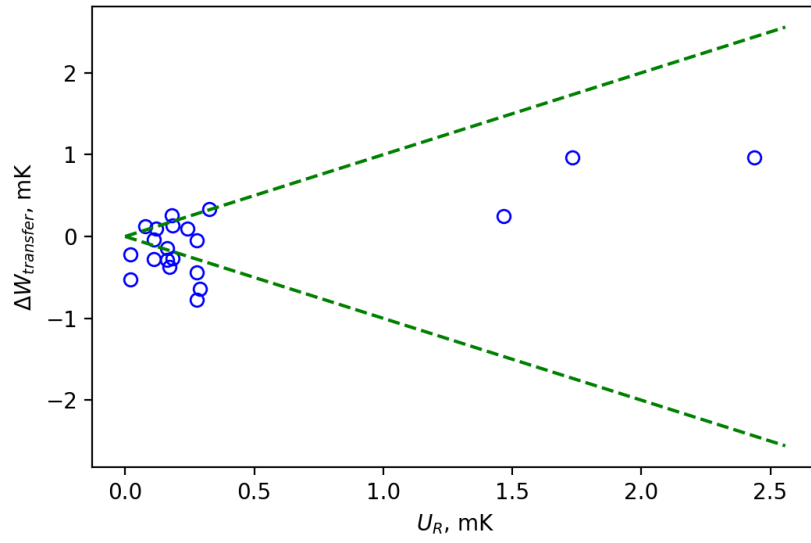


Figure 4.9: Shift in measured W upon recalibration for each SPRT used in this study, at the Sn point. Dashed lines represent the uncertainty of the shift (i.e. the random components of the budgeted uncertainty).

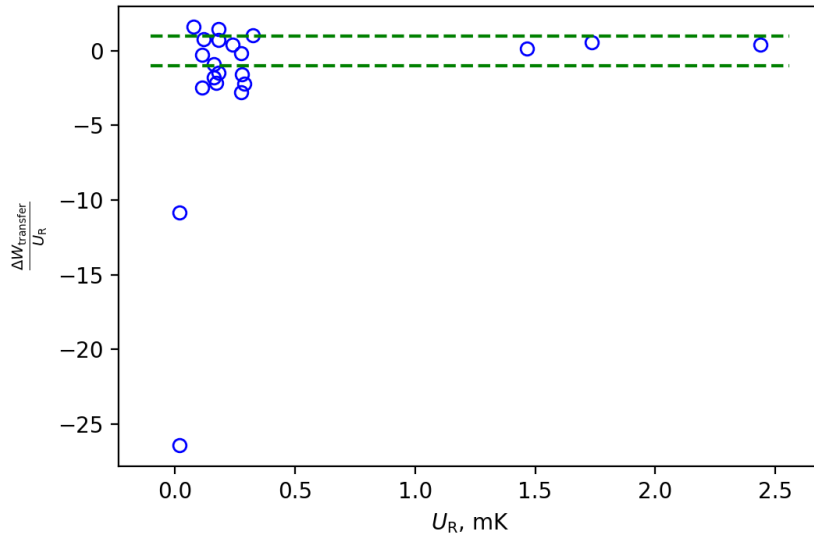


Figure 4.10: Shift in measured W upon recalibration for each SPRT used in this study, at the Sn point, scaled by the random uncertainty of that shift.

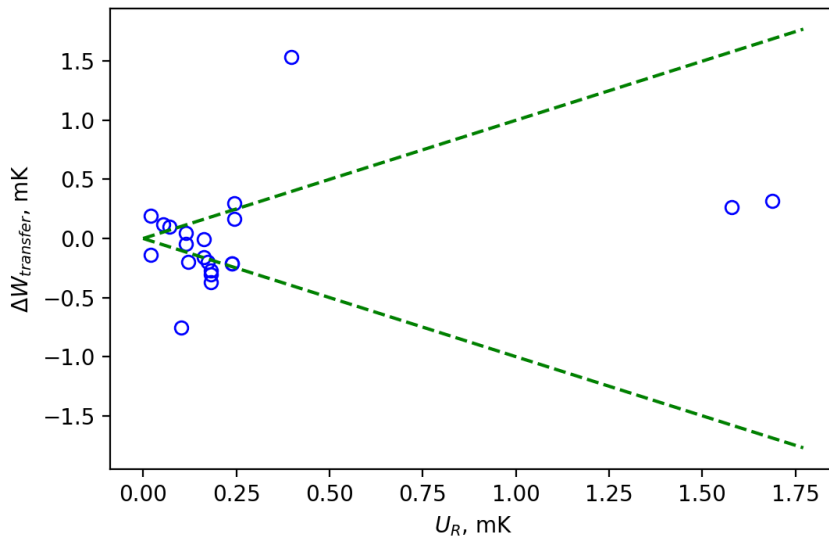


Figure 4.11: Shift in measured W upon recalibration for each SPRT used in this study, at the In point. Dashed lines represent the uncertainty of the shift (i.e. the random components of the budgeted uncertainty).

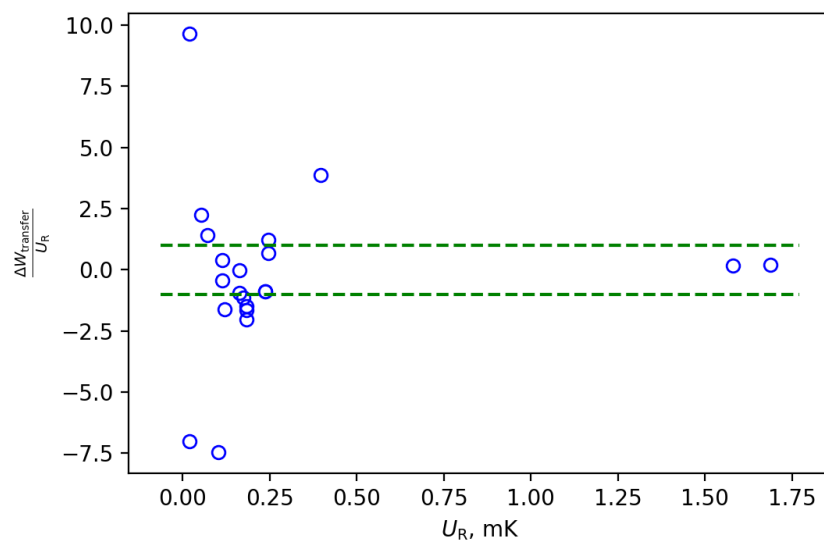


Figure 4.12: Shift in measured W upon recalibration for each SPRT used in this study, at the In point, scaled by the random uncertainty of that shift.

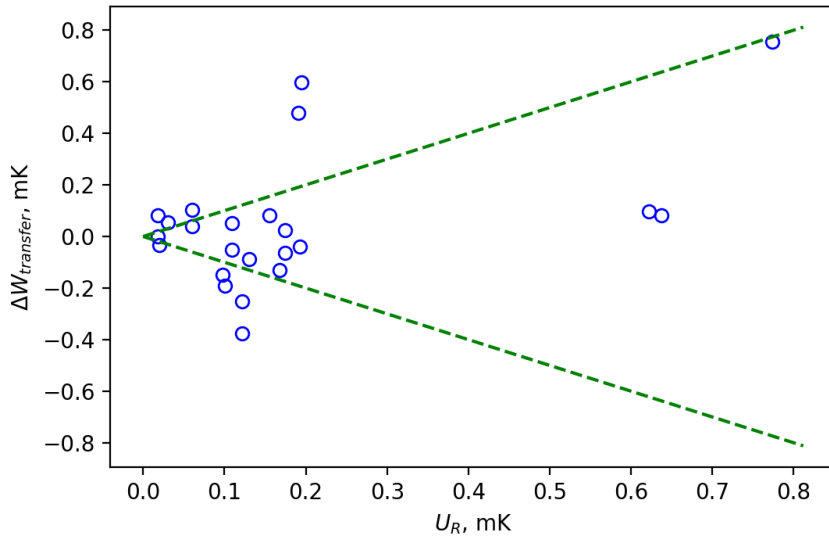


Figure 4.13: Shift in measured W upon recalibration for each SPRT used in this study, at the Ga point. Dashed lines represent the uncertainty of the shift (i.e. the random components of the budgeted uncertainty).

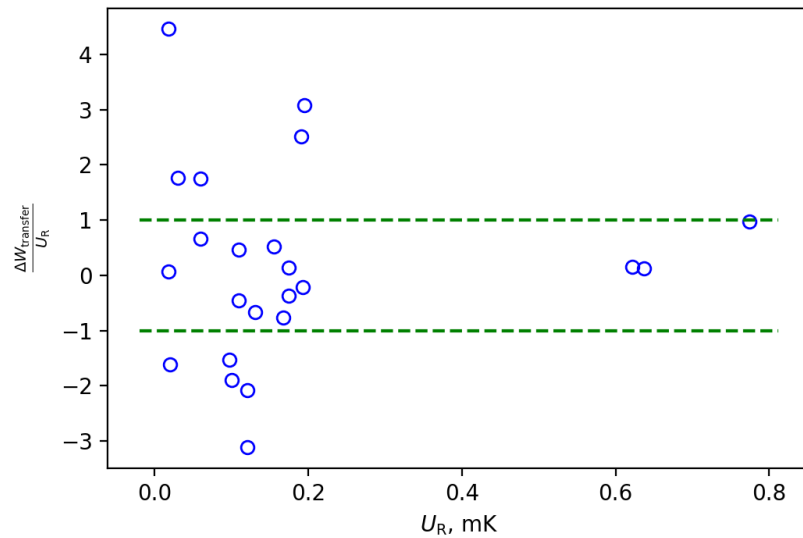


Figure 4.14: Shift in measured W upon recalibration for each SPRT used in this study, at the Ga point, scaled by the random uncertainty of that shift.

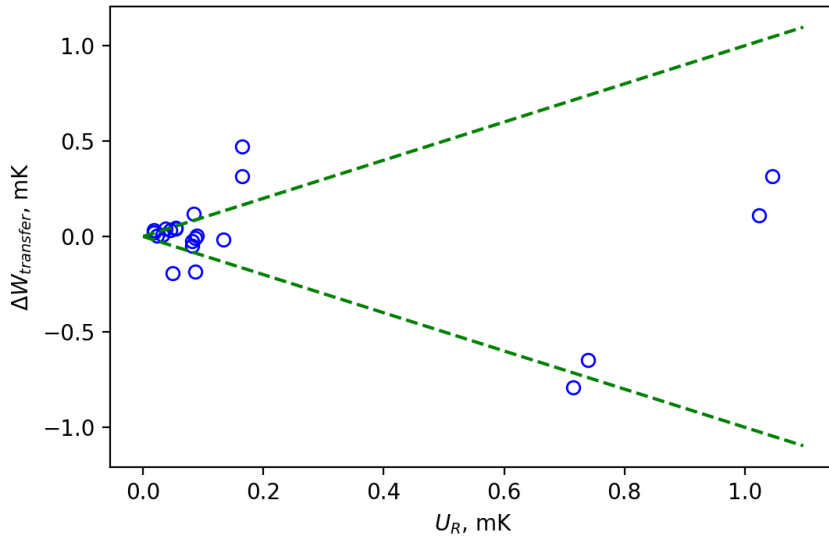


Figure 4.15: Shift in measured W upon recalibration for each SPRT used in this study, at the Hg point. Dashed lines represent the uncertainty of the shift (i.e. the random components of the budgeted uncertainty).

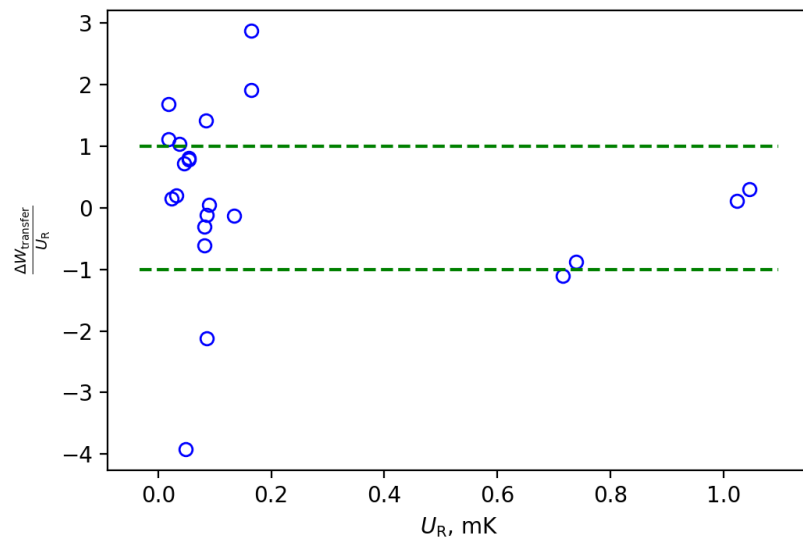


Figure 4.16: Shift in measured W upon recalibration for each SPRT used in this study, at the Hg point, scaled by the random uncertainty of that shift.

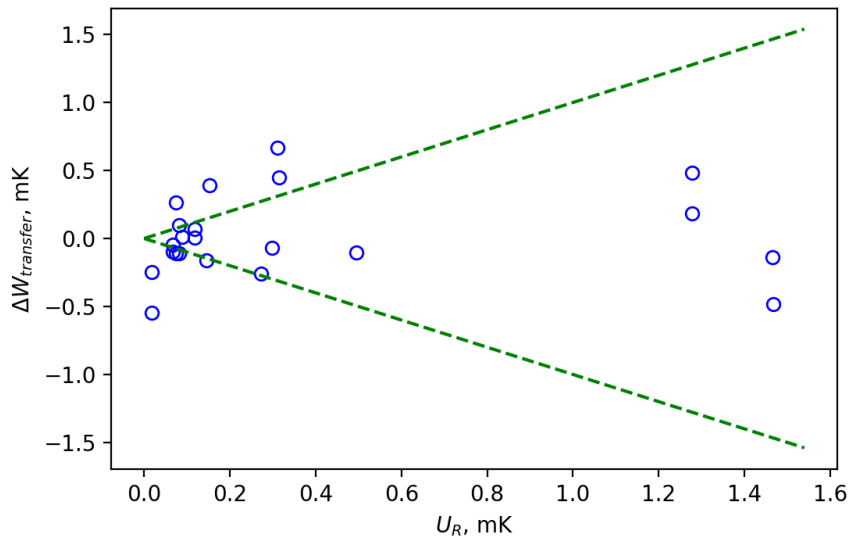


Figure 4.17: Shift in measured W upon recalibration for each SPRT used in this study, at the Ar point. Dashed lines represent the uncertainty of the shift (i.e. the random components of the budgeted uncertainty).

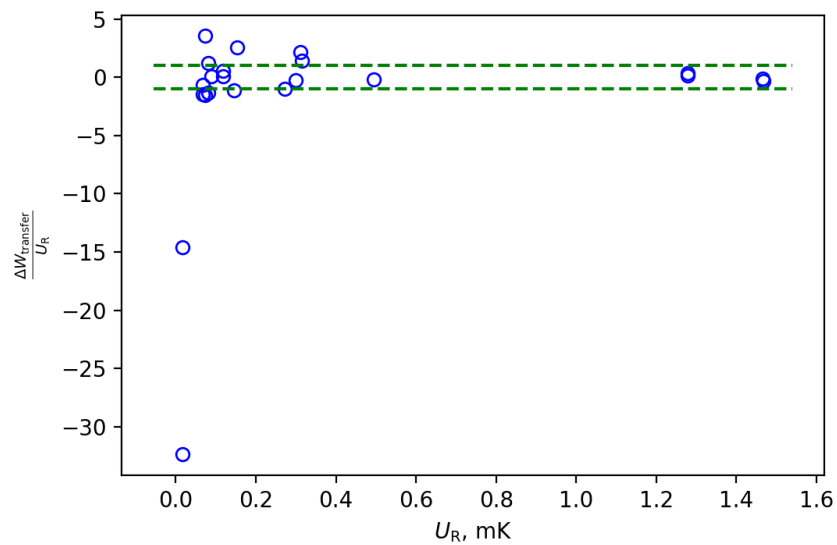


Figure 4.18: Shift in measured W upon recalibration for each SPRT used in this study, at the Ar point, scaled by the random uncertainty of that shift.

	σ (mK)	u_R (mK)
Zn	0.24	0.18
Sn	0.08	0.12
In	0.10	0.05
Ga	0.17	0.02
Hg	0.09	0.07
Ar	0.43	0.03

Table 4.2: The scatter in measurements of the NIST proxy SPRT at each fixed point, expressed as the standard deviation of all nine measurements at each fixed-point and compared to the uncorrelated (random) contributions to uncertainty.

4.3 Scatter in NIST proxy measurements contrasted with uncertainty budget

The distribution of measured “temperature shifts” at NIST shown in Table 4.1 is incompatible with the NIST uncertainty budget at some fixed points. To explicitly address this inconsistency, Table 4.2 compares the magnitude of the random component of NIST’s budget to the observed scatter in the nine realizations measured by the proxy SPRT at each fixed point.

The scatter in measurements exceeds the variation expected from the uncertainty budget at all but one fixed point, although the source of this additional variation is unclear and clearly depends on fixed point. From a practical standpoint, this implies that NMI results are dependent on identity of the batch, or batches, that included their SPRTs when measured at NIST.

The easiest way to remove this dependency is to increase the magnitude of uncertainty of the NIST measurements used to calculate ΔT_{NMI} . We use a simple statistical approach since there is no clear physical source for this variation: the standard deviation of the measurements (shown in Table 4.2) is compared to $u_R(\text{NIST})$. The larger of these two values is used as $u_R(\text{NIST})$ when calculating ΔT_{NMI} . Note that this does not represent a change in the NIST uncertainty budget – the NIST SPRT data for this comparison are processed identically to other NMIs, using the NIST uncertainty budget supplied in Appendix C.

The results presented in the body of this report incorporate this unexpected additional variation. For completeness, we include in Appendix E the results calculated as originally proposed, without accounting for this variation.

Chapter 5

Key comparison reference value

5.1 Calculation of key comparison reference value

Table 5.1 reports the key comparison reference value (KCRV) $\overline{\Delta T}$ at each fixed point using the average NMI measured W (i.e. the average of ante- and post- NIST measurements). As outlined in the previous section, it incorporates an increased uncertainty for the measurements taken, at NIST, at fixed points where we observed greater than expected variation. This $\overline{\Delta T}$ is not meant to have any intrinsic meaning – it is a computational tool allowing comparisons across labs linked through measurements at the pilot lab.

The numerical magnitude of $\overline{\Delta T}$ at each fixed point is related to the average offset of the NIST realization of that fixed point from those of the other participating labs. However, using this as the metric for evaluating NIST relative to the other NMIs is problematic since the uncertainty of such a comparison is ambiguous. Instead, in the tables and graphs that follow, the NIST data plotted are those of the proxy SPRT as described in the earlier chapters.

While $\overline{\Delta T}$ was computed using a simple mean as originally proposed, some variations on this approach are included in Appendix E, including weighting an SPRT’s contribution based on its performance at other fixed points or weighting a laboratory’s results based on their stated uncertainty. The appendix also includes calculations using specific subsets of measurements, and calculations that neglect the additional variation noted in the “at NIST” measurements.

	$\overline{\Delta T}$ (mK)	$U(\overline{\Delta T})$ (mK)	#NMIs
Zn	-0.20	0.22	12
Sn	0.06	0.16	10
In	-0.08	0.09	11
Ga	0.23	0.07	12
Hg	0.28	0.08	10
Ar	0.80	0.17	11

Table 5.1: Values, with uncertainty, for the KCRV ($\overline{\Delta T}$) at each fixed-point, as well as a tally of the number of NMIs with measurements contributing to the calculation.

5.2 NMI results with respect to $\overline{\Delta T}$, organized by fixed point

Tables 5.2 through 5.7 and Figures 5.1 through 5.6 summarize deviations of NMI results from $\overline{\Delta T}$ at each fixed point. Error bars in all of these plots show the uncertainty in the value $\Delta T_{\text{NMI-KCRV}}$ at the $k = 2$ level. Values for $\Delta T_{\text{NMI-KCRV}}$ were computed using all measurements at an NMI, regardless of whether they passed the cutoff criteria.

These tables also include a column showing the uncertainty of a single value of \overline{W} using the budgets supplied by each lab. By default the value is for SPRT #1 (i.e. \overline{W}_1), but data from SPRT #2 are used if no data are available from SPRT #1. This uncertainty is based entirely on the NMI uncertainty budget; it includes no components from NIST, nor does it include transfer uncertainty. It is included to illustrate the accuracy claimed by each lab, since that may or may not come across effectively in $U(\Delta T_{\text{NMI-KCRV}})$. The magnitude of $U(\overline{W}_1)$ may be less than, equal to, or greater than $U(\Delta T_{\text{NMI-KCRV}})$ depending on the contribution of NIST uncertainties, the magnitude of the transfer uncertainties for the NMI's SPRTs, and the number of NMI SPRTs that contributed to the calculation of $\Delta T_{\text{NMI-KCRV}}$.

5.2.1 Zinc

All labs which had facilities for realizing the zinc freezing point had at least one measurement that contributed to the calculation of $\overline{\Delta T}$ for zinc. The results of this comparison at the zinc point are summarized in Table 5.2 and Fig. 5.1.

	$\Delta T_{\text{NMI-KCRV}}$ (mK)	$U(\Delta T_{\text{NMI-KCRV}})$ (mK)	$U(\overline{W}_1)$ (mK)
BIPM	—	—	—
INMETRO	-0.69	1.37	1.51
INRIM	-0.61	0.91	0.79
INTI	-1.56	3.37	3.88
KRISS	0.61	0.99	0.92
LNE-CNAM	1.01	0.96	0.97
NIM	0.13	0.74	0.61
NIST	0.02	0.61	0.44
NMIA	-1.07	0.64	0.41
NMIJ/AIST	0.19	0.78	0.68
NPL	-1.78	0.64	0.43
NRC	0.30	0.75	0.58
PTB	1.69	1.23	1.27
VSL	2.53	1.04	0.74

Table 5.2: Deviation of ΔT_{NMI} from $\overline{\Delta T}$ measured by each NMI at the zinc point. Uncertainties are displayed at the $k = 2$ level.

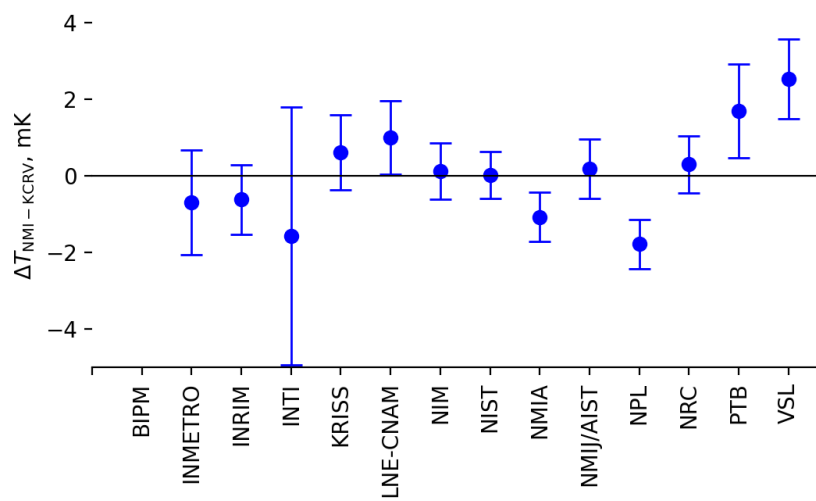


Figure 5.1: Deviation of ΔT_{NMI} from $\overline{\Delta T}$ at the zinc point measured by each NMI. Error bars represent uncertainty calculated using the uncertainty budget supplied by the NMI for this key comparison, at the $k = 2$ level.

5.2.2 Tin

Ten of the twelve labs which had facilities for realizing the tin freezing point had at least one measurement that contributed to the calculation of $\overline{\Delta T}$ for tin. The results of this comparison at the tin point are summarized in Table 5.3 and Fig. 5.2.

	$\Delta T_{\text{NMI-KCRV}}$ (mK)	$U(\Delta T_{\text{NMI-KCRV}})$ (mK)	$U(\overline{W}_1)$ (mK)
BIPM	—	—	—
INMETRO	-0.91	0.84	0.90
INRIM	0.09	0.59	0.50
INTI	-1.10	1.88	2.10
KRISS	0.22	0.75	0.81
LNE-CNAM	0.29	0.64	0.48
NIM	0.33	0.54	0.51
NIST	-0.11	0.37	0.23
NMIA	-0.21	0.46	0.31
NMIJ/AIST	-0.03	0.53	0.51
NPL	0.09	0.50	0.25
NRC	0.65	0.47	0.34
PTB	0.28	0.79	0.88
VSL	0.54	0.56	0.47

Table 5.3: Deviation of ΔT_{NMI} from $\overline{\Delta T}$ measured by each NMI at the tin point. Uncertainties are displayed at the $k = 2$ level.

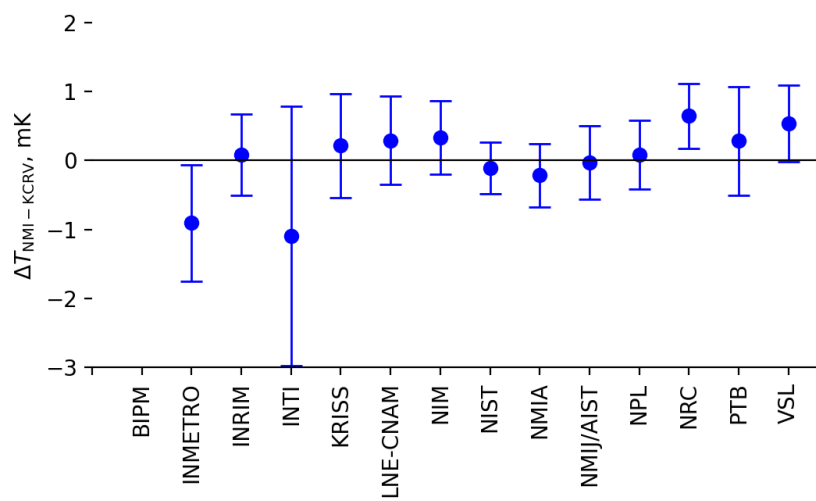


Figure 5.2: Deviation of ΔT_{NMI} from $\overline{\Delta T}$ at the tin point measured by each NMI. Error bars represent uncertainty calculated using the uncertainty budget supplied by the NMI for this key comparison, at the $k = 2$ level.

5.2.3 Indium

Eleven of the twelve labs which had facilities for realizing the indium freezing point had at least one measurement that contributed to the calculation of $\overline{\Delta T}$ for indium. The results of this comparison at the indium point are summarized in Table 5.3 and Fig. 5.3.

	$\Delta T_{\text{NMI-KCRV}}$ (mK)	$U(\Delta T_{\text{NMI-KCRV}})$ (mK)	$U(\overline{W}_1)$ (mK)
BIPM	—	—	—
INMETRO	-0.65	0.61	0.82
INRIM	-0.02	0.58	0.59
INTI	0.45	2.35	2.15
KRISS	0.27	0.97	1.13
LNE-CNAM	0.64	0.49	0.51
NIM	0.13	0.43	0.45
NIST	0.13	0.25	0.17
NMIA	-0.04	0.39	0.39
NMIJ/AIST	0.16	0.36	0.34
NPL	-0.29	0.29	0.24
NRC	0.12	0.29	0.22
PTB	0.06	0.75	0.87
VSL	-0.02	0.40	0.31

Table 5.4: Deviation of ΔT_{NMI} from $\overline{\Delta T}$ measured by each NMI at the indium point. Uncertainties are displayed at the $k = 2$ level.

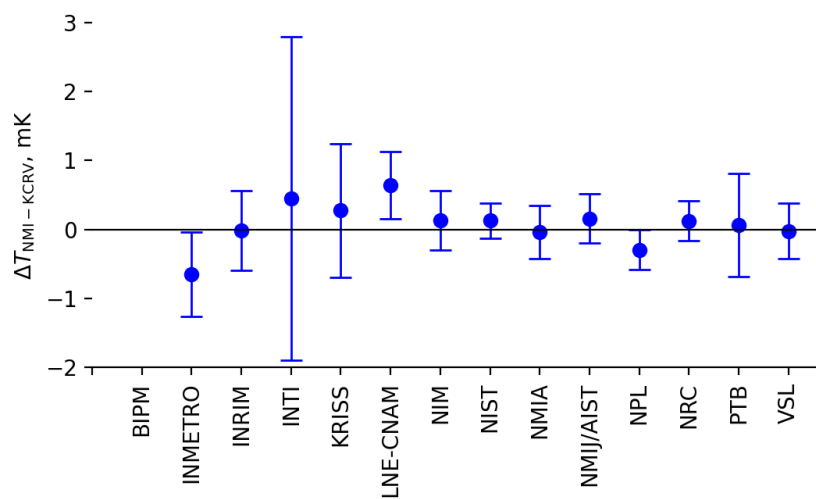


Figure 5.3: Deviations of ΔT_{NMI} from $\overline{\Delta T}$ at the indium point measured by each NMI. Error bars represent uncertainty calculated using the uncertainty budget supplied by the NMI for this key comparison, at the $k = 2$ level.

5.2.4 Gallium

Twelve of the thirteen labs which had facilities for realizing the gallium melting point had at least one measurement that contributed to the calculation of $\overline{\Delta T}$ for gallium. The results of this comparison at the gallium point are summarized in Table 5.3 and Fig. 5.2.

	$\Delta T_{\text{NMI-KCRV}}$ (mK)	$U(\Delta T_{\text{NMI-KCRV}})$ (mK)	$U(\overline{W}_1)$ (mK)
BIPM	0.11	0.32	0.25
INMETRO	0.29	0.34	0.36
INRIM	0.04	0.35	0.15
INTI	0.15	0.87	0.72
KRISS	-0.08	0.41	0.31
LNE-CNAM	-0.36	0.38	0.40
NIM	0.26	0.38	0.34
NIST	-0.22	0.23	0.07
NMIA	-0.33	0.35	0.34
NMIJ/AIST	-0.24	0.30	0.23
NPL	-0.06	0.26	0.12
NRC	0.12	0.27	0.14
PTB	-0.05	0.30	0.22
VSL	-0.14	0.36	0.27

Table 5.5: Deviation of ΔT_{NMI} from $\overline{\Delta T}$ measured by each NMI at the gallium point. Uncertainties are displayed at the $k = 2$ level.

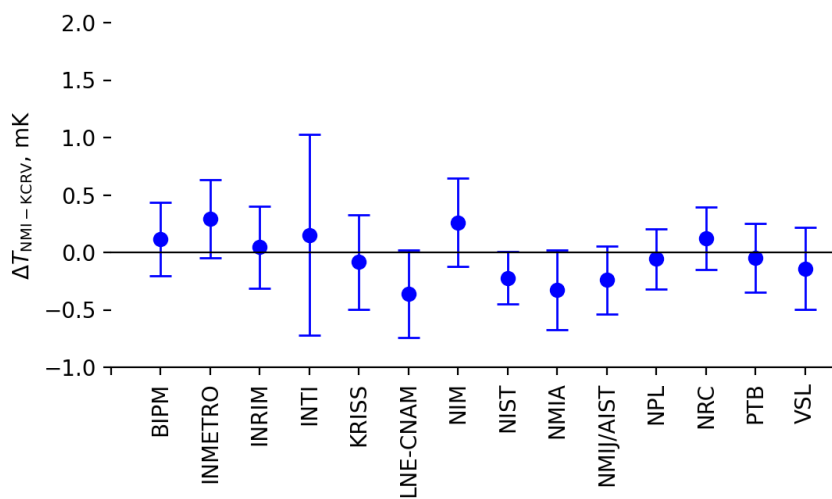


Figure 5.4: Deviations of ΔT_{NMI} from $\overline{\Delta T}$ at the gallium point measured by each NMI. Error bars represent uncertainty calculated using the uncertainty budget supplied by the NMI for this key comparison, at the $k = 2$ level.

5.2.5 Mercury

Ten of the twelve labs which had facilities for realizing the mercury triple point had at least one measurement that contributed to the calculation of $\overline{\Delta T}$ for mercury. The results of this comparison at the mercury point are summarized in Table 5.6 and Fig. 5.5.

	$\Delta T_{\text{NMI-KCRV}}$ (mK)	$U(\Delta T_{\text{NMI-KCRV}})$ (mK)	$U(\overline{W}_1)$ (mK)
BIPM	—	—	—
INMETRO	-0.11	0.41	0.54
INRIM	0.18	0.30	0.12
INTI	-0.08	0.66	0.71
KRISS	-0.19	0.40	0.42
LNE-CNAM	0.76	0.64	0.52
NIM	0.24	0.31	0.29
NIST	-0.32	0.25	0.12
NMIA	-0.04	0.29	0.27
NMIJ/AIST	0.18	0.59	0.70
NPL	0.06	0.24	0.18
NRC	0.01	0.24	0.18
PTB	0.12	0.29	0.28
VSL	-0.07	0.25	0.22

Table 5.6: Deviation of ΔT_{NMI} from $\overline{\Delta T}$ measured by each NMI at the mercury point. Uncertainties are displayed at the $k = 2$ level.

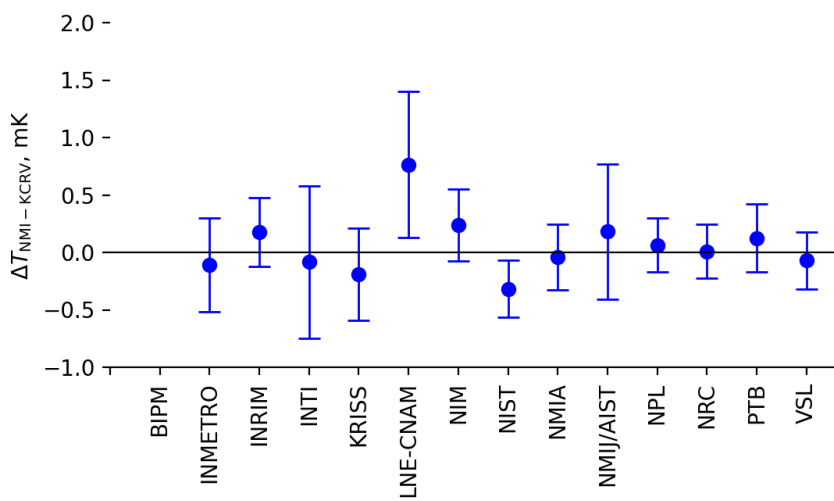


Figure 5.5: Deviations of ΔT_{NMI} from $\overline{\Delta T}$ at the mercury point measured by each NMI. Error bars represent uncertainty calculated using the uncertainty budget supplied by the NMI for this key comparison, at the $k = 2$ level.

5.2.6 Argon

Eleven of the twelve labs which had facilities for realizing the argon triple point had at least one measurement that contributed to the calculation of $\overline{\Delta T}$ for argon. The results of this comparison at the argon point are summarized in Table 5.7 and Fig. 5.6.

	$\Delta T_{\text{NMI-KCRV}}$ (mK)	$U(\Delta T_{\text{NMI-KCRV}})$ (mK)	$U(\overline{W}_1)$ (mK)
BIPM	—	—	—
INMETRO	0.21	0.79	0.75
INRIM	0.22	1.08	0.36
INTI	0.95	1.74	1.95
KRISS	0.28	1.03	0.81
LNE-CNAM	-0.17	0.80	0.61
NIM	-0.67	0.66	0.33
NIST	-1.41	0.54	0.13
NMIA	-0.36	0.99	0.95
NMIJ/AIST	0.20	1.30	1.41
NPL	0.35	0.66	0.32
NRC	-0.06	0.65	0.30
PTB	0.10	0.73	0.49
VSL	-0.82	0.63	0.33

Table 5.7: Deviation of ΔT_{NMI} from $\overline{\Delta T}$ measured by each NMI at the argon point. Uncertainties are displayed at the $k = 2$ level.

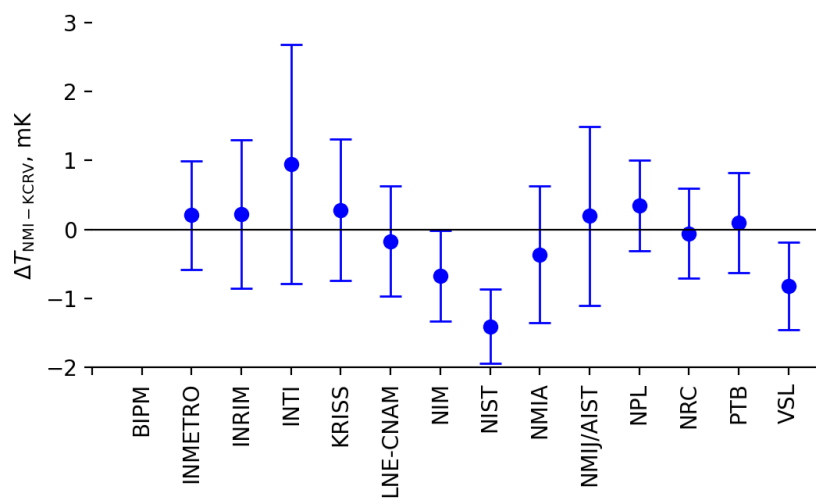


Figure 5.6: Deviations of ΔT_{NMI} from $\overline{\Delta T}$ at the argon point measured by each NMI. Error bars represent uncertainty calculated using the uncertainty budget supplied by the NMI for this key comparison, at the $k = 2$ level.

5.3 NMI results with respect to $\overline{\Delta T}$, organized by lab

5.3.1 BIPM

	$\Delta T_{\text{NMI-KCRV}}$ (mK)	$U(\Delta T_{\text{NMI-KCRV}})$ (mK)	$U(\overline{W_1})$ (mK)
Zn	—	—	—
Sn	—	—	—
In	—	—	—
Ga	0.11	0.32	0.25
Hg	—	—	—
Ar	—	—	—

Table 5.8: Deviation from $\overline{\Delta T}$ at each fixed-point measured at BIPM. Uncertainties are displayed at the $k = 2$ level.

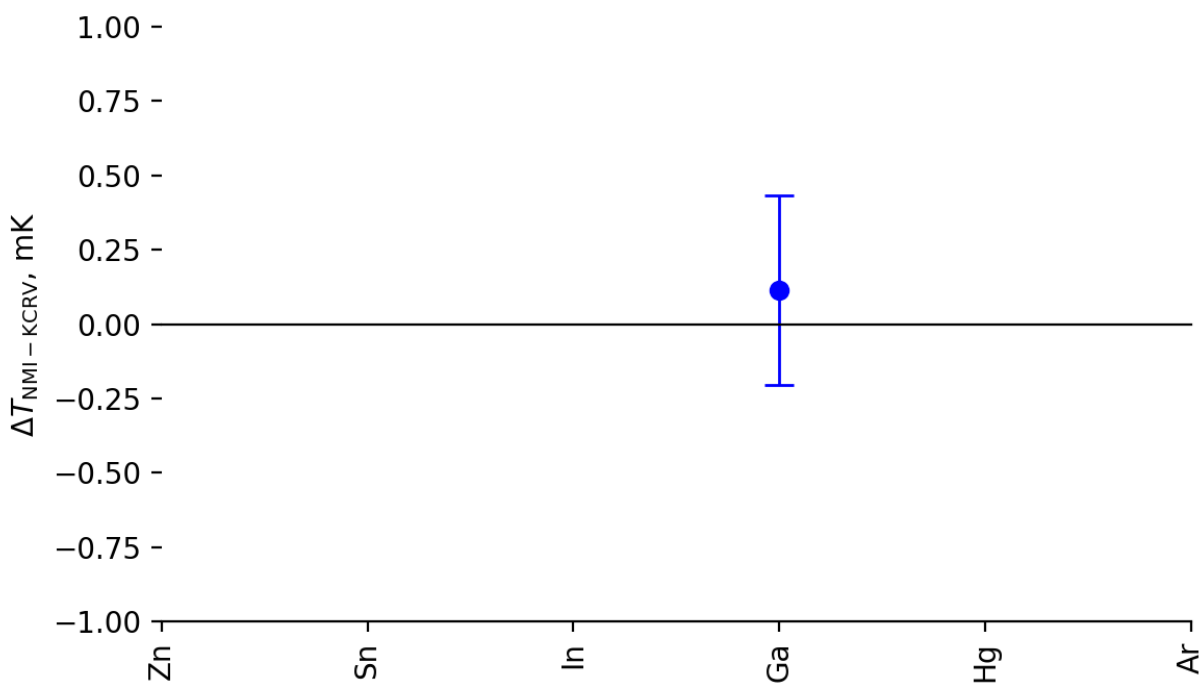


Figure 5.7: Deviation of ΔT_{NMI} from $\overline{\Delta T}$ at each fixed-point measured at BIPM.

5.3.2 INMETRO

	$\Delta T_{\text{NMI-KCRV}}$ (mK)	$U(\Delta T_{\text{NMI-KCRV}})$ (mK)	$U(\overline{W_1})$ (mK)
Zn	-0.69	1.37	1.51
Sn	-0.91	0.84	0.90
In	-0.65	0.61	0.82
Ga	0.29	0.34	0.36
Hg	-0.11	0.41	0.54
Ar	0.21	0.79	0.75

Table 5.9: Deviation from $\overline{\Delta T}$ at each fixed-point measured at INMETRO. Uncertainties are displayed at the $k = 2$ level.

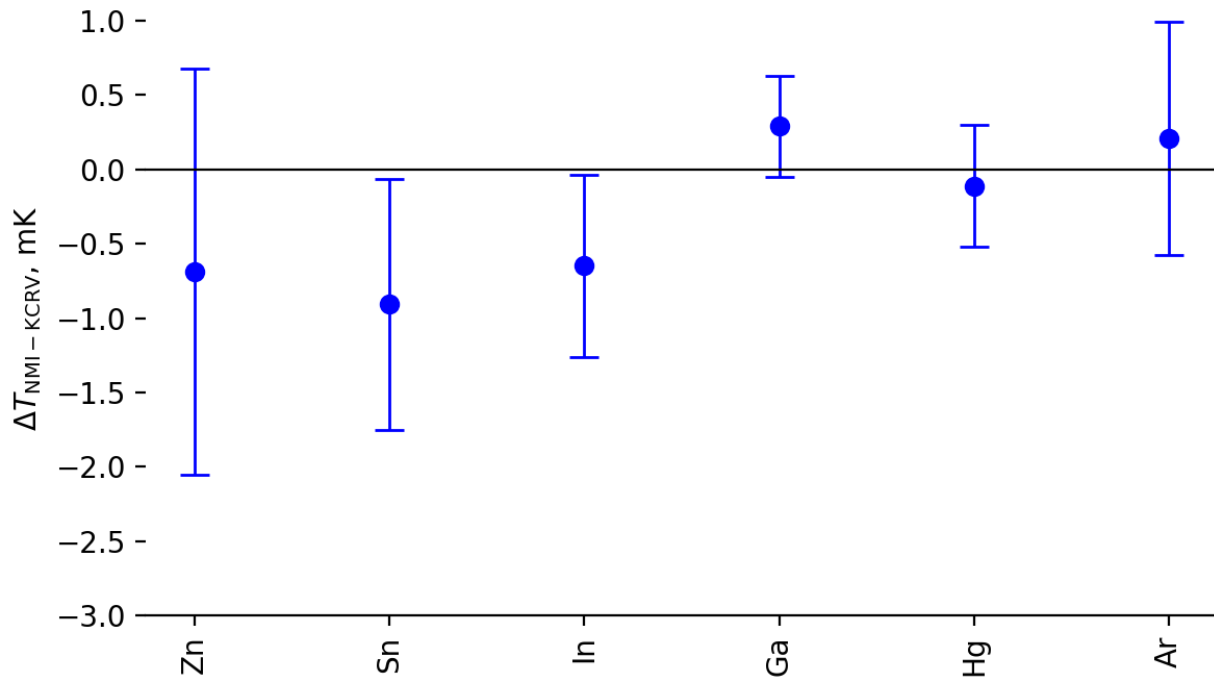


Figure 5.8: Deviation of ΔT_{NMI} from $\overline{\Delta T}$ at each fixed-point measured at INMETRO.

5.3.3 INRIM

	$\Delta T_{\text{NMI-KCRV}}$ (mK)	$U(\Delta T_{\text{NMI-KCRV}})$ (mK)	$U(\overline{W_1})$ (mK)
Zn	-0.61	0.91	0.79
Sn	0.09	0.59	0.50
In	-0.02	0.58	0.59
Ga	0.04	0.35	0.15
Hg	0.18	0.30	0.12
Ar	0.22	1.08	0.36

Table 5.10: Deviation from $\overline{\Delta T}$ at each fixed-point measured at INRIM. Uncertainties are displayed at the $k = 2$ level.

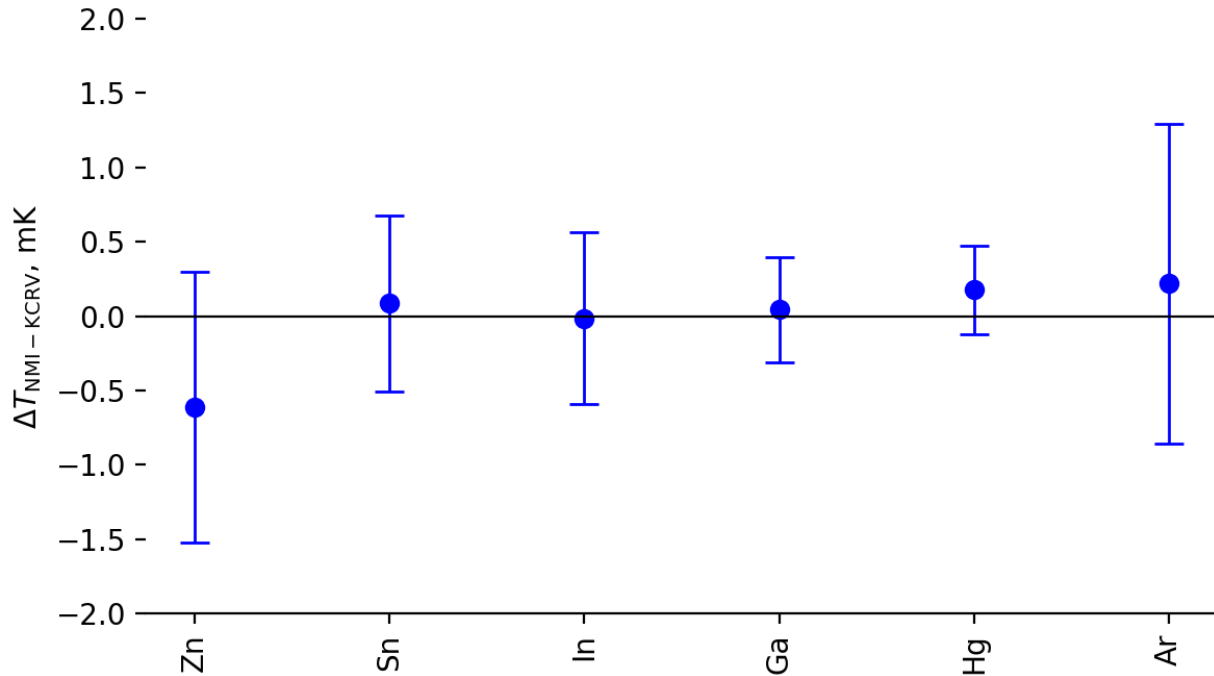


Figure 5.9: Deviation of ΔT_{NMI} from $\overline{\Delta T}$ at each fixed-point measured at INRIM.

5.3.4 INTI

	$\Delta T_{\text{NMI-KCRV}}$ (mK)	$U(\Delta T_{\text{NMI-KCRV}})$ (mK)	$U(\bar{W}_1)$ (mK)
Zn	-1.56	3.37	3.88
Sn	-1.10	1.88	2.10
In	0.45	2.35	2.15
Ga	0.15	0.87	0.72
Hg	-0.08	0.66	0.71
Ar	0.95	1.74	1.95

Table 5.11: Deviation from $\bar{\Delta T}$ at each fixed-point measured at INTI. Uncertainties are displayed at the $k = 2$ level.

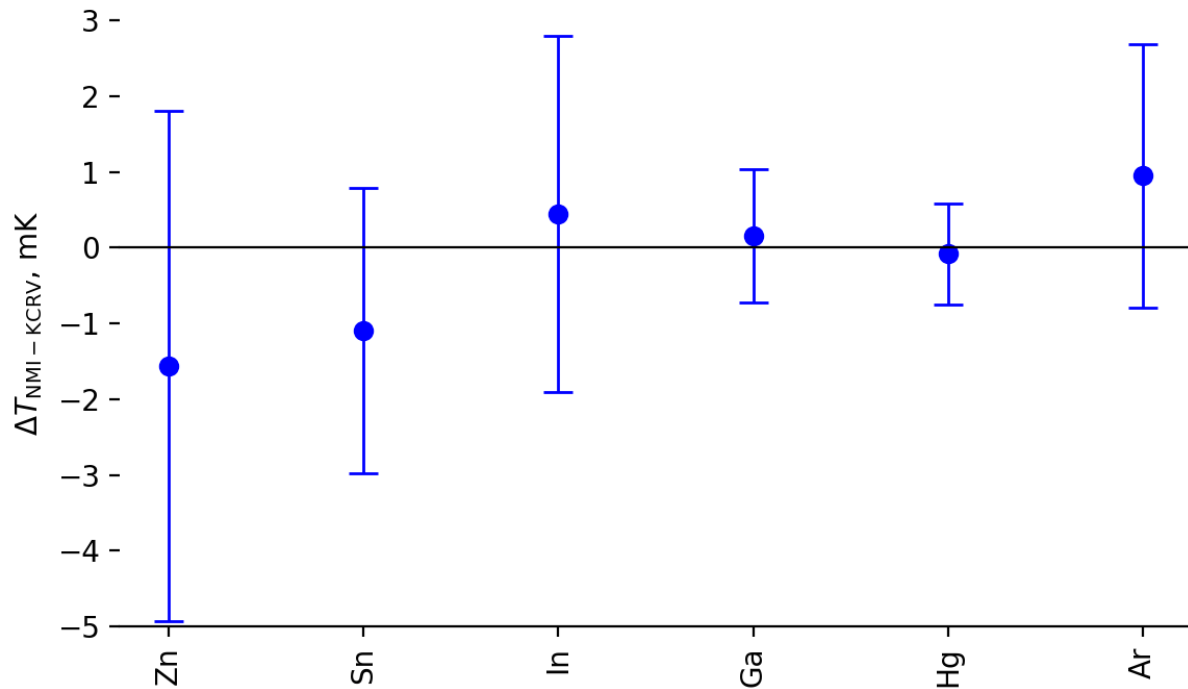


Figure 5.10: Deviation of ΔT_{NMI} from $\bar{\Delta T}$ at each fixed-point measured at INTI.

5.3.5 KRISS

	$\Delta T_{\text{NMI-KCRV}}$ (mK)	$U(\Delta T_{\text{NMI-KCRV}})$ (mK)	$U(\bar{W}_1)$ (mK)
Zn	0.61	0.99	0.92
Sn	0.22	0.75	0.81
In	0.27	0.97	1.13
Ga	-0.08	0.41	0.31
Hg	-0.19	0.40	0.42
Ar	0.28	1.03	0.81

Table 5.12: Deviation from \bar{T} at each fixed-point measured at KRISS. Uncertainties are displayed at the $k = 2$ level.

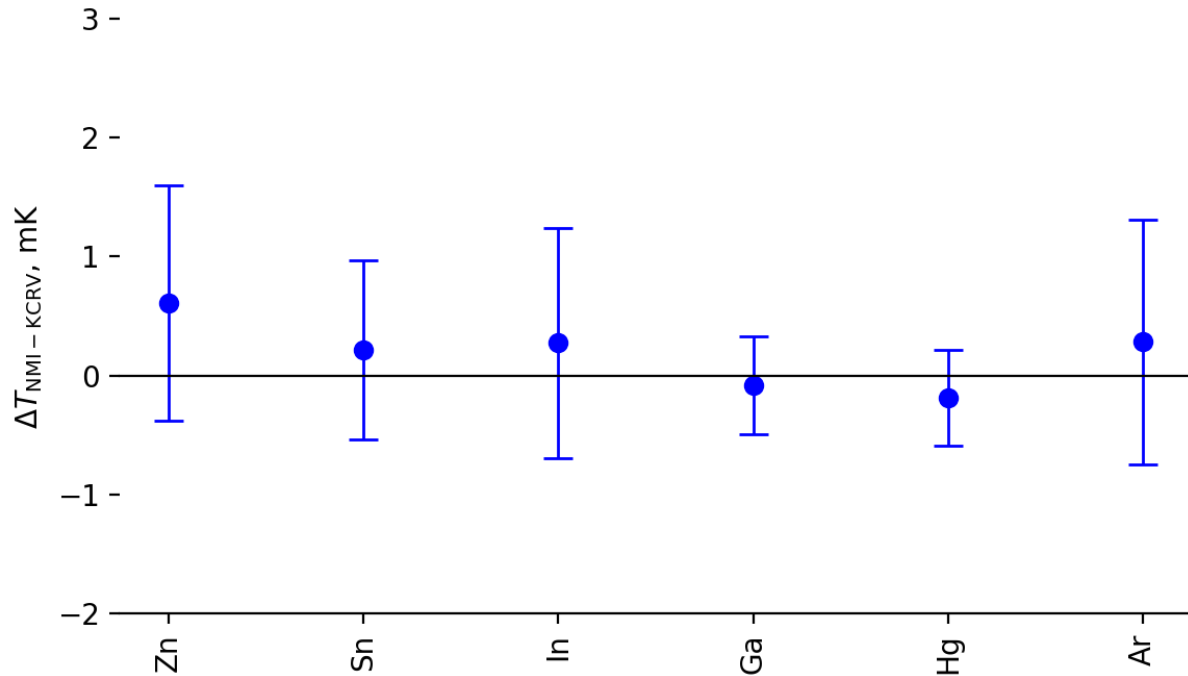


Figure 5.11: Deviation of ΔT_{NMI} from \bar{T} at each fixed-point measured at KRISS.

5.3.6 LNE-CNAM

	$\Delta T_{\text{NMI-KCRV}}$ (mK)	$U(\Delta T_{\text{NMI-KCRV}})$ (mK)	$U(\overline{W_1})$ (mK)
Zn	1.01	0.96	0.97
Sn	0.29	0.64	0.48
In	0.64	0.49	0.51
Ga	-0.36	0.38	0.40
Hg	0.76	0.64	0.52
Ar	-0.17	0.80	0.61

Table 5.13: Deviation from $\overline{\Delta T}$ at each fixed-point measured at LNE-CNAM. Uncertainties are displayed at the $k = 2$ level.

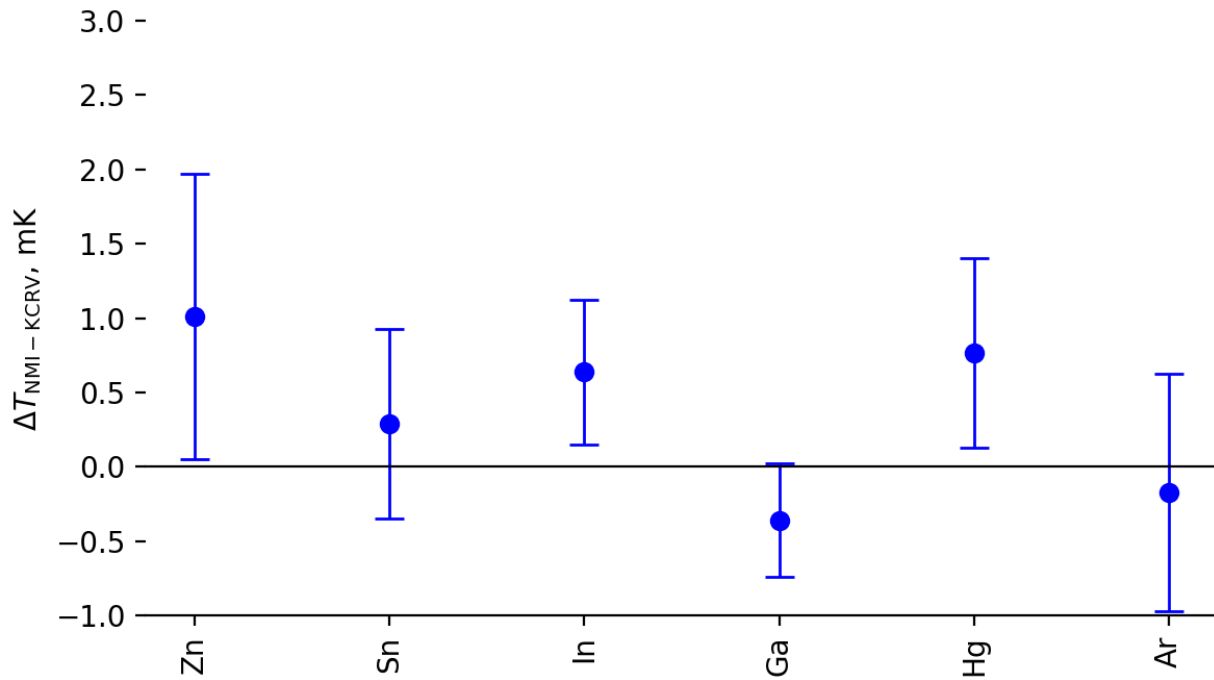


Figure 5.12: Deviation of ΔT_{NMI} from $\overline{\Delta T}$ at each fixed-point measured at LNE-CNAM.

5.3.7 NIM

	$\Delta T_{\text{NMI-KCRV}}$ (mK)	$U(\Delta T_{\text{NMI-KCRV}})$ (mK)	$U(\overline{W}_1)$ (mK)
Zn	0.13	0.74	0.61
Sn	0.33	0.54	0.51
In	0.13	0.43	0.45
Ga	0.26	0.38	0.34
Hg	0.24	0.31	0.29
Ar	-0.67	0.66	0.33

Table 5.14: Deviation from $\overline{\Delta T}$ at each fixed-point measured at NIM. Uncertainties are displayed at the $k = 2$ level.

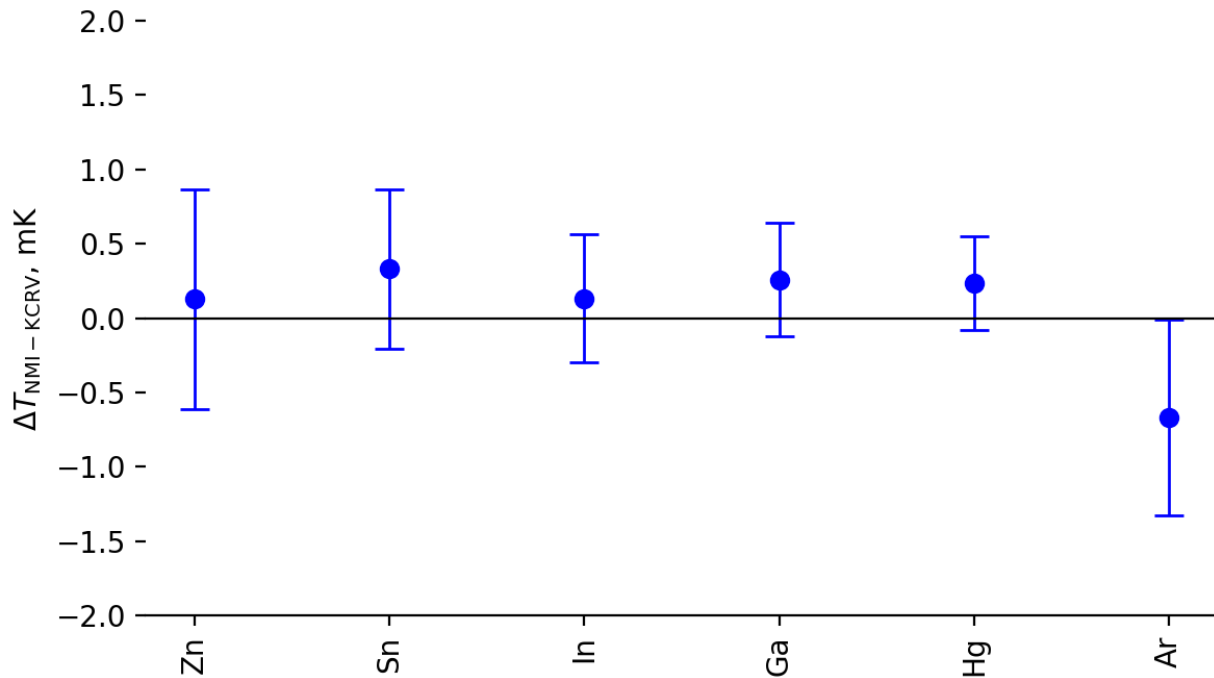


Figure 5.13: Deviation of ΔT_{NMI} from $\overline{\Delta T}$ at each fixed-point measured at NIM.

5.3.8 NIST

	$\Delta T_{\text{NMI-KCRV}}$ (mK)	$U(\Delta T_{\text{NMI-KCRV}})$ (mK)	$U(\bar{W}_1)$ (mK)
Zn	0.02	0.61	0.44
Sn	-0.11	0.37	0.23
In	0.13	0.25	0.17
Ga	-0.22	0.23	0.07
Hg	-0.32	0.25	0.12
Ar	-1.41	0.54	0.13

Table 5.15: Deviation from $\bar{\Delta T}$ at each fixed-point measured at NIST. Uncertainties are displayed at the $k = 2$ level.

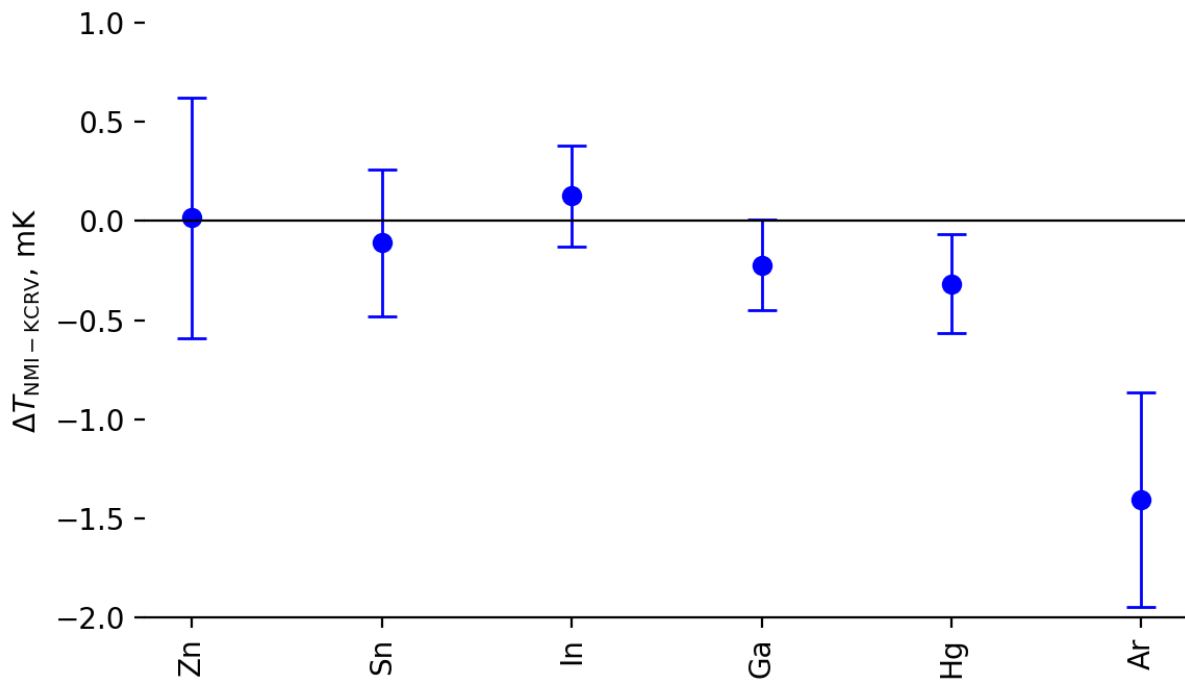


Figure 5.14: Deviation of ΔT_{NMI} from $\bar{\Delta T}$ at each fixed-point measured at NIST.

5.3.9 NMIA

	$\Delta T_{\text{NMI-KCRV}}$ (mK)	$U(\Delta T_{\text{NMI-KCRV}})$ (mK)	$U(\overline{W_1})$ (mK)
Zn	-1.07	0.64	0.41
Sn	-0.21	0.46	0.31
In	-0.04	0.39	0.39
Ga	-0.33	0.35	0.34
Hg	-0.04	0.29	0.27
Ar	-0.36	0.99	0.95

Table 5.16: Deviation from $\overline{\Delta T}$ at each fixed-point measured at NMIA. Uncertainties are displayed at the $k = 2$ level.

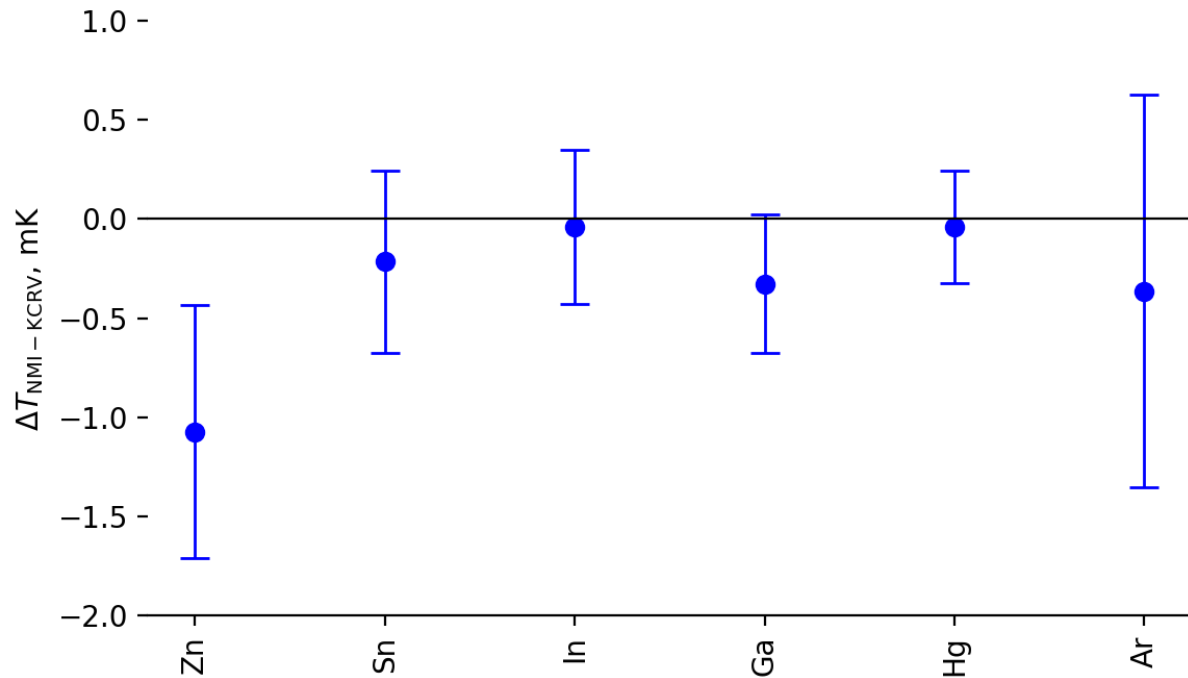


Figure 5.15: Deviation of ΔT_{NMI} from $\overline{\Delta T}$ at each fixed-point measured at NMIA.

5.3.10 NMIJ/AIST

	$\Delta T_{\text{NMI-KCRV}}$ (mK)	$U(\Delta T_{\text{NMI-KCRV}})$ (mK)	$U(\overline{W_1})$ (mK)
Zn	0.19	0.78	0.68
Sn	-0.03	0.53	0.51
In	0.16	0.36	0.34
Ga	-0.24	0.30	0.23
Hg	0.18	0.59	0.70
Ar	0.20	1.30	1.41

Table 5.17: Deviation from $\overline{\Delta T}$ at each fixed-point measured at NMIJ/AIST. Uncertainties are displayed at the $k = 2$ level.

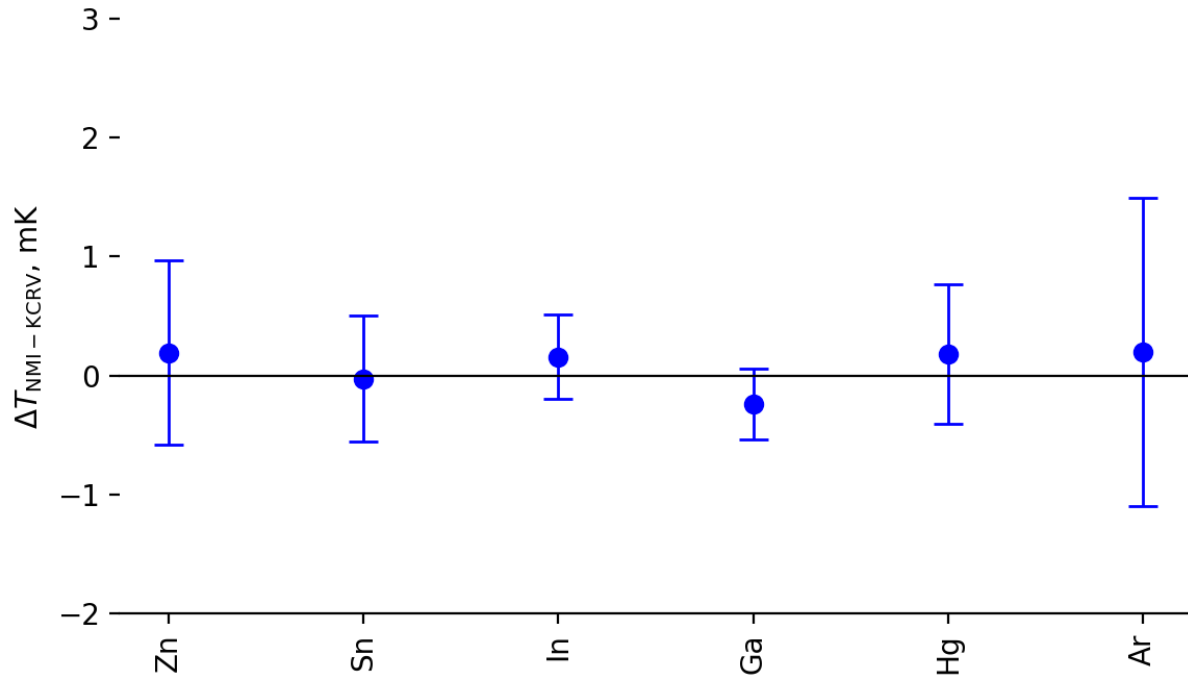


Figure 5.16: Deviation of ΔT_{NMI} from $\overline{\Delta T}$ at each fixed-point measured at NMIJ/AIST.

5.3.11 NPL

	$\Delta T_{\text{NMI-KCRV}}$ (mK)	$U(\Delta T_{\text{NMI-KCRV}})$ (mK)	$U(\overline{W_1})$ (mK)
Zn	-1.78	0.64	0.43
Sn	0.09	0.50	0.25
In	-0.29	0.29	0.24
Ga	-0.06	0.26	0.12
Hg	0.06	0.24	0.18
Ar	0.35	0.66	0.32

Table 5.18: Deviation from $\overline{\Delta T}$ at each fixed-point measured at NPL. Uncertainties are displayed at the $k = 2$ level.

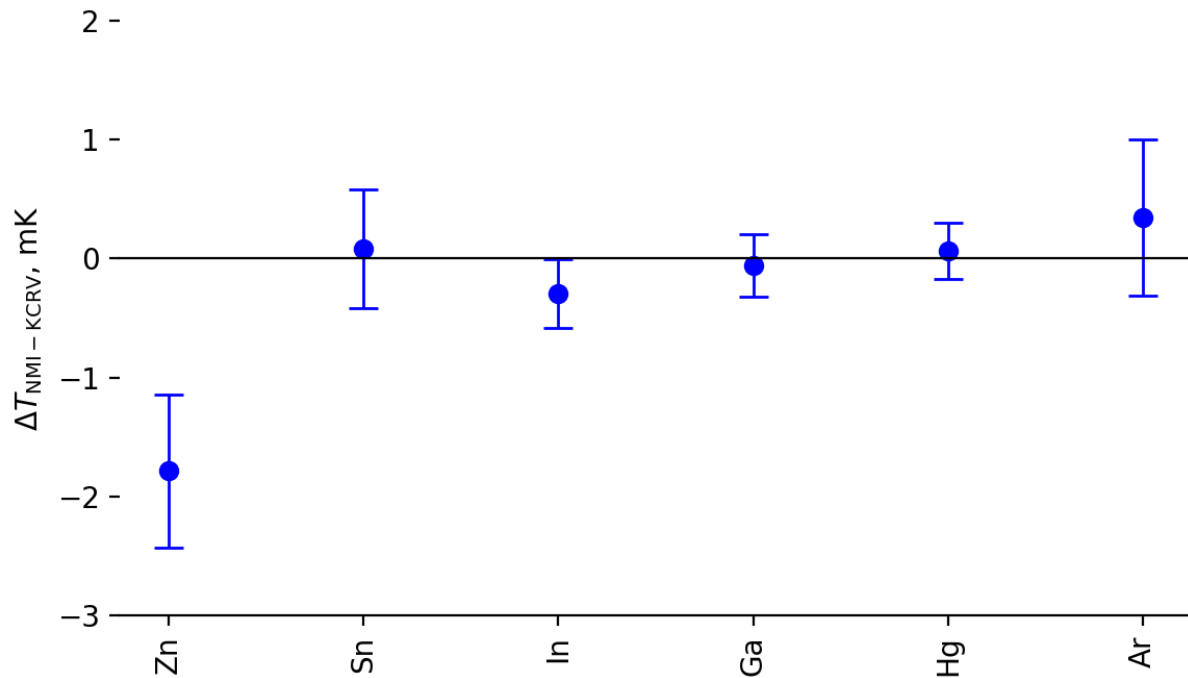


Figure 5.17: Deviation of ΔT_{NMI} from $\overline{\Delta T}$ at each fixed-point measured at NPL.

5.3.12 NRC

	$\Delta T_{\text{NMI-KCRV}}$ (mK)	$U(\Delta T_{\text{NMI-KCRV}})$ (mK)	$U(\overline{W_1})$ (mK)
Zn	0.30	0.75	0.58
Sn	0.65	0.47	0.34
In	0.12	0.29	0.22
Ga	0.12	0.27	0.14
Hg	0.01	0.24	0.18
Ar	-0.06	0.65	0.30

Table 5.19: Deviation from $\overline{\Delta T}$ at each fixed-point measured at NRC. Uncertainties are displayed at the $k = 2$ level.

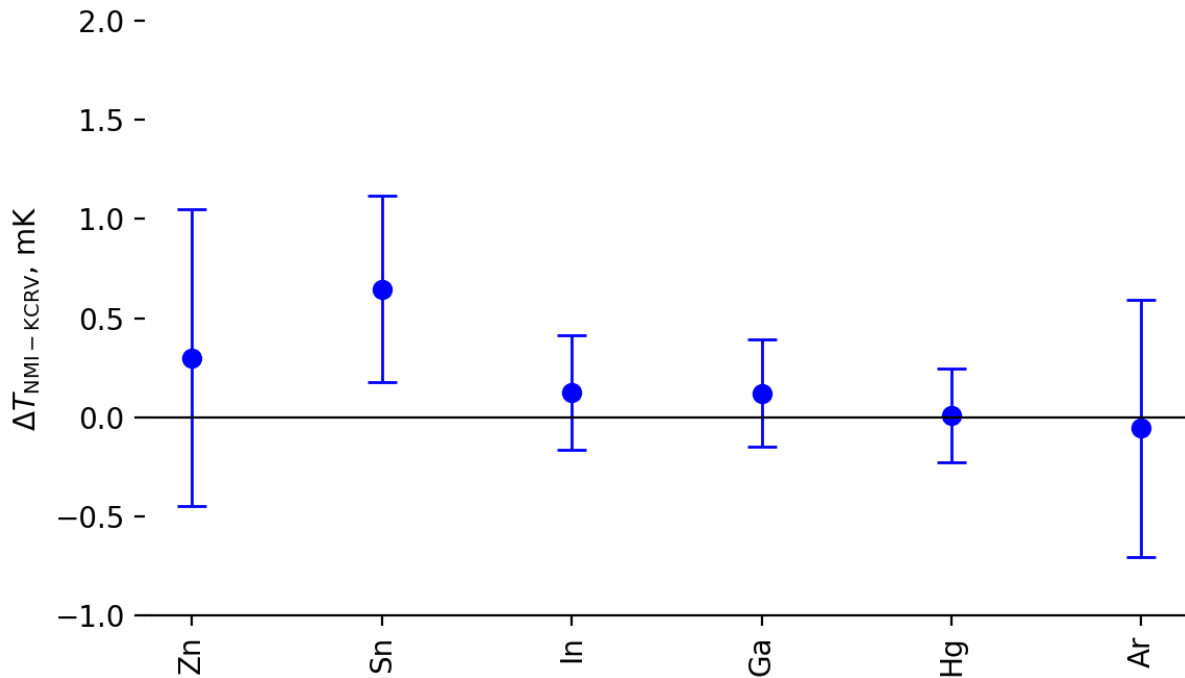


Figure 5.18: Deviation of ΔT_{NMI} from $\overline{\Delta T}$ at each fixed-point measured at NRC.

5.3.13 PTB

	$\Delta T_{\text{NMI-KCRV}}$ (mK)	$U(\Delta T_{\text{NMI-KCRV}})$ (mK)	$U(\overline{W_1})$ (mK)
Zn	1.69	1.23	1.27
Sn	0.28	0.79	0.88
In	0.06	0.75	0.87
Ga	-0.05	0.30	0.22
Hg	0.12	0.29	0.28
Ar	0.10	0.73	0.49

Table 5.20: Deviation from $\overline{\Delta T}$ at each fixed-point measured at PTB. Uncertainties are displayed at the $k = 2$ level.

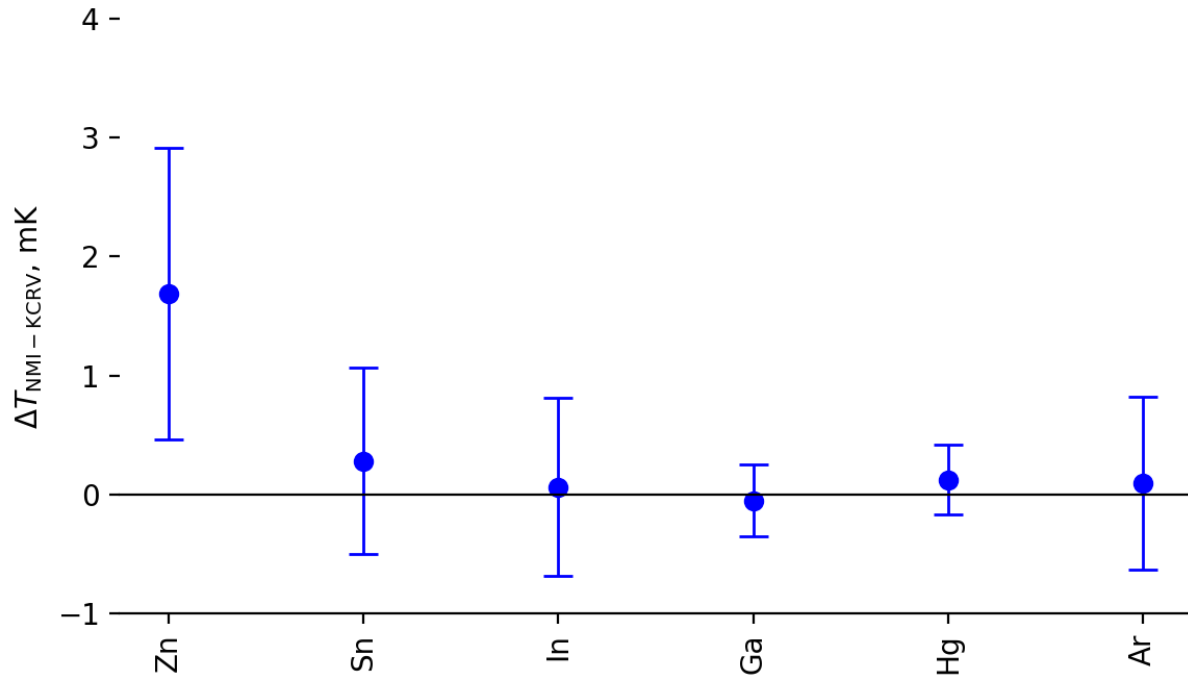


Figure 5.19: Deviation of ΔT_{NMI} from $\overline{\Delta T}$ at each fixed-point measured at PTB.

5.3.14 VSL

	$\Delta T_{\text{NMI-KCRV}}$ (mK)	$U(\Delta T_{\text{NMI-KCRV}})$ (mK)	$U(\overline{W_1})$ (mK)
Zn	2.53	1.04	0.74
Sn	0.54	0.56	0.47
In	-0.02	0.40	0.31
Ga	-0.14	0.36	0.27
Hg	-0.07	0.25	0.22
Ar	-0.82	0.63	0.33

Table 5.21: Deviation from $\overline{\Delta T}$ at each fixed-point measured at VSL. Uncertainties are displayed at the $k = 2$ level.

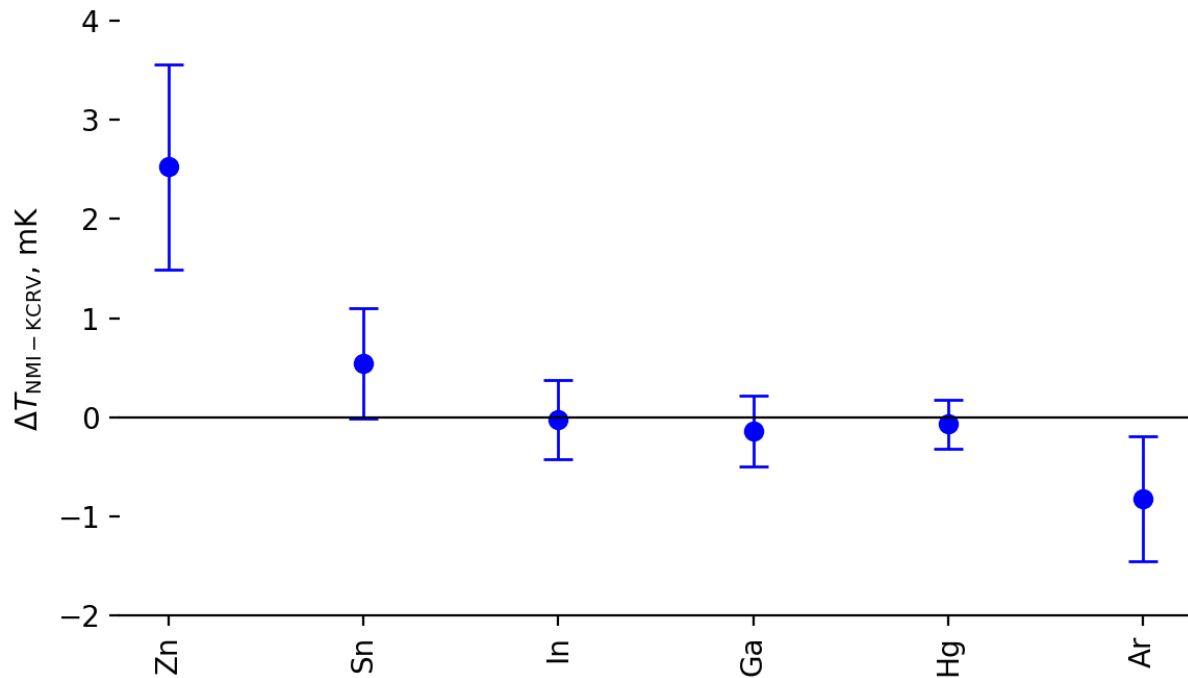


Figure 5.20: Deviation of ΔT_{NMI} from $\overline{\Delta T}$ at each fixed-point measured at VSL.

Appendix A

Original protocol

The original protocol, as distributed to participants, follows.

Key Comparison 9 Protocol

ITS-90 SPRT Calibration from the Ar TP to the Zn FP

Objective: This comparison is designed to compare the realization of the ITS-90 through the calibration of SPRTs. The range of temperature covered in this comparison is from the triple point of Ar (83.8058 K) to the freezing point of Zn (692.677 K). The transfer standards used will be long-stem SPRTs.

Method: Collapsed Star



NMI Participants:

Pilot: NIST, Gregory Strouse, gstrouse@nist.gov

AFRIMETS: NMISA, Hans Liedberg, hliedber@nmisa.org

APMP: KRISS, Inseok Yang, iyang@kriss.re.kr

APMP: NIM, Jianping Sun (孙建平), sunjp@nim.ac.cn

APMP: NMIIJ, Jun Tamba, j-tamba@aist.go.jp

APMP: NMIA, Kim Nguyen, kim.nguyen@measurement.gov.au

COOMET: VNIIM, Anatoly Pokhodun, a.i.pokhodun@vniim.ru

EURAMET: NPL, Helen McEvoy, helen.mcevoy@npl.co.uk

EURAMET: VSL, Andrea Peruzzi, aperuzzi@vsl.nl

EURAMET: PTB, Joachim Fischer, joachim.fischer@ptb.de

EURAMET: INRIM, Peter Steur, p.steur@inrim.it

EURAMET: LNE-INM/CNAM, Yves Hermier, hermier@cnam.fr

SIM: INMETRO, Renato Nunes Teixeira, rnteixeira@inmetro.gov.br

SIM: INTI, Javier Skabar, jskabar@inti.gob.ar

SIM: NRC, Ken Hill, ken.hill@nrc-cnrc.gc.ca

Projected Timeline:

Protocol Agreement	January 31, 2011
Transfer Standards Sent to NIST	March 31, 2011
Transfer Standards Returned to NMIs	September 30, 2011
Transfer Standards Re-Measured by NMIs	December 31, 2011
Draft A Report Completed	March 31, 2012

Participants will supply the following information:

- ◆ 2 ITS-90 calibrated SPRTs
 - NMI participant will select their own SPRTs based on their own criteria for suitability and will convey the selection criteria to the Pilot Laboratory
 - SPRTs must be calibrated by NMI participant before measurements are made by the pilot and then again on return from the pilot
 - SPRTs are to be measured at every available fixed-point over the range of the comparison including the In FP and Ga MP
 - The calibration of SPRTs by an NMI participant is to be performed by either fixed-point cells or by comparison with an ITS-90 calibrated reference SPRT
- ◆ Calibration results supplied in $\bar{W}(FP)$ with all corrections applied by the NMI such that the $\bar{W}(FP)$ values are equivalent to the ITS-90 assigned temperature values for 0 mA. Uncertainties, $u\left[\bar{W}(FP)_{SPRT_i}\right]$, may be specific to each SPRT or a nominal uncertainty may be given for both SPRTs
 - Appendix A gives a reporting worksheet

-
- ◆ The measurement equation used to compute each calibration result with an indication of which inputs vary randomly for each realized equilibrium and which inputs are systematic across all equilibria for each fixed point within this comparison
 - Any quantities in the measurement equation that are a mixture of random and systematic effects for each SPRT should be broken into constituent parts that are either purely random or purely systematic within this comparison.
 - An example of an SPRT measurement is given in Appendix B
 - ◆ Uncertainty budget compliant with CCT WG3 that includes degrees of freedom associated each component
 - A suggested fixed-point cell uncertainty budget is given in Appendix C
 - Sources of uncertainty may be added or deleted as needed
 - An NMI may choose to supply their own uncertainty budget (CMC and WG3 compliant) that includes degrees of freedom for each source of uncertainty
 - Please identify which components of the uncertainty budget are associated with random effects in $\bar{W}(FP)$ and which are associated with systematic effects in $\bar{W}(FP)$ within this comparison.
 - ◆ Heat Flux (Immersion) profile for each fixed-point cell using the SPRTs of this comparison
 - [R(FP), 0 mA] and corresponding [immersion depth (sensor midpoint), cm]
 - ◆ All results and required information will be e-mailed to the NIST statistician
 - Will Guthrie, william.guthrie@nist.gov

If you have questions about any aspect of the protocol or are not sure how to report something that is requested, please contact Greg Strouse and Will Guthrie prior to submitting your report. After reviewing all submitted reports, we will contact you if there is anything that is unclear to us or if any additional information is needed to complete the analysis of the data.

Measurement Matrix for Measurements Made at Pilot Laboratory:

SPRT 1

Batch 1	E1	S1	AP1	C1
Batch 2	E2	S2	AP2	AF1
Batch 3	E3	S3	AP3	E4
Batch 4	E5	N1	AP4	

SPRT 2

Batch 5	E2	S1	AP3	C1
Batch 6	E3	S3	AP2	AF1
Batch 7	E1	S2	AP1	E4
Batch 8	E5	N1	AP4	

Note: RMO numbers assigned to NMI SPRTs by arrival date

Method of Analysis:

The fixed-point realization temperature differences for each NMI from the KCRV will be calculated using the following equations:

$$\Delta T_{NMI-KCRV} = \Delta T_{NMI} - \overline{\Delta T} \text{ based on a KCRV of } \overline{\Delta T} = \frac{1}{15} \sum_{i=1}^{15} \Delta T_{NMI_i}$$

where $\Delta T_{NMI} = \frac{1}{2} (\Delta T_{NMI,SPRT_1} + \Delta T_{NMI,SPRT_2})$, in general, and

$$\Delta T_{NMI,SPRT_i} = \frac{[\bar{W}(FP)_{NMI,SPRT_i} - \bar{W}(FP)_{NIST,SPRT_i}]}{dW_r/dT} + C_{SPRT_i}.$$

C_{SPRT_i} is a term used to account for uncertainty associated with the travel, handling, or stability of each SPRT and is taken to have a value of $C_{SPRT_i} = 0$ and a standard uncertainty, $u(C_{SPRT_i})$, of

$$u(C_{SPRT_i}) = \frac{|\bar{W}(FP)_{NMI,SPRT_i,Post-NIST} - \bar{W}(FP)_{NMI,SPRT_i,Pre-NIST}|}{(dW_r/dT)\sqrt{12}}.$$

The uncertainty for each fixed-point realization temperature difference will be calculated using the following equation:

$$\begin{aligned} u_{NMI-KCRV}^2(k=1) &= u(\Delta T_{NMI})^2 + u(\overline{\Delta T})^2 - 2u(\Delta T_{NMI}\overline{\Delta T}) \\ &= u(\Delta T_{NMI})^2 + u(\overline{\Delta T})^2 - 2u(\Delta T_{NMI})u(\overline{\Delta T})\rho(\Delta T_{NMI}\overline{\Delta T}) \end{aligned}$$

where $u(\Delta T_{NMI})$ is the standard uncertainty of ΔT_{NMI} ,

$u(\overline{\Delta T})$ is the standard uncertainty of $\overline{\Delta T}$,

$u(\Delta T_{NMI}\overline{\Delta T})$ is the covariance of ΔT_{NMI} and $\overline{\Delta T}$, and

$\rho(\Delta T_{NMI}\overline{\Delta T})$ is the correlation of ΔT_{NMI} and $\overline{\Delta T}$

An SPRT cutoff criterion for use in calculating values of ΔT_{NMI} will be used to ensure that uncertainty associated with the travel, handling, or stability of either SPRT does not dominate the standard uncertainty of ΔT_{NMI} . $u(\Delta T_{NMI})$. The cutoff criterion will be based on the statistical agreement between each SPRT's resistance ratios before and after its travel to NIST and the magnitude of $u(C_{SPRT_i})$.

The mathematical definition for the cutoff criterion will be:

$$\left. \begin{aligned} & \frac{\left| \bar{W}(FP)_{NMI, SPRT_i, \text{Post-NIST}} - \bar{W}(FP)_{NMI, SPRT_i, \text{Pre-NIST}} \right|}{(dW_r/dT) \sqrt{u_R \left[\bar{W}(FP)_{NMI, SPRT_i, \text{Post-NIST}} \right]^2 + u_R \left[\bar{W}(FP)_{NMI, SPRT_i, \text{Pre-NIST}} \right]^2}} > t_{0.95, v_{\text{eff}}} \\ & \text{and} \\ & u(C_{SPRT_i}) > \frac{\sqrt{u(\Delta T_{NMI})^2 - u(C_{SPRT_i})^2}}{3} \end{aligned} \right\} \text{Results from } SPRT_i \text{ will not be used}$$

In the cutoff criterion above, $u_R \left[\bar{W}(FP)_{NMI, SPRT_i} \right]$ is the combined standard uncertainty from all sources of random uncertainty for each SPRT and $t_{0.95, v_{\text{eff}}}$ is the appropriate quantile of the Student's t distribution with v_{eff} degrees of freedom needed to compute an approximate 95% confidence interval for the temperature difference observed after travel to and from NIST for each SPRT.

Appendix A: Measurement Reporting Worksheet (active Excel Spreadsheet)

Participating NMI

Before sending SPRTs to Pilot Laboratory

	SPRT 1 $u[\bar{W}(FP)_{SPRT_1}]$, mK	Number of Equilibria Realized*	SPRT 2 $u[\bar{W}(FP)_{SPRT_2}]$, mK	Number of Equilibria Realized*
\bar{W} (Zn)				
\bar{W} (Sn)				
\bar{W} (In)				
\bar{W} (Ga)				
\bar{W} (Hg)				
\bar{W} (Ar)				

Final $R(TPW)$

On return to participating NMI

	SPRT 1 On Receipt $R(TPW)$ <input type="text"/>	SPRT 2 <input type="text"/>
	SPRT 1 $u[\bar{W}(FP)_{SPRT_1}]$, mK	SPRT 2 $u[\bar{W}(FP)_{SPRT_2}]$, mK
\bar{W} (Zn)		
\bar{W} (Sn)		
\bar{W} (In)		
\bar{W} (Ga)		
\bar{W} (Hg)		
\bar{W} (Ar)		

Final $R(TPW)$

Fixed-Point Cell Information**

s/n	Immersion depth, cm	Pressure, kPa
Zn		
Sn		
In		
Ga		
Hg		
Ar		

* or number of comparison measurements

** or supply sufficient information of the comparison method

	Resistance Ratio Bridge Model	Reference Resistor Model	Resistor Enclosure Stability, mK
Measurement System			

Appendix B: Example of an SPRT measurement (active Excel spreadsheet)**

$T_{\text{meas.}}(\text{FP}) = T_{90}(\text{FP}) + \text{pressure correction} + \text{immersion correction}$

$W(\text{FP}) = W_{\text{calc.}}(\text{FP}) + (T_{\text{meas.}} - T_{90}) / dWr/dT$

Before sending SPRTs to Pilot Laboratory

	pressure		immersion	
	correction mK	$u_{\text{correction}}$ mK	correction mK	$u_{\text{correction}}$ mK
\bar{W} (Zn)				
\bar{W} (Sn)				
\bar{W} (In)				
\bar{W} (Ga)				
\bar{W} (Hg)				
\bar{W} (Ar)				

After sending SPRTs to Pilot Laboratory

	pressure		immersion	
	correction mK	$u_{\text{correction}}$ mK	correction mK	$u_{\text{correction}}$ mK
\bar{W} (Zn)				
\bar{W} (Sn)				
\bar{W} (In)				
\bar{W} (Ga)				
\bar{W} (Hg)				
\bar{W} (Ar)				

** or supply sufficient information of the comparison method

Appendix C: Suggested Fixed-Point Cell Uncertainty Budget (active Excel Spreadsheet)**

Participating NMI

Type A	Ar mK	df	Hg mK	df	Ga mK	df	In mK	df	Sn mK	df	Zn mK	Systematic or Random
Phase Transition												
Realization Repeatability												
Total A	0.00		0.00		0.00		0.00		0.00		0.00	
Type B												
Chemical Impurities												
Hydrostatic-head												
Propagated TPW												
SPRT self-heating												
Heat Flux												
Moisture												
Gas pressure												
Slope of Plateau												
Total B	0		0		0		0		0		0	
Combined Standard Uncertainty	0		0		0		0		0		0	
Expanded Uncertainty ($k=2$ level, using effective df)	0.00		0.00		0.00		0.00		0.00		0.00	

** or supply sufficient information of the comparison method

Appendix B

Raw Data tables

B.1 W values and uncertainty

The following tables contain ante-NIST and post-NIST data supplied by each NMI in the “Appendix A: Measurement Reporting Worksheet” from the original K9 protocol, along with the at-NIST measurements performed in Gaithersburg, USA. Columns containing quantities required to calculate the ‘cutoff criteria’ described in Chapter 2 have been added, displaying the total random contribution to the uncertainty and its corresponding degrees of freedom respectively. These quantities were calculated from the uncertainty budgets supplied by each NMI.

Fixed point	SPRT #1				SPRT #2				
	W	u_C (mK)	u_R (mK)	dof	realizations	W	u_C (mK)	u_R (mK)	
Zn	—	—	—	—	—	—	—	—	—
Sn	—	—	—	—	—	—	—	—	—
In	—	—	—	—	—	—	—	—	—
Before NIST	1.1181086	0.160	0.107	1	3	1.1180695	0.160	0.107	1
Ga	—	—	—	—	—	—	—	—	—
Hg	—	—	—	—	—	—	—	—	—
Ar	—	—	—	—	—	—	—	—	—
At NIST	Zn	—	—	—	—	—	—	—	—
	Sn	—	—	—	—	—	—	—	—
	In	—	—	—	—	—	—	—	—
	Ga	1.1181065	—	0.023	—	1	1.1180688	—	0.023
	Hg	—	—	—	—	—	—	—	—
	Ar	—	—	—	—	—	—	—	—
After NIST	Zn	—	—	—	—	—	—	—	—
	Sn	—	—	—	—	—	—	—	—
	In	—	—	—	—	—	—	—	—
	Ga	1.1181083	0.160	0.107	1	3	1.1180696	0.160	0.107
	Hg	—	—	—	—	—	—	—	—
	Ar	—	—	—	—	—	—	—	—

Table B.1: Raw data for BIPM SPRT measurements. Uncertainties correspond to $k = 1$.

Fixed point	SPRT #1				SPRT #2			
	W	u_C (mK)	u_R (mK)	dof realizations	W	u_C (mK)	u_R (mK)	dof realizations
Before NIST	Zn	2.5687284	1.227	1.223	—	1	2.5684806	1.368
	Sn	1.8926961	0.717	0.708	—	1	1.8925510	0.997
	In	1.6097336	0.654	0.645	—	1	1.6096324	0.692
	Ga	1.1181273	0.270	0.254	—	1	1.1181080	0.262
	Hg	0.8441531	0.428	0.418	—	1	0.8441778	0.430
	Ar	0.2159181	0.602	0.598	—	1	0.2160553	0.600
At NIST	Zn	2.5687365	—	0.181	—	1	2.5684853	—
	Sn	1.8927003	—	0.121	—	1	1.8925567	—
	In	1.6097354	—	0.046	—	1	1.6096372	—
	Ga	1.1181242	—	0.023	—	1	1.1181073	—
	Hg	0.8441523	—	0.070	—	1	0.8441781	—
	Ar	0.2159144	—	0.032	—	1	0.2160489	—
After NIST	Zn	2.5687352	1.227	1.223	—	2	2.5684870	1.368
	Sn	1.8926997	0.717	0.708	—	2	1.8925546	0.997
	In	1.6097346	0.654	0.645	—	2	1.6096336	0.692
	Ga	1.1181277	0.270	0.254	—	2	1.1181083	0.262
	Hg	0.8441535	0.428	0.418	—	2	0.8441791	0.430
	Ar	0.2159175	0.602	0.598	—	2	0.2160532	0.600

Table B.2: Raw data for INMETRO SPRT measurements. Uncertainties correspond to $k = 1$.

Fixed point	W	SPRT #1			SPRT #2					
		u_C (mK)	u_R (mK)	dof	realizations	W	u_C (mK)	u_R (mK)	dof	realizations
Zn	-	-	-	-	-	2.5687195	0.420	0.180	-	3
Sn	-	-	-	-	-	1.8926917	0.300	0.200	-	3
In	-	-	-	-	-	1.6097291	0.320	0.150	-	3
Ga	-	-	-	-	-	1.1181263	0.090	0.080	-	3
Hg	-	-	-	-	-	0.8441556	0.060	0.030	-	3
Ar	-	-	-	-	-	0.2159222	0.250	0.190	-	3
Before NIST										
Zn	-	-	-	-	-	2.5687225	-	0.181	-	1
Sn	-	-	-	-	-	1.8926918	-	0.121	-	1
In	-	-	-	-	-	1.6097300	-	0.046	-	1
Ga	-	-	-	-	-	1.1181250	-	0.023	-	1
Hg	-	-	-	-	-	0.8441534	-	0.070	-	1
Ar	-	-	-	-	-	0.2159192	-	0.032	-	1
At NIST										
Zn	-	-	-	-	-	2.5687197	0.440	0.180	-	3
Sn	-	-	-	-	-	1.8926930	0.320	0.200	-	3
In	-	-	-	-	-	1.6097302	0.330	0.150	-	3
Ga	-	-	-	-	-	1.1181259	0.120	0.080	-	3
Hg	-	-	-	-	-	0.8441549	0.070	0.030	-	3
Ar	-	-	-	-	-	0.2159251	0.250	0.190	-	3
After NIST										

Table B.3: Raw data for INRIM SPRT measurements. Uncertainties correspond to $k = 1$.

Fixed point	SPRT #1				SPRT #2				Before NIST
	W	u_C (mK)	u_R (mK)	dof	realizations	W	u_C (mK)	u_R (mK)	
Zn	—	—	—	—	—	2.5687490	1.960	0.328	
Sn	—	—	—	—	—	1.8927055	1.150	0.597	
In	—	—	—	—	—	1.6097400	1.080	0.162	
Ga	—	—	—	—	—	1.1181279	0.440	0.316	
Hg	0.8441674	0.420	0.291	11	2	0.8441534	0.420	0.292	12
Ar	0.2159900	1.060	0.521	7	2	0.2159130	1.060	0.522	7
Zn	2.5685894	—	0.181	—	1	2.5687531	—	0.181	—
Sn	1.8926191	—	0.121	—	1	1.8927098	—	0.121	—
In	1.6096812	—	0.046	—	1	1.6097415	—	0.046	—
Ga	1.1181163	—	0.023	—	1	1.1181279	—	0.023	—
Hg	0.8441658	—	0.070	—	1	0.8441505	—	0.070	—
Ar	0.2159820	—	0.032	—	1	0.2159073	—	0.032	—
Zn	2.5685812	2.150	0.954	19	1	2.5687449	1.960	0.330	11
Sn	1.8926208	1.220	0.713	20	1	1.8927064	1.150	0.600	15
In	1.6096804	1.090	0.180	51	1	1.6097458	1.080	0.162	54
Ga	1.1181183	0.440	0.316	16	1	1.1181309	0.440	0.316	16
Hg	0.8441648	0.430	0.307	14	1	0.8441502	0.420	0.292	12
Ar	0.2159908	1.060	0.522	7	1	0.2159151	1.060	0.522	7

Table B.4: Raw data for INTI SPRT measurements. Uncertainties correspond to $k = 1$.

Fixed point	SPRT #1				SPRT #2				Before NIST
	W	u_C (mK)	u_R (mK)	dof	realizations	W	u_C (mK)	u_R (mK)	
Zn	2.5685577	0.509	0.237	12	3	2.5686243	0.509	0.237	
Sn	1.8925980	0.427	0.148	43	3	1.8926350	0.427	0.148	
In	1.6096650	0.582	0.150	75	3	1.6096898	0.582	0.150	
Ga	1.1181133	0.188	0.118	30	3	1.1181180	0.188	0.118	
Hg	0.8441715	0.223	0.082	74	3	0.8441655	0.223	0.082	
Ar	0.2160184	0.438	0.183	166	3	0.2159871	0.438	0.183	
Zn	2.5685566	—	0.181	—	1	2.5686258	—	0.181	—
Sn	1.8925971	—	0.121	—	1	1.8926356	—	0.121	—
In	1.6096646	—	0.046	—	1	1.6096909	—	0.046	—
Ga	1.1181126	—	0.023	—	1	1.1181175	—	0.023	—
Hg	0.8441711	—	0.070	—	1	0.8441635	—	0.070	—
Ar	0.2160135	—	0.032	—	1	0.2159808	—	0.032	—
Zn	2.5685584	0.509	0.237	12	3	—	—	—	—
Sn	1.8925983	0.427	0.148	43	3	—	—	—	—
In	1.6096656	0.582	0.150	75	3	—	—	—	—
Ga	1.1181131	0.188	0.118	30	3	—	—	—	—
Hg	0.8441715	0.223	0.082	74	3	—	—	—	—
Ar	0.2160181	0.438	0.183	166	3	—	—	—	—

Table B.5: Raw data for KRISS SPRT measurements. Uncertainties correspond to $k = 1$.

Fixed point	SPRT #1				SPRT #2					
	W	u_C (mK)	u_R (mK)	dof	realizations	W	u_C (mK)	u_R (mK)	dof	realizations
Zn	2.5685546	0.520	0.216	197	2	2.5680572	0.520	0.216	197	3
Sn	1.8925961	0.290	0.183	191	3	1.8923152	0.290	0.183	191	3
In	1.6096656	0.280	0.121	79	3	1.6094739	0.280	0.121	79	3
Ga	1.1181106	0.350	0.146	31	3	1.1180734	0.350	0.146	31	3
Hg	0.8441746	0.280	0.113	3	3	0.8442228	0.280	0.113	3	3
Ar	0.2160135	0.341	0.172	11	4	0.2162457	0.341	0.172	11	3
Zn	2.5685520	—	0.181	—	1	2.5680540	—	0.181	—	1
Sn	1.8925948	—	0.121	—	1	1.8923120	—	0.121	—	1
In	1.6096626	—	0.046	—	1	1.6094713	—	0.046	—	1
Ga	1.1181114	—	0.023	—	1	1.1180758	—	0.023	—	1
Hg	0.8441691	—	0.070	—	1	0.8442195	—	0.070	—	1
Ar	0.2160102	—	0.032	—	1	0.2162439	—	0.032	—	1
Zn	2.5685549	0.570	0.324	99	4	2.5680567	0.570	0.324	99	4
Sn	1.8925945	0.320	0.222	116	6	1.8923128	0.320	0.222	116	5
In	1.6096641	0.280	0.117	280	4	1.6094728	0.280	0.117	280	4
Ga	1.1181125	0.130	0.109	53	6	1.1180758	0.130	0.109	53	5
Hg	0.8441759	0.269	0.087	8	3	0.8442247	0.269	0.087	8	3
Ar	0.2160124	0.370	0.212	14	4	0.2162477	0.370	0.212	14	3

Table B.6: Raw data for LNE-CNAM SPRT measurements. Uncertainties correspond to $k = 1$.

Fixed point	SPRT #1				SPRT #2				Before NIST
	W	u_C (mK)	u_R (mK)	dof	realizations	W	u_C (mK)	u_R (mK)	
Zn	2.5687780	0.320	0.100	6	3	2.5686731	0.320	0.100	
Sn	1.8927250	0.270	0.100	6	3	1.8926673	0.270	0.100	
In	1.6097524	0.240	0.100	6	2	1.6097126	0.240	0.100	
Ga	1.1181315	0.180	0.070	6	2	1.1181235	0.180	0.070	
Hg	0.8441500	0.150	0.050	6	2	0.8441600	0.150	0.050	
Ar	0.2158901	0.170	0.040	6	2	0.2159477	0.170	0.040	
Zn	2.5687750	—	0.181	—	1	2.5686754	—	0.181	At NIST
Sn	1.8927223	—	0.121	—	1	1.8926663	—	0.121	
In	1.6097511	—	0.046	—	1	1.6097126	—	0.046	
Ga	1.1181285	—	0.023	—	1	1.1181214	—	0.023	
Hg	0.8441457	—	0.070	—	1	0.8441579	—	0.070	
Ar	0.2158893	—	0.032	—	1	0.2159471	—	0.032	
Zn	2.5687766	0.320	0.100	6	3	2.5686721	0.320	0.100	After NIST
Sn	1.8927244	0.270	0.100	6	3	1.8926663	0.270	0.100	
In	1.6097513	0.240	0.100	6	3	1.6097119	0.240	0.100	
Ga	1.1181300	0.180	0.070	6	4	1.1181225	0.180	0.070	
Hg	0.8441492	0.150	0.050	6	4	0.8441600	0.150	0.050	
Ar	0.2158897	0.170	0.040	6	5	0.2159475	0.170	0.040	

Table B.7: Raw data for NIM SPRT measurements. Uncertainties correspond to $k = 1$.

Fixed point	SPRT #1				SPRT #2				realizations
	W	u_C (mK)	u_R (mK)	dof	realizations	W	u_C (mK)	u_R (mK)	
Before NIST	Zn	2.5687664	0.254	0.181	—	1	2.5687661	0.254	0.181
	Sn	1.8927182	0.141	0.121	—	1	1.8927175	0.141	0.121
	In	1.6097484	0.089	0.046	—	1	1.6097492	0.089	0.046
	Ga	1.1181345	0.037	0.023	—	1	1.1181353	0.037	0.023
	Hg	0.8441560	0.077	0.070	—	1	0.8441542	0.077	0.070
	Ar	0.2159041	0.070	0.032	—	1	0.2159039	0.070	0.032
At NIST	Zn	2.5687667	—	0.181	—	1	2.5687668	—	0.181
	Sn	1.8927178	—	0.121	—	1	1.8927180	—	0.121
	In	1.6097489	—	0.046	—	1	1.6097494	—	0.046
	Ga	1.1181354	—	0.023	—	1	1.1181352	—	0.023
	Hg	0.8441562	—	0.070	—	1	0.8441562	—	0.070
	Ar	0.2159070	—	0.032	—	1	0.2159042	—	0.032
After NIST	Zn	2.5687657	0.254	0.181	—	1	2.5687659	0.254	0.181
	Sn	1.8927178	0.141	0.121	—	1	1.8927184	0.141	0.121
	In	1.6097493	0.089	0.046	—	1	1.6097498	0.089	0.046
	Ga	1.1181360	0.037	0.023	—	1	1.1181360	0.037	0.023
	Hg	0.8441561	0.077	0.070	—	1	0.8441566	0.077	0.070
	Ar	0.2159059	0.070	0.032	—	1	0.2159035	0.070	0.032

Table B.8: Raw data for NIST SPRT measurements. Uncertainties correspond to $k = 1$.

Fixed point	SPRT #1				SPRT #2					
	W	u_C (mK)	u_R (mK)	dof	realizations	W	u_C (mK)	u_R (mK)	dof	realizations
Before NIST	Zn	2.5687669	0.254	0.181	—	1	—	—	—	—
	Sn	1.8927178	0.141	0.121	—	1	—	—	—	—
	In	1.6097495	0.089	0.046	—	1	—	—	—	—
	Ga	1.1181365	0.037	0.023	—	1	—	—	—	—
	Hg	0.8441571	0.077	0.070	—	1	—	—	—	—
	Ar	0.2159041	0.070	0.032	—	1	—	—	—	—
At NIST	Zn	2.5687680	—	0.181	—	1	—	—	—	—
	Sn	1.8927185	—	0.121	—	1	—	—	—	—
	In	1.6097489	—	0.046	—	1	—	—	—	—
	Ga	1.1181366	—	0.023	—	1	—	—	—	—
	Hg	0.8441560	—	0.070	—	1	—	—	—	—
	Ar	0.2159096	—	0.032	—	1	—	—	—	—
After NIST	Zn	2.5687683	0.254	0.181	—	1	—	—	—	—
	Sn	1.8927177	0.141	0.121	—	1	—	—	—	—
	In	1.6097493	0.089	0.046	—	1	—	—	—	—
	Ga	1.1181364	0.037	0.023	—	1	—	—	—	—
	Hg	0.8441621	0.077	0.070	—	1	—	—	—	—
	Ar	0.2159041	0.070	0.032	—	1	—	—	—	—

Table B.9: Raw data for NIST SPRT measurements. Uncertainties correspond to $k = 1$.

Fixed point	SPRT #1				SPRT #2					
	W	u_C (mK)	u_R (mK)	dof	realizations	W	u_C (mK)	u_R (mK)	dof	realizations
Zn	2.5688588	0.205	0.015	—	4	2.5688349	0.225	0.015	—	4
Sn	1.8927710	0.158	0.014	—	4	1.8927571	0.193	0.014	—	4
In	1.6097831	0.194	0.014	—	4	1.6097735	0.192	0.014	—	4
Ga	1.1181351	0.169	0.013	—	4	1.1181336	0.135	0.013	—	4
Hg	0.8441409	0.138	0.013	—	4	0.8441437	0.136	0.013	—	4
Ar	0.2158628	0.475	0.012	—	4	0.2158763	0.474	0.012	—	4
Zn	2.5688622	—	0.181	—	1	2.5688394	—	0.181	—	1
Sn	1.8927713	—	0.121	—	1	1.8927565	—	0.121	—	1
In	1.6097837	—	0.046	—	1	1.6097740	—	0.046	—	1
Ga	1.1181354	—	0.023	—	1	1.1181342	—	0.023	—	1
Hg	0.8441404	—	0.070	—	1	0.8441423	—	0.070	—	1
Ar	0.2158603	—	0.032	—	1	0.2158733	—	0.032	—	1
Zn	2.5688579	0.205	0.015	—	4	2.5688339	0.225	0.015	—	4
Sn	1.8927691	0.158	0.014	—	4	1.8927563	0.195	0.014	—	4
In	1.6097839	0.194	0.014	—	4	1.6097730	0.191	0.014	—	4
Ga	1.1181354	0.169	0.013	—	4	1.1181336	0.135	0.013	—	4
Hg	0.8441409	0.138	0.013	—	4	0.8441439	0.135	0.013	—	4
Ar	0.2158604	0.475	0.012	—	4	0.2158752	0.475	0.012	—	4

Table B.10: Raw data for NMIA SPRT measurements. Uncertainties correspond to $k = 1$.

Fixed point	SPRT #1				SPRT #2			
	W	u_C (mK)	u_R (mK)	dof realizations	W	u_C (mK)	u_R (mK)	dof realizations
Before NIST	Zn 2.5688167	0.339	0.032	8	4	2.5688645	0.346	0.072
	Sn 1.8927428	0.265	0.065	4	4	1.8927718	0.264	0.058
	In 1.6097642	0.165	0.033	5	4	1.6097840	0.166	0.040
	Ga 1.1181313	0.116	0.015	9	4	1.1181355	0.116	0.012
	Hg 0.8441473	0.348	0.025	4	4	0.8441418	0.345	0.014
	Ar 0.2158900	0.696	0.050	2	3	0.2158644	0.709	0.050
At NIST	Zn 2.5688161	—	0.181	—	1	2.5688650	—	0.181
	Sn 1.8927430	—	0.121	—	1	1.8927718	—	0.121
	In 1.6097639	—	0.046	—	1	1.6097841	—	0.046
	Ga 1.1181313	—	0.023	—	1	1.1181357	—	0.023
	Hg 0.8441454	—	0.070	—	1	0.8441400	—	0.070
	Ar 0.2158847	—	0.032	—	1	0.2158611	—	0.032
After NIST	Zn 2.5688168	0.345	0.052	9	4	2.5688642	0.349	0.043
	Sn 1.8927431	0.273	0.100	4	4	1.8927722	0.253	0.052
	In 1.6097646	0.185	0.062	5	4	1.6097844	0.167	0.036
	Ga 1.1181316	0.118	0.027	12	4	1.1181354	0.095	0.016
	Hg 0.8441474	0.350	0.038	8	4	0.8441418	0.347	0.019
	Ar 0.2158904	0.717	0.050	2	3	0.2158640	0.690	0.050

Table B.11: Raw data for NMIJ/AIST SPRT measurements. Uncertainties correspond to $k = 1$.

Fixed point	SPRT #1				SPRT #2			
	W	u_C (mK)	u_R (mK)	dof realizations	W	u_C (mK)	u_R (mK)	dof realizations
Before NIST	Zn	2.5686000	0.223	0.105	8	3	2.5685731	0.223
	Sn	1.8926293	0.144	0.078	8	3	1.8926127	0.144
	In	1.6096856	0.145	0.080	8	3	1.6096747	0.145
	Ga	1.1181170	0.069	0.040	8	3	1.1181149	0.069
	Hg	0.8441658	0.095	0.040	9	3	0.8441685	0.095
	Ar	0.2159828	0.158	0.027	8	3	0.2159938	0.158
	Zn	2.5686077	—	0.181	—	1	2.5685793	—
At NIST	Sn	1.8926283	—	0.121	—	1	—	—
	In	1.6096868	—	0.046	—	1	1.6096763	—
	Ga	1.1181162	—	0.023	—	1	1.1181146	—
	Hg	0.8441645	—	0.070	—	1	0.8441673	—
	Ar	0.2159762	—	0.032	—	1	0.2159906	—
	Zn	2.5685997	0.279	0.180	5	3	2.5685736	0.279
	Sn	1.8926283	0.140	0.058	5	3	1.8926126	0.140
After NIST	In	1.6096854	0.124	0.058	5	3	1.6096749	0.124
	Ga	1.1181172	0.073	0.033	6	3	1.1181153	0.073
	Hg	0.8441660	0.093	0.024	6	3	0.8441687	0.093
	Ar	0.2159828	0.193	0.113	7	4	0.2159941	0.193
	Zn	2.5685997	—	—	—	—	0.181	—
	Sn	1.8926283	—	—	—	—	—	—
	In	1.6096854	—	—	—	—	0.046	—

Table B.12: Raw data for NPL SPRT measurements. Uncertainties correspond to $k = 1$.

Fixed point	SPRT #1				SPRT #2			
	W	u_C (mK)	u_R (mK)	dof realizations	W	u_C (mK)	u_R (mK)	dof realizations
Before NIST	Zn 2.5674577	0.295	0.050	10	3	2.5685350	0.295	0.050
	Sn 1.8919779	0.231	0.170	10	3	1.8925851	0.231	0.170
	In 1.6092414	0.143	0.100	10	3	1.6096557	0.143	0.100
	Ga 1.1180323	0.126	0.110	10	4	1.1181126	0.126	0.110
	Hg 0.8442790	0.103	0.055	10	4	0.8441737	0.103	0.055
	Ar 0.2165675	0.155	0.044	10	5	0.2160256	0.155	0.044
	Zn 2.5674563	—	0.181	—	1	2.5685346	—	0.181
At NIST	Sn 1.8919750	—	0.121	—	1	1.8925812	—	0.121
	In 1.6092408	—	0.046	—	1	1.6096557	—	0.046
	Ga 1.1180311	—	0.023	—	1	1.1181109	—	0.023
	Hg 0.8442783	—	0.070	—	1	0.8441723	—	0.070
	Ar 0.2165632	—	0.032	—	1	0.2160232	—	0.032
	Zn 2.5674545	0.295	0.050	10	3	2.5685359	0.295	0.050
	Sn 1.8919750	0.231	0.170	10	3	1.8925849	0.231	0.170
After NIST	In 1.6092408	0.143	0.100	10	3	1.6096557	0.143	0.100
	Ga 1.1180326	0.126	0.110	10	4	1.1181121	0.126	0.110
	Hg 0.8442795	0.103	0.055	10	3	0.8441737	0.103	0.055
	Ar 0.2165670	0.155	0.044	10	2	0.2160256	0.155	0.044

Table B.13: Raw data for NRC SPRT measurements. Uncertainties correspond to $k = 1$.

Fixed point	SPRT #1				SPRT #2			
	W	u_C (mK)	u_R (mK)	dof realizations	W	u_C (mK)	u_R (mK)	dof realizations
Zn	2.5683498	0.650	0.140	—	2.5688460	0.650	0.140	—
Sn	1.8924797	0.450	0.100	—	1.8927607	0.450	0.100	—
In	1.6095850	0.450	0.130	—	1.6097754	0.450	0.130	—
Ga	1.1180979	0.120	0.060	—	1.1181345	0.120	0.060	—
Hg	0.8441932	0.150	0.050	—	0.8441438	0.150	0.050	—
Ar	0.2161150	0.260	0.100	—	0.2158714	0.260	0.100	—
Zn	2.5683486	—	0.181	—	1	2.5688403	—	0.181
Sn	1.8924789	—	0.121	—	1	1.8927587	—	0.121
In	1.6095847	—	0.046	—	1	1.6097750	—	0.046
Ga	1.1180974	—	0.023	—	1	1.1181336	—	0.023
Hg	0.8441914	—	0.070	—	1	0.8441422	—	0.070
Ar	0.2161107	—	0.032	—	1	0.2158684	—	0.032
Zn	—	—	—	—	2.5688451	0.650	0.140	—
Sn	1.8924802	0.450	0.100	—	1.8927597	0.450	0.100	—
In	1.6095842	0.450	0.130	—	1.6097746	0.450	0.130	—
Ga	1.1180981	0.120	0.060	—	1.1181343	0.120	0.060	—
Hg	0.8441930	0.150	0.050	—	0.8441437	0.150	0.050	—
Ar	0.2161143	0.260	0.100	—	0.2158731	0.260	0.100	—

Table B.14: Raw data for PTB SPRT measurements. Uncertainties correspond to $k = 1$.

Fixed point	SPRT #1				SPRT #2				
	W	u_C (mK)	u_R (mK)	dof	realizations	W	u_C (mK)	u_R (mK)	
Before NIST	Zn	2.5686691	0.367	0.039	7	6	2.5684333	0.685	0.181
	Sn	1.8926613	0.250	0.119	4	5	1.8925252	0.288	0.110
	In	1.6097074	0.161	0.087	4	5	1.6096145	0.173	0.097
	Ga	1.1181208	0.158	0.104	4	5	1.1181030	0.160	0.098
	Hg	0.8441607	0.115	0.029	2	3	0.8441840	0.102	0.024
	Ar	0.2159540	0.438	0.424	5	3	0.2160758	0.115	0.029
At NIST	Zn	2.5686569	—	0.181	—	1	2.5684275	—	0.181
	Sn	1.8926570	—	0.121	—	1	1.8925249	—	0.121
	In	1.6097051	—	0.046	—	1	1.6096158	—	0.046
	Ga	1.1181195	—	0.023	—	1	1.1181029	—	0.023
	Hg	0.8441599	—	0.070	—	1	0.8441831	—	0.070
	Ar	0.2159536	—	0.032	—	1	0.2160767	—	0.032
After NIST	Zn	2.5686673	0.380	0.038	7	5	2.5684317	0.736	0.306
	Sn	1.8926600	0.277	0.136	4	4	1.8925262	0.325	0.160
	In	1.6097046	0.181	0.073	6	5	1.6096138	0.192	0.085
	Ga	1.1181201	0.157	0.044	7	5	1.1181024	0.163	0.043
	Hg	0.8441608	0.111	0.023	2	7	0.8441840	0.098	0.017
	Ar	0.2159536	0.128	0.061	5	3	0.2160769	0.127	0.057

Table B.15: Raw data for VSL SPRT measurements. Uncertainties correspond to $k = 1$.

Appendix C

Uncertainty budgets

This section contains the uncertainty budgets submitted (“Appendix C: Suggested Fixed-Point Cell Uncertainty Budget” in the original K9 protocol) by each NMI. In the first table for each NMI, individual components are enumerated and identified as:

- (i) Type A or
- (ii) Type B

and also as

- (i) Random (R) or
- (ii) Systemmatic (S)

In cases where the submitted budget only denoted uncertainty type, we assumed Type A components to be random and Type B components to be systematic.

The second table(s) for each NMI detail the quantitative contributions of each uncertainty component at each fixed point. In this table, the component names have been truncated to save space; readers are directed to the first table for the full names of each component. In some cases, we identified minor inconsistencies in the reported combined uncertainties, likely due to rounding in the budget forwarded to NIST. We have presented the budgets as they were provided to NIST, rather than recalculating combined uncertainties or degrees of freedom. The final row of this table displays the expanded combined uncertainty at $k = 2$.

A dash represents a value that was not supplied.

Component	Type	Systematic/Random
typical statistical uncertainty of the phase transition realization (including bridge noise and short term resistor stability)	A	R
chemical impurities and evolution of thermometer well	B	R
immersion depth correction	B	R
heat flux	B	S
fixed point realization (including slope)	B	R
isotopic correction	B	S
precision and linearity of resistance bridge	B	S
precision of standard resistor	B	S
SPRT oxidation	B	S
SPRT moisture	B	S
SPRT self-heating correction	B	R
Propagated TPW	-	-

Table C.1: Uncertainty budget components at BIPM.

	Type	Ar mK	dof	Hg mK	dof	Ga mK	dof	In mK	dof	Sn mK	dof	Zn mK	dof
typical...	A	-	-	-	-	0.010	12	-	-	-	-	-	-
chemical...	B	-	-	-	-	0.035	1	-	-	-	-	-	-
immersion depth...	B	-	-	-	-	0.007	1	-	-	-	-	-	-
heat flux	B	-	-	-	-	0.030	1	-	-	-	-	-	-
fixed point...	B	-	-	-	-	0.100	1	-	-	-	-	-	-
isotopic correction	B	-	-	-	-	0	1	-	-	-	-	-	-
precision and...	B	-	-	-	-	0.050	1	-	-	-	-	-	-
precision of...	B	-	-	-	-	0.013	1	-	-	-	-	-	-
SPRT oxidation	B	-	-	-	-	0.005	1	-	-	-	-	-	-
SPRT moisture	B	-	-	-	-	0.020	1	-	-	-	-	-	-
SPRT self-heating...	B	-	-	-	-	0.005	1	-	-	-	-	-	-
Propagated TPW	-	-	-	-	-	0.115	3	-	-	-	-	-	-
Total type A	A	-	-	-	-	0.01	-	-	-	-	-	-	-
Total type B	B	-	-	-	-	0.12	-	-	-	-	-	-	-
Combined standard...	-	-	-	-	-	0.16	5	-	-	-	-	-	-
Expanded...	-	-	-	-	-	0.32	-	-	-	-	-	-	-

Table C.2: Uncertainty budget at BIPM.

Component	Type	Systematic/Random
Phase Transition Realization Repeatability	A	R
Chemical Impurities	B	R
Hydrostatic-head	B	S
Propagated TPW	B	R
SPRT self-heating	B	S
Heat Flux	B	R
Bridge Linearity	B	R
Standard Resistor	B	R
Gas pressure	B	R
Slope of Plateau	B	R
R(TPW) Stability	B	R

Table C.3: Uncertainty budget components at INMETRO.

	Type	Ar	Hg	Ga	In	Sn	Zn						
Phase Transition...		mK	dof										
Chemical Impurities	B	0.003	32	0.005	36	0.003	65	0.004	68	0.004	73	0.005	67
Hydrostatic-head	B	0.550	∞	0.380	∞	0.110	∞	0.540	∞	0.570	∞	1.100	∞
Propagated TPW	B	0.019	∞	0.041	∞	0.007	∞	0.019	∞	0.013	∞	0.016	∞
SPRT self-heating	B	0.026	∞	0.100	∞	0.133	∞	0.191	∞	0.225	∞	0.305	∞
Heat Flux	B	0.068	∞	0.084	∞	0.091	∞	0.109	∞	0.112	∞	0.102	∞
Bridge Linearity	B	0.032	∞	0.050	∞	0.063	∞	0.048	∞	0.148	∞	0.080	∞
Standard Resistor	B	0.016	∞	0.068	∞	0.092	∞	0.138	∞	0.166	∞	0.239	∞
Gas pressure	B	0	∞	0	∞	0.029	∞	0.070	∞	0.047	∞	0.061	∞
Slope of Plateau	B	0.230	∞	0.110	∞	0.140	∞	0.200	∞	0.080	∞	0.190	∞
R(TPW) Stability	B	0.010	∞	0.010	∞	0.021	∞	0.134	∞	0.249	∞	0.280	∞
Total A	A	0.00	32	0.01	36	0.00	65	0.00	68	0.00	73	0.01	67
Total B	B	0.60	∞	0.43	∞	0.27	∞	0.65	∞	0.72	∞	1.23	∞
Combined Standard...		0.60	∞	0.43	∞	0.27	∞	0.65	∞	0.72	∞	1.23	∞
Expanded...		1.20	-	0.86	-	0.54	-	1.31	-	1.43	-	2.45	-

Table C.4: Uncertainty budget at INMETRO for SPRT 1.

	Type	Ar	Hg	Ga	In	Sn	Zn
Phase Transition...		mK dof					
Chemical Impurities	B	0.005 32	0.002 69	0.003 63	0.005 70	0.005 66	0.007 70
Hydrostatic-head	B	0.550 ∞	0.380 ∞	0.110 ∞	0.540 ∞	0.570 ∞	1.100 ∞
Propagated TPW	B	0.019 ∞	0.041 ∞	0.007 ∞	0.019 ∞	0.013 ∞	0.016 ∞
SPRT self-heating	B	0.025 ∞	0.100 ∞	0.132 ∞	0.190 ∞	0.223 ∞	0.303 ∞
Heat Flux	B	0.016 ∞	0.026 ∞	0.032 ∞	0.062 ∞	0.063 ∞	0.050 ∞
Bridge Linearity	B	0.032 ∞	0.099 ∞	0.078 ∞	0.270 ∞	0.750 ∞	0.658 ∞
Standard Resistor	B	0.017 ∞	0.069 ∞	0.092 ∞	0.138 ∞	0.166 ∞	0.239 ∞
Gas pressure	B	0 ∞	0 ∞	0.029 ∞	0.070 ∞	0.047 ∞	0.061 ∞
Slope of Plateau	B	0.230 ∞	0.110 ∞	0.140 ∞	0.200 ∞	0.080 ∞	0.190 ∞
R(TPW) Stability	B	0.030 ∞	0.008 ∞	0.041 ∞	0.081 ∞	0.108 ∞	0.164 ∞
Total A	A	0.01 32	0.00 69	0.00 64	0.01 70	0.01 67	0.01 70
Total B	B	0.60 ∞	0.43 ∞	0.26 ∞	0.69 ∞	1.00 ∞	1.37 ∞
Combined Standard...		0.60 ∞	0.43 ∞	0.26 ∞	0.69 ∞	1.00 ∞	1.37 ∞
Expanded...		1.20 -	0.86 -	0.52 -	1.38 -	1.99 -	2.74 -

Table C.5: Uncertainty budget at INMETRO for SPRT 2.

Component	Type	Systematic/Random
Phase Transition Realization Repeatability	A	R
Bridge (repeatability, non-linearity, AC quadrature)	A	S
Reference Resistor Stability	A	S
Chemical Impurities	B	S
Hydrostatic-head	B	S
Propagated TPW	B	S
SPRT self-heating	B	S
Heat Flux	B	S
Moisture	B	-
SPRT Pt Oxidation	B	-
Gas pressure	B	S
Slope of Plateau	B	S

Table C.6: Uncertainty budget components at INRIM.

	Type	Ar	Hg	Ga	In	Sn	Zn		
	mK	dof	mK	dof	mK	dof	mK	dof	
Phase Transition... Bridge... Reference...	A	0.190	3	0.030	3	0.080	3	0.150	3
	A	0.020	40	0.020	40	0.020	40	0.020	40
	A	0.010	∞	0.010	∞	0.010	∞	0.010	∞
Chemical Impurities	B	0.028	-	0.010	-	0.008	-	0.270	-
Hydrostatic-head	B	0.012	-	0.036	-	0.004	-	0.012	-
Propagated TPW	B	0.018	-	0.051	-	0.067	-	0.094	-
SPRT self-heating	B	0.010	-	0.006	-	0.020	-	0.010	-
Heat Flux	B	0.115	-	0.010	-	0.060	-	0.010	-
Moisture	B	-	-	-	-	-	-	-	-
SPRT Pt Oxidation	B	-	-	-	-	-	-	-	-
Gas pressure	B	-	-	-	-	0.010	-	0.010	-
Slope of Plateau	B	0.115	-	0.003	-	0.005	-	0.060	-
Total A	A	0.19	-	0.04	-	0.08	-	0.15	-
Total B	B	0.17	-	0.06	-	0.09	-	0.29	-
Combined Standard...		0.25	-	0.07	-	0.12	-	0.33	-
Expanded...		0.51	-	0.15	-	0.25	-	0.66	-

Table C.7: Uncertainty budget at INRIM.

Component	Type	Systematic/Random
Reading Repeatability	A	R
Slope of Plateau	A	S
Repeatability of Phase Transition	A	R
SPRT self-heating	A	S
Chemical Impurities	B	S
Hydrostatic-head	B	S
Propagated TPW	B	S
Heat Flux	B	S
Bridge error	B	R
Reference Resistor Stability	B	R
Gas pressure	B	S

Table C.8: Uncertainty budget components at INTI.

	Type	Ar	Hg	Ga	In	Sn	Zn
	mK	dof	mK	dof	mK	dof	mK
Reading...	A	0.035	11	0.017	15	-	-
Slope of Plateau	A	0.866	7	0.058	11	-	-
Repeatability of...	A	0.520	7	0.289	11	-	-
SPRT self-heating	A	0.095	5	0.027	7	-	-
Chemical Impurities	B	0.290	50	0.250	50	-	-
Hydrostatic-head	B	0.040	50	0.080	50	-	-
Propagated TPW	B	0.031	50	0.131	50	-	-
Heat Flux	B	0.076	50	0.020	50	-	-
Bridge error	B	0.027	50	0.029	50	-	-
Reference...	B	0.001	50	0.005	50	-	-
Gas pressure	B	-	-	0.010	50	-	-
Total A	A	1.01	-	0.30	-	-	-
Total B	B	0.31	-	0.30	-	-	-
Combined Standard...		1.06	14	0.42	43	-	-
Expanded...		2.29	-	0.84	-	-	-

Table C.9: Uncertainty budget at INTI for SPRT 1 Ante-NIST.

	Type	Ar	Hg	Ga	In	Sn	Zn
	mK	dof	mK	mK	dof	mK	dof
Reading...							
Slope of Plateau	A	0.045	11	0.100	15	0.053	13
	A	0.866	7	0.058	11	0.144	11
Repeatability of...	A	0.520	7	0.289	11	0.289	8
SPRT self-heating	A	0.061	5	0.037	5	0.034	6
Chemical Impurities	B	0.290	50	0.250	50	0.200	50
Hydrostatic-head	B	0.040	50	0.080	50	0.010	50
Propagated TPW	B	0.032	50	0.136	50	0.185	50
Heat Flux	B	0.020	50	0.020	50	0.010	50
Bridge error	B	0.027	50	0.029	50	0.117	50
Reference...	B	0.001	50	0.005	50	0.006	50
Gas pressure	B	-	0.010	50	0.010	50	0.630
Total A	A	1.01	-	0.31	-	0.33	-
Total B	B	0.30	-	0.30	-	0.30	-
Combined Standard...		1.06	14	0.43	48	0.44	53
Expanded...		2.28	-	0.87	-	0.89	-
						2.15	-
						2.41	-
						4.27	-

Table C.10: Uncertainty budget at INTI for SPRT 1 Post-NIST.

	Type	Ar	Hg	Ga	In	Sn	Zn
	mK	dof	mK	mK	dof	mK	dof
Reading...							
Slope of Plateau	A	0.045	11	0.034	15	0.053	13
	A	0.866	7	0.058	11	0.144	11
Repeatability of...	A	0.520	7	0.289	11	0.289	8
SPRT self-heating	A	0.061	5	0.037	5	0.034	6
Chemical Impurities	B	0.290	50	0.250	50	0.200	50
Hydrostatic-head	B	0.040	50	0.080	50	0.010	50
Propagated TPW	B	0.032	50	0.136	50	0.185	50
Heat Flux	B	0.020	50	0.020	50	0.010	50
Bridge error	B	0.027	50	0.029	50	0.117	50
Reference...	B	0.001	50	0.005	50	0.006	50
Gas pressure	B	-	0.010	50	0.010	50	0.630
Total A	A	1.01	-	0.30	-	0.33	-
Total B	B	0.30	-	0.30	-	0.30	-
Combined Standard...		1.06	14	0.42	44	0.44	53
Expanded...		2.28	-	0.85	-	0.89	-

Table C.11: Uncertainty budget at INTI for SPRT 2.

Component	Type	Systematic/Random
Phase Transition Realization Repeatability	A	R
Bridge (repeatability)	A	R
Reference Resistor Stability	A	R
Chemical Impurities	B	S
Bridge (non-linearity, AC quadrature)	B	S
Hydrostatic-head	B	S
Propagated TPW	B	S
TPW Resistance change	B	R
SPRT self-heating	B	R
Heat Flux	B	S
Moisture	B	-
SPRT Pt Oxidation	B	-
Gas pressure	B	S
Slope of Plateau	B	S

Table C.12: Uncertainty budget components at KRISS.

	Type	Ar	Hg	Ga	In	Sn	Zn
	mK	dof	mK	mK	mK	mK	mK
Phase Transition...	A	0.080	6	0.050	10	0.090	6
Bridge...	A	0.020	∞	0.020	∞	0.020	0.200
Reference...	A	0.001	∞	0.001	∞	0.001	∞
Chemical Impurities	B	0.280	∞	0.114	∞	0.008	0.540
Bridge (non-...)	B	0.070	∞	0.070	∞	0.070	0.070
Hydrostatic-head	B	0.033	∞	0.071	∞	0.012	0.033
Propagated TPW	B	0.013	∞	0.055	∞	0.074	0.111
TPW Resistance...	B	0.085	∞	0.017	∞	0.043	0.037
SPRT self-heating	B	0.140	∞	0.060	∞	0.060	0.120
Heat Flux	B	0.210	∞	0.062	∞	0.077	0.064
Moisture	B	0	-	0	-	0	-
SPRT Pt Oxidation	B	0	-	0	-	0	-
Gas pressure	B	0	-	0	-	0	-
Slope of Plateau	B	0.173	∞	0.115	∞	0.069	0.035
Total A	A	0.08	7	0.05	13	0.09	7
Total B	B	0.43	∞	0.22	∞	0.16	0.58
Combined Standard...		0.44	5412	0.22	3971	0.19	1.90
Expanded...		0.88	-	0.45	-	0.38	-
						1.16	-
						0.85	-
						1.02	-

Table C.13: Uncertainty budget at KRISS.

Component	Type	Systematic/Random
W repeatability	A	R
Self heating correction	A	R
Bridge linearity	A	S
Short-term thermometer repeatability at TPW	A	R
Purity and gas pressure	B	S
Hydrostatic pressure correction	B	S
Spurious heat fluxes	B	S
AC/DC current	B	S
Interpretation of the plateau	B	S
Propagated TPW reproducibility	B	R
Propagated TPW purity and isotopic composition	B	S
Propagated TPW hydrostatic pressure correction	B	S
Propagated TPW spurious heat fluxes	B	S
Propagated TPW self-heating correction	B	R
Internal insulation leakage	B	S
Stability of Rs	B	-
Temperature correction for Rs	B	-

Table C.14: Uncertainty budget components at LNE-CNAM.

	Type	Ar	Hg	Ga	In	Sn	Zn
	mK	dof	mK	dof	mK	dof	mK
W repeatability...	A	0.140	6	0.100	2	0.128	18
Self heating...	A	0.089	6	0.016	2	0.032	30
Bridge linearity...	A	0.003	2	0.003	2	0.013	2
Short-term...	A	0.042	2	0.020	3	0.021	35
Purity and gas...	B	0.060	∞	0.220	∞	0.047	∞
Hydrostatic...	B	0.048	∞	0.040	∞	0.004	∞
Spurious heat fluxes...	B	0.290	∞	0.130	∞	0.029	∞
AC/DC current...	B	0	-	0	-	0	-
Interpretation of...	B	0	-	0	-	0.031	∞
Propagated TPW...	B	0.010	∞	0.038	∞	0.050	∞
Propagated TPW...	B	0.001	∞	0.002	∞	0.003	∞
Propagated TPW...	B	0	∞	0.002	∞	0.002	∞
Propagated TPW...	B	0.006	∞	0.024	∞	0.033	∞
Propagated TPW...	B	0.006	∞	0.024	∞	0.033	∞
Internal...	B	0.002	∞	0.008	∞	0.011	∞
Stability of Rs...	B	0	-	0	-	0	-
Temperature...	B	0.012	∞	0.012	∞	0.012	∞
Total A	A	0.17	-	0.10	-	0.13	-
Total B	B	0.30	-	0.26	-	0.09	-
Combined Standard...		0.34	197	0.28	115	0.16	49
Expanded...		0.68	-	0.56	-	0.33	-

Table C.15: Uncertainty budget at LNE-CNAM Ante-NIST.

	Type	Ar	Hg	Ga	In	Sn	Zn
	mK	dof	mK	dof	mK	dof	mK
W repeatability	A	0.200	11	0.058	2	0.042	1.9
Self heating...	A	0.068	11	0.020	2	0.074	1.2
Bridge linearity	A	0.003	2	0.003	2	0.013	2
Short-term...	A	0.006	2	0.043	3	0.034	20
Purity and gas...	B	0.060	∞	0.220	∞	0.047	∞
Hydrostatic...	B	0.048	∞	0.040	∞	0.004	∞
Spurious heat fluxes	B	0.290	∞	0.130	∞	0.029	∞
AC/DC current	B	0	-	0	-	0	-
Interpretation of...	B	0	-	0	-	0.031	∞
Propagated TPW...	B	0.010	∞	0.038	∞	0.050	∞
Propagated TPW...	B	0.001	∞	0.002	∞	0.003	∞
Propagated TPW...	B	0	∞	0.002	∞	0.002	∞
Propagated TPW...	B	0.006	∞	0.024	∞	0.033	∞
Propagated TPW...	B	0.006	∞	0.024	∞	0.033	∞
Internal...	B	0.002	∞	0.008	∞	0.011	∞
Stability of Rs	B	0	-	0	-	0	-
Temperature....	B	0.012	∞	0.012	∞	0.012	∞
Total A	A	0.21	-	0.07	-	0.09	-
Total B	B	0.30	-	0.26	-	0.09	-
Combined Standard...		0.37	116	0.27	810	0.13	114
Expanded...		0.73	-	0.54	-	0.26	-
						0.54	-
						0.63	-
						1.12	-

Table C.16: Uncertainty budget at LNE-CNAM Post-NIST.

Component	Type	Systematic/Random
Phase Transition Realization Repeatability	A	R
Chemical Impurities	B	S
Hydrostatic-head	B	S
Reference resistors	B	S
Non-linearity of bridge	B	S
Repeatability of bridge	B	S
Propagated TPW	B	S
SPRT self-heating	B	S
Heat Flux	B	S
Gas pressure	B	S
Slope of Plateau	B	S

Table C.17: Uncertainty budget components at NIM.

	Type	Ar	Hg	Ga	In	Sn	Zn
	mK	dof	mK	dof	mK	dof	mK
Phase Transition...	A	0.040	6	0.050	6	0.070	6
Chemical Impurities	B	0.050	2	0.080	2	0.100	2
Hydrostatic-head	B	0.020	2	0.070	2	0.040	2
Reference resistors	B	0.010	8	0.010	8	0.030	8
Non-linearity of...	B	0.010	2	0.020	2	0.040	2
Repeatability of...	B	0.010	2	0.020	2	0.030	2
Propagated TPW	B	0.010	8	0.050	8	0.090	8
SPRT self-heating	B	0.020	6	0.020	6	0.020	6
Heat Flux	B	0.110	8	0.060	8	0.080	8
Gas pressure	B	-	-	-	0.010	12	0.010
Slope of Plateau	B	0.110	6	0.060	6	0.060	6
Total A	A	0.04	6	0.05	6	0.07	6
Total B	B	0.17	17	0.15	13	0.18	16
Combined Standard...		0.17	19	0.16	16	0.20	20
Expanded...		0.34	-	0.31	-	0.39	-
					0.26	33	0.29
					0.52	-	0.58
						0.58	-
						0.66	-

Table C.18: Uncertainty budget at NIM.

Component	Type	Systematic/Random
Bridge Repeatability	A	R
Bridge Non-Linearity	A	S
Phase Transition Realization Repeatability	A	R
AC Bridge Quadrature	B	S
Reference Resistor Stability	B	R
Chemical Impurities	B	S
Hydrostatic-Head Correction	B	S
SPRT Self-Heating Correction	B	R
Heat Flux	B	S
Gas Pressure	B	R
Slope of Plateau	B	S
Isotopic Variation	B	R
Propagation of TPW	B	R

Table C.19: Uncertainty budget components at NIST.

	Type	A_r	H_g	G_a	In	Sn	Zn				
		mK	dof	mK	dof	mK	dof	mK	dof	mK	dof
Bridge Repeatability	A	0.002	-	0.002	-	0.002	-	0.003	-	0.003	-
Bridge Non-Linearity	A	0.018	-	0.019	-	0.020	-	0.021	-	0.022	-
Phase Transition...	A	0.030	-	0.069	-	0.020	-	0.040	-	0.120	-
AC Bridge Quadrature Reference...	B	0.003	-	0.003	-	0.003	-	0.003	-	0.003	-
Chemical Impurities	B	0.050	-	0.010	-	0.010	-	0.070	-	0.060	-
Hydrostatic-Head...	B	0.005	-	0.009	-	0.002	-	0.005	-	0.003	-
SPRT Self-Heating...	B	0.006	-	0.007	-	0.006	-	0.006	-	0.006	-
Heat Flux	B	0.030	-	0.004	-	0.002	-	0.002	-	0.003	-
Gas Pressure	B	0	-	0	-	0	-	0.011	-	0.008	-
Slope of Plateau	B	0	-	0	-	0	-	0	-	0	-
Isotopic Variation	B	0	-	0	-	0	-	0	-	0	-
Propagation of TPW	B	0.002	-	0.008	-	0.009	-	0.010	-	0.019	-
Total A	A	0.04	-	0.07	-	0.03	-	0.05	-	0.12	-
Total B	B	0.06	-	0.02	-	0.02	-	0.07	-	0.06	-
Combined Uncertainty		0.07	-	0.08	-	0.04	-	0.09	-	0.14	-
Expanded...		0.14	-	0.15	-	0.07	-	0.18	-	0.28	-
										0.51	-

Table C.20: Uncertainty budget at NIST.

Component	Type	Systematic/Random
Electrical Noise	A	R
Reference Resistor Stability	A	R
Chemical Impurities	B	S
FP realization/Slope of plateau	B	S
SPRT self-heating	B	S
Bridge non-linearity	B	S
Bridge quadrature	B	S
AC/DC effect	B	-
Hydrostatic-head	B	S
Heat flux/conduction	B	S
Moisture/Insulation	B	S
Gas pressure	B	S
Propagated SPRT stability/ Pt oxidation	B	S
Propagated TPW	B	S

Table C.21: Uncertainty budget components at NMIA.

	Type	Ar	Hg	Ga	In	Sn	Zn
		mK dof					
Electrical Noise Reference...	A	0.012 -	0.013 -	0.013 -	0.013 -	0.014 -	0.015 -
	A	0.003 -	0.003 -	0.003 -	0.003 -	0.003 -	0.003 -
Chemical Impurities	B	0.400 -	0.100 -	0.100 -	0.100 -	0.100 -	0.100 -
	B	0.250 -	0.050 -	0.050 -	0.050 -	0.050 -	0.075 -
SPRT self-heating	B	0.010 -	0.005 -	0.005 -	0.005 -	0.005 -	0.010 -
	B	0.046 -	0.050 -	0.051 -	0.052 -	0.054 -	0.057 -
Bridge non-linearity	B	0.009 -	0.010 -	0.010 -	0.011 -	0.011 -	0.011 -
	B	0.005 -	0.010 -	0.010 -	0.015 -	0.020 -	0.025 -
Bridge quadrature	B	- -	0.035 -	0.006 -	0.017 -	0.011 -	0.013 -
	B	- -	0.015 -	0.040 -	0.035 -	0.055 -	0.050 -
AC/DC effect	B	- -	- -	0.005 -	0.005 -	0.005 -	0.010 -
	B	- -	- -	0.020 -	0.049 -	0.033 -	0.043 -
Hydrostatic-head	B	- -	0.017 -	0.006 -	0.101 -	0.111 -	0.008 -
	B	0.007 -	0.029 -	0.039 -	0.059 -	0.070 -	0.101 -
Total A	A	0.01 -	0.02 -				
	B	0.47 -	0.14 -	0.17 -	0.19 -	0.16 -	0.20 -
Combined Uncertainty		0.47 -	0.14 -	0.17 -	0.19 -	0.16 -	0.20 -
Expanded...		0.95 -	0.28 -	0.34 -	0.39 -	0.32 -	0.41 -

Table C.22: Uncertainty budget at NIMA for SPRT 1.

	Type	Ar	Hg	Ga	In	Sn	Zn
		mK dof					
Electrical Noise Reference...	A	0.012 -	0.013 -	0.013 -	0.013 -	0.014 -	0.015 -
	A	0.003 -	0.003 -	0.003 -	0.003 -	0.003 -	0.003 -
Chemical Impurities	B	0.400 -	0.100 -	0.100 -	0.100 -	0.100 -	0.100 -
	B	0.250 -	0.050 -	0.050 -	0.050 -	0.050 -	0.075 -
SPRT self-heating	B	0.010 -	0.005 -	0.005 -	0.005 -	0.005 -	0.010 -
	B	0.046 -	0.050 -	0.051 -	0.052 -	0.054 -	0.057 -
Bridge non-linearity	B	0.009 -	0.010 -	0.010 -	0.011 -	0.011 -	0.011 -
	B	0.005 -	0.010 -	0.010 -	0.015 -	0.020 -	0.025 -
Bridge quadrature	B	- -	0.035 -	0.006 -	0.017 -	0.011 -	0.013 -
	B	- -	0.010 -	0.025 -	0 -	0.030 -	0.050 -
AC/DC effect	B	- -	- -	0.005 -	0.005 -	0.005 -	0.010 -
	B	- -	- -	0.020 -	0.049 -	0.033 -	0.043 -
Hydrostatic-head	B	- -	0.015 -	0.025 -	0.117 -	0.111 -	0.117 -
	B	0.007 -	0.029 -	0.039 -	0.059 -	0.070 -	0.101 -
Total A	A	0.01 -	0.02 -				
	B	0.47 -	0.13 -	0.13 -	0.19 -	0.19 -	0.23 -
Combined Uncertainty		0.47 -	0.14 -	0.13 -	0.19 -	0.19 -	0.23 -
Expanded...		0.95 -	0.27 -	0.27 -	0.38 -	0.39 -	0.45 -

Table C.23: Uncertainty budget at NIMA for SPRT 2.

Component	Type	Systematic/Random
Repeatability of Measured Resistance Ratio	A	R
Short-term Repeatability of the Resistance Measurements at the Fixed Point	A	R
Reproducibility of the Resistance of the SPRT at TPW	A	R
Short-term Repeatability of the Resistance Measurements at the TPW	A	R
Fixed Point Reproducibility	B	S
Chemical Impurities in Fixed Point Cell	B	S
Variation of the Liquid Fraction during the Measurement Period of a Fixed Point Plateau Realization	B	S
Gas Pressure Correction in Fixed Point Cell	B	S
Calibration to National Standard	B	S
Heat Flux at Fixed Point	B	S
Hydrostatic-head Correction in Fixed Point Cell	B	S
Water Triple Point Reproducibility	B	S
Isotopes and Chemical Impurities in Water Triple Point Cell	B	S
Residual Gas in Water Triple Point Cell	B	S
Heat Flux at Water Triple Point	B	S
Hydrostatic-head Correction in Water Triple Point Cell	B	S
Moisture	B	-
SPRT Pt Oxidation	B	-
Bridge and Reference Resistor Stability	B	S

Table C.24: Uncertainty budget components at NMIJ/AIST.

	Type	Ar	Hg	Ga	In	Sn	Zn	
	mK	dof	mK	dof	mK	dof	mK	
Repeatability of...	A	-	0.023	3	0.007	3	0.011	3
Short-term...	A	-	0.005	9	0.004	12	0.005	9
Reproducibility...	A	-	0.005	4	0.012	4	0.032	4
Short-term...	A	-	0.004	9	0.005	9	0.007	11
Fixed Point...	B	-	0.100	∞	0.017	∞	0.058	∞
Chemical...	B	-	0.250	∞	-	-	0.100	∞
Variation of the...	B	-	0.115	∞	0.046	∞	0.058	∞
Gas Pressure...	B	-	0.150	∞	-	-	0.028	∞
Calibration to...	B	-	-	-	0.086	∞	-	-
Heat Flux at...	B	-	0.020	∞	0.015	∞	0.028	∞
Hydrostatic-head...	B	-	0.094	∞	0.016	∞	0.044	∞
Water Triple...	B	-	0.012	∞	0.015	∞	0.022	∞
Isotopes and...	B	-	0.017	∞	0.022	∞	0.032	∞
Residual Gas in...	B	-	0.013	∞	0.017	∞	0.024	∞
Heat Flux at...	B	-	0.024	∞	0.007	∞	0.016	∞
Hydrostatic-head...	B	-	0.008	∞	0.011	∞	0.016	∞
Moisture	B	-	-	-	-	-	-	-
SPRT Pt Oxidation	B	-	-	-	-	-	-	-
Bridge and...	B	-	0.037	∞	0.044	∞	0.058	∞
Total A	A	-	0.02	-	0.03	-	0.07	-
Total B	B	-	0.35	-	0.12	-	0.16	-
Combined Standard...	0.70	-	0.35	148185	0.12	30516	0.17	2847
Expanded...	1.39	-	0.70	-	0.23	-	0.33	-
							0.53	-
							0.68	-

Table C.25: Uncertainty budget at NMIJ/AIST for SPRJ 1 Ante-NIST.

	Type	Ar	Hg	Ga	In	Sn	Zn
	mK	dof	mK	mK	mK	mK	mK
Repeatability of...	A	-	0.012	3	0.003	3	0.032
Short-term...	A	-	0.003	10	0.007	11	0.004
Reproducibility...	A	-	0.006	4	0.007	4	0.035
Short-term...	A	-	0.005	12	0.006	9	0.009
Fixed Point...	B	-	0.100	∞	0.017	∞	0.058
Chemical...	B	-	0.250	∞	-	0.100	∞
Variation of the...	B	-	0.115	∞	0.046	∞	0.058
Gas Pressure...	B	-	0.150	∞	-	0.028	∞
Calibration to...	B	-	-	∞	0.086	∞	-
Heat Flux at...	B	-	0.007	∞	0.016	∞	0.024
Hydrostatic-head...	B	-	0.094	∞	0.016	∞	0.044
Water Triple...	B	-	0.012	∞	0.015	∞	0.022
Isotopes and...	B	-	0.017	∞	0.022	∞	0.032
Residual Gas in...	B	-	0.013	∞	0.017	∞	0.024
Heat Flux at...	B	-	0.004	∞	0.006	∞	0.011
Hydrostatic-head...	B	-	0.008	∞	0.011	∞	0.016
Moisture	B	-	-	-	-	-	-
SPRT Pt Oxidation	B	-	-	-	-	-	-
Bridge and...	B	-	0.037	∞	0.044	∞	0.058
Total A	A	-	0.01	-	0.04	-	0.06
Total B	B	-	0.35	-	0.12	-	0.16
Combined Standard...	0.71	-	0.35	2066655	0.12	158646	0.17
Expanded...	1.42	-	0.69	-	0.23	-	0.33
							-
							0.69

Table C.26: Uncertainty budget at NMIJ/AIST for SPRJ 2 Ante-NIST.

	Type	Ar	Hg	Ga	In	Sn	Zn	
	mK	dof	mK	dof	mK	dof	mK	dof
Repeatability of...	A	-	0.017	3	0.011	3	0.006	3
Short-term...	A	-	0.009	11	0.009	9	0.009	9
Reproducibility...	A	-	0.032	4	0.020	4	0.058	4
Short-term...	A	-	0.009	9	0.012	10	0.010	9
Fixed Point...	B	-	0.100	∞	0.009	∞	0.058	∞
Chemical...	B	-	0.250	∞	-	-	0.100	∞
Variation of the...	B	-	0.115	∞	0.046	∞	0.058	∞
Gas Pressure...	B	-	0.150	∞	-	-	0.028	∞
Calibration to...	B	-	-	-	0.086	∞	-	-
Heat Flux at...	B	-	0.038	∞	0.016	∞	0.068	∞
Hydrostatic-head...	B	-	0.094	∞	0.016	∞	0.044	∞
Water Triple...	B	-	0.012	∞	0.015	∞	0.022	∞
Isotopes and...	B	-	0.017	∞	0.022	∞	0.32	∞
Residual Gas in...	B	-	0.013	∞	0.017	∞	0.024	∞
Heat Flux at...	B	-	0.019	∞	0.015	∞	0.019	∞
Hydrostatic-head...	B	-	0.008	∞	0.011	∞	0.016	∞
Moisture	B	-	-	-	-	-	-	-
SPRT Pt Oxidation	B	-	-	-	-	-	-	-
Bridge and...	B	-	0.037	∞	0.044	∞	0.058	∞
Total A	A	-	0.04	-	0.03	-	0.06	-
Total B	B	-	0.35	-	0.12	-	0.17	-
Combined Standard...	0.72	-	0.35	52815	0.12	4480	0.18	396
Expanded...	1.43	-	0.70	-	0.24	-	0.37	-
							0.55	-
							0.69	-

Table C.27: Uncertainty budget at NMLJ/AIST for SPRT 1 Post-NIST.

	Type	Ar	Hg	Ga	In	Sn	Zn	
	mK	dof	mK	mK	dof	mK	dof	
Repeatability of...	A	-	0.019	3	0.009	3	0.015	3
Short-term...	A	-	0.003	11	0.008	12	0.005	17
Reproducibility...	A	-	0.002	4	0.011	4	0.032	4
Short-term...	A	-	0.003	13	0.004	12	0.006	12
Fixed Point...	B	-	0.100	∞	0.017	∞	0.058	∞
Chemical...	B	-	0.250	∞	0.049	∞	0.100	∞
Variation of the...	B	-	0.115	∞	0.046	∞	0.058	∞
Gas Pressure...	B	-	0.150	∞	0.012	∞	0.028	∞
Calibration to...	B	-	-	-	-	-	-	-
Heat Flux at...	B	-	0.017	∞	0.021	∞	0.039	∞
Hydrostatic-head...	B	-	0.094	∞	0.016	∞	0.044	∞
Water Triple...	B	-	0.012	∞	0.015	∞	0.022	∞
Isotopes and...	B	-	0.017	∞	0.022	∞	0.032	∞
Residual Gas in...	B	-	0.013	∞	0.017	∞	0.024	∞
Heat Flux at...	B	-	0.005	∞	0.010	∞	0.005	∞
Hydrostatic-head...	B	-	0.008	∞	0.011	∞	0.016	∞
Moisture	B	-	-	-	-	-	-	-
SPRT Pt Oxidation	B	-	-	-	-	-	-	-
Bridge and...	B	-	0.037	∞	0.044	∞	0.058	∞
Total A	A	-	0.02	-	0.02	-	0.04	-
Total B	B	-	0.35	-	0.09	-	0.16	-
Combined Standard...	0.69	-	0.35	352821	0.10	13776	0.17	2763
Expanded...	1.38	-	0.69	-	0.19	-	0.33	-
							0.51	-
							0.70	-

Table C.28: Uncertainty budget at NMLJ/AIST for SPRT 2 Post-NIST.

Component	Type	Systematic/Random
Repeatability	A	R
Estimation of the triple point temperature of Ar by Reference SPRT	B	S
Longitudinal temperature gradient	B	S
Reference Resistor Stability for Reference SPRT	B	S
Bridge for Reference SPRT	B	S
Reference SPRT self-heating	B	S
Calibration of Reference SPRT at the triple point of Ar	B	S
Reference SPRT Stability	B	S
Reference Resistor Stability for DUT	B	S
Bridge for Reference DUT	B	S
DUT self-heating	B	S
Estimation of the value of DUT at the Fixed point by comparison	B	S
Propagated TPW	B	S

Table C.29: Uncertainty budget components at NMIJ/AIST.

	Type	Ar	Hg	Ga	In	Sn	Zn
		mK	dof	mK	dof	mK	dof
Repeatability	A	0.050	2				
Estimation of the...	B	0.110	∞				
Longitudinal...	B	0.160	∞				
Reference...	B	0.010	∞				
Bridge for...	B	0.080	∞				
Reference SPRT...	B	0.150	∞				
Calibration of...	B	0.080	∞				
Reference SPRT...	B	0.100	∞				
Reference...	B	0.010	∞				
Bridge for...	B	0.080	∞				
DUT self-heating	B	0.170	∞				
Estimation of the...	B	0.600	∞				
Propagated TPW	B	0.050	∞				
Total A	A	0.05	-				
Total B	B	0.69	-				
Combined Standard...		0.70	74807				
Expanded...		1.39	-				

Table C.30: Uncertainty budget at NMLJ/AIST for SPRT 1 Ante-NIST.

	Type	Ar	Hg	Ga	In	Sn	Zn
		mK	dof	mK	dof	mK	dof
Repeatability	A	0.050	2				
Estimation of the...	B	0.100	∞				
Longitudinal...	B	0.160	∞				
Reference...	B	0.010	∞				
Bridge for...	B	0.080	∞				
Reference SPRT...	B	0.180	∞				
Calibration of...	B	0.080	∞				
Reference SPRT...	B	0.100	∞				
Reference...	B	0.010	∞				
Bridge for...	B	0.080	∞				
DUT self-heating	B	0.200	∞				
Estimation of the...	B	0.600	∞				
Propagated TPW	B	0.050	∞				
Total A	A	0.05	-				
Total B	B	0.71	-				
Combined Standard...		0.71	84674				
Expanded...		1.42	-				

Table C.31: Uncertainty budget at NMLJ/AIST for SPRT 2 Ante-NIST.

	Type	Ar	Hg	Ga	In	Sn	Zn
		mK	dof	mK	dof	mK	dof
Repeatability	A	0.050	2				
Estimation of the...	B	0.120	∞				
Longitudinal...	B	0.160	∞				
Reference...	B	0.010	∞				
Bridge for...	B	0.080	∞				
Reference SPRT...	B	0.200	∞				
Calibration of...	B	0.080	∞				
Reference SPRT...	B	0.100	∞				
Reference...	B	0.010	∞				
Bridge for...	B	0.080	∞				
DUT self-heating	B	0.200	∞				
Estimation of the...	B	0.600	∞				
Propagated TPW	B	0.050	∞				
Total A	A	0.05	-				
Total B	B	0.72	-				
Combined Standard...		0.72	80769				
Expanded...		1.43	-				

Table C.32: Uncertainty budget at NMIJ/AIST for SPRT 1 Post-NIST.

	Type	Ar	Hg	Ga	In	Sn	Zn
		mK	dof	mK	dof	mK	dof
Repeatability	A	0.050	2				
Estimation of the...	B	0.100	∞				
Longitudinal...	B	0.160	∞				
Reference...	B	0.010	∞				
Bridge for...	B	0.080	∞				
Reference SPRT...	B	0.130	∞				
Calibration of...	B	0.080	∞				
Reference SPRT...	B	0.100	∞				
Reference...	B	0.010	∞				
Bridge for...	B	0.080	∞				
DUT self-heating	B	0.170	∞				
Estimation of the...	B	0.600	∞				
Propagated TPW	B	0.050	∞				
Total A	A	0.05	-				
Total B	B	0.69	-				
Combined Standard...		0.69	72443				
Expanded...		1.38	-				

Table C.33: Uncertainty budget at NMIJ/AIST for SPRT 2 Post-NIST.

Component	Type	Systematic/Random
FP repeatability	A	R
Bridge repeatability	A	R
Stability of Rs	B	S
Chemical Impurities	B	S
Hydrostatic-head	B	S
Propagated TPW	B	S
Bridge non-linearity	B	S
Freq, quadrature	B	S
SPRT self-heating	B	S
Heat Flux	B	S
Moisture	B	S
SPRT Pt Oxidation	B	S
Gas Pressure	B	S
Slope of Plateau	B	S

Table C.34: Uncertainty budget components at NPL.

	Type	Ar	Hg	Ga	In	Sn	Zn
	mK dof	mK dof	mK dof	mK dof	mK dof	mK dof	mK dof
FP repeatability	A	0.027	8	0.039	8	0.040	8
Bridge repeatability	A	0.004	29	0.008	29	0.005	29
Stability of Rs	B	0.001	∞	0.002	∞	0.003	∞
Chemical Impurities	B	0.139	∞	0.058	∞	0.012	∞
Hydrostatic-head	B	0.019	∞	0.041	∞	0.007	∞
Propagated TPW	B	0.006	13448	0.024	17742	0.032	37432
Bridge non-linearity	B	0.027	∞	0.029	∞	0.029	∞
Freq, quadrature	B	0.013	∞	0.014	∞	0.016	∞
SPRT self-heating	B	0.017	∞	0.020	∞	0.024	∞
Heat Flux	B	0.058	∞	0.012	∞	0.006	∞
Moisture	B	0	∞	0	∞	0	∞
SPRT Pt Oxidation	B	0	∞	0	∞	0	∞
Gas Pressure	B	0	∞	0.016	∞	0.015	∞
Slope of Plateau	B	0	∞	0	∞	0	∞
Total A	A	0.03	8	0.04	9	0.04	8
Total B	B	0.16	-	0.09	-	0.06	-
Combined Standard...		0.16	9420	0.09	266	0.07	73
Expanded...		0.32	-	0.19	-	0.14	-
						0.29	-
						0.29	-
						0.45	-

Table C.35: Uncertainty budget at NPL Ante-NIST.

	Type	Ar	Hg	Ga	In	Sn	Zn
	mK	dof	mK	mK	dof	mK	dof
FP repeatability	A	0.113	7	0.023	5	0.058	5
Bridge repeatability	A	0.001	19	0.007	19	0.003	19
Stability of Rs	B	0.001	∞	0.002	∞	0.004	∞
Chemical Impurities	B	0.139	∞	0.058	∞	0.058	∞
Hydrostatic-head	B	0.019	∞	0.041	∞	0.007	∞
Propagated TPW	B	0.007	6702	0.030	10373	0.041	3858
Bridge non-linearity	B	0.027	∞	0.029	∞	0.029	∞
Freq, quadrature	B	0.021	∞	0.023	∞	0.027	∞
SPRT self-heating	B	0.017	∞	0.020	∞	0.024	∞
Heat Flux	B	0.058	∞	0.012	∞	0.006	∞
Moisture	B	0	∞	0	∞	0	∞
SPRT Pt Oxidation	B	0	∞	0	∞	0	∞
Gas Pressure	B	0	∞	0.016	∞	0.015	∞
Slope of Plateau	B	0	∞	0	∞	0	∞
Total A	A	0.11	7	0.02	6	0.06	5
Total B	B	0.16	-	0.09	-	0.07	-
Combined Standard...		0.19	59	0.09	1309	0.07	145
Expanded...		0.39	-	0.19	-	0.15	-
						0.25	-
						0.28	-
						0.56	-

Table C.36: Uncertainty budget at NPL Post-NIST.

Component	Type	Systematic/Random
Phase Transition Realization Repeatability	A	R
Bridge (repeatability, non-linearity, AC quadrature)	B	S
Reference Resistor Stability	B	S
Chemical Impurities	B	S
Hydrostatic-head	B	S
Propagated TPW	B	S
SPRT self-heating	B	S
Heat Flux	B	S
Moisture	B	-
SPRT Pt Oxidation	B	-
Gas pressure	B	S
Slope of Plateau	B	S

Table C.37: Uncertainty budget components at NRC.

Type	Phase Transition...	Ar	Hg	Ga	In	Sn	Zn						
	A	mK	dof										
Bridge...	B	0.030	8	0.030	8	0.030	8	0.030	8	0.030	8	0.030	8
Reference...	B	0.004	50	0.004	50	0.004	50	0.004	50	0.004	50	0.004	50
Chemical Impurities	B	0.142	8	0.006	8	0.008	8	0.058	8	0.127	8	0.266	8
Hydrostatic-head	B	0.030	50	0.071	50	0.012	50	0.033	50	0.022	50	0.027	50
Propagated TPW	B	0.009	16	0.036	16	0.048	16	0.069	16	0.081	16	0.110	16
SPRT self-heating	B	0.010	50	0.010	50	0.010	50	0.010	50	0.010	50	0.010	50
Heat Flux	B	0.005	8	0.005	8	0.005	8	0.005	8	0.005	8	0.005	8
Moisture	B	-	-	-	-	-	-	-	-	-	-	-	-
SPRT Pt Oxidation	B	-	-	-	-	-	-	-	-	-	-	-	-
Gas pressure	B	0	8	0.010	8	0.003	8	0.006	8	0.004	8	0.006	8
Slope of Plateau	B	0.010	8	0.010	8	0.010	8	0.010	8	0.010	8	0.010	8
Total A	A	0.04	10	0.06	10	0.11	10	0.10	10	0.17	10	0.05	10
Total B	B	0.15	10	0.09	81	0.06	31	0.10	37	0.16	17	0.29	11
Combined Standard...		0.16	11	0.10	69	0.13	16	0.14	32	0.23	24	0.30	12
Expanded Standard...		0.31	-	0.21	-	0.25	-	0.29	-	0.46	-	0.59	-

Table C.38: Uncertainty budget at NRC.

Component	Type	Systematic/Random
Phase Transition Realization Repeatability	A	R
Hydrostatic Pressure	B	S
Residual Gas Pressure	B	S
Impurities	B	S
Thermal Effects	B	S
Choice of Fixed-Point Value (includ. Slope of the Plateau)	B	S
Propagated TPW	B	S
SPRT Self-Heating	B	S
SPRT Instability	B	S
Resistance-Ratio Measurement	B	S
Reference Resistor Stability	B	S

Table C.39: Uncertainty budget components at PTB.

	Type	Ar	Hg	Ga	In	Sn	Zn
	mK	dof	mK	dof	mK	dof	mK
Phase Transition...	A	0.100	-	0.050	-	0.130	-
Hydrostatic Pressure	B	0.040	-	0.030	-	0.020	-
Residual Gas...	B	-	-	0.010	-	0.030	-
Impurities	B	0.200	-	0.060	-	0.040	-
Thermal Effects	B	0.100	-	0.020	-	0.060	-
Choice of Fixed...	B	0.070	-	0.070	-	0.050	-
Propagated TPW	B	0.020	-	0.060	-	0.060	-
SPRT Self-Heating	B	0.020	-	0.050	-	0.010	-
SPRT Instability	B	0	-	0	-	0.010	-
Resistance-Ratio...	B	0.010	-	0.050	-	0.030	-
Reference...	B	0.010	-	0.010	-	0.020	-
Total A	A	0.10	-	0.05	-	0.13	-
Total B	B	0.24	-	0.14	-	0.11	-
Combined Standard...		0.26	-	0.15	-	0.12	-
Expanded...		0.52	-	0.30	-	0.24	-

Table C.40: Uncertainty budget at PTB.

Component	Type	Systematic/Random
Realization repeatability	A	R
SPRT resistance measurement	A	R
Chemical Impurities	B	S
Hydrostatic head	B	S
SPRT self-heating (current)	B	S
SPRT self-heating (extrapolation)	B	S
Standard resistor	B	S
Resistance ratio bridge	B	S
TPW propagation	B	S
Gas pressure	B	S
Heat flux (evaluated during return measurements)	B	S

Table C.41: Uncertainty budget components at VSL.

	Type	Ar	Hg	Ga	In	Sn	Zn
	mK	dof	mK	dof	mK	dof	mK
Realization...	A	0.424	5	0.028	2	0.103	4
SPRT resistance...	A	0.006	57	0.009	57	0.011	57
Chemical Impurities	B	0.032	∞	0.012	∞	0.079	∞
Hydrostatic head	B	0.032	∞	0.071	∞	0.012	∞
SPRT self-heating...	B	0.004	∞	0.001	∞	0.001	∞
SPRT self-heating...	B	0.002	29	0.027	29	0.027	29
Standard resistor	B	0.007	49	0.023	49	0.031	49
Resistance ratio...	B	0.001	29	0.016	29	0.016	29
TPW propagation	B	0.009	74	0.038	74	0.052	74
Gas pressure	B	0	∞	0.004	∞	0.040	∞
Heat flux...	B	0.100	∞	0.064	3	0.038	4
Total type A	A	0.42	5	0.03	2	0.10	4
Total type B	B	0.11	1081893	0.11	27	0.12	298
Combined standard...		0.44	6	0.11	29	0.16	34
Expanded...		0.88	-	0.23	-	0.32	-
						0.50	-
						0.73	-

Table C.42: Uncertainty budget at VSL for SPRT 1 Ante-NIST.

	Type	Ar	Hg	Ga	In	Sn	Zn	
	mK	dof	mK	dof	mK	dof	mK	dof
Realization...	A	0.061	5	0.023	2	0.038	4	0.067
SPRT resistance...	A	0.005	57	0.007	57	0.021	57	0.028
Chemical Impurities	B	0.032	∞	0.012	∞	0.079	∞	0.027
Hydrostatic head	B	0.032	∞	0.071	∞	0.012	∞	0.033
SPRT self-heating...	B	0.004	∞	0.001	∞	0.001	∞	0.003
SPRT self-heating...	B	0.020	29	0.021	29	0.086	29	0.089
Standard resistor	B	0.005	49	0.021	49	0.028	49	0.042
Resistance ratio...	B	0.011	29	0.012	29	0.050	29	0.051
TPW propagation	B	0.009	74	0.038	74	0.052	74	0.078
Gas pressure	B	0	∞	0.004	∞	0.040	∞	0.049
Heat flux...	B	0.100	∞	0.064	3	0.038	4	0.069
Total type A	A	0.06	5	0.02	2	0.04	7	0.07
Total type B	B	0.11	28396	0.11	25	0.15	191	0.17
Combined standard...	0.13	96	0.11	26	0.16	187	0.18	78
Expanded...	0.26	-	0.22	-	0.31	-	0.36	-
							0.55	-
							0.76	-

Table C.43: Uncertainty budget at VSL for SPRT 1 Post-NIST.

	Type	mK	dof	Ar	mK	dof	Hg	mK	dof	Ga	mK	dof	In	mK	dof	Sn	mK	dof	Zn	mK	dof
Realization...	A	0.028	2	0.022	2	0.097	4	0.096	4	0.109	3	0.181	5								
SPRT resistance...	A	0.006	57	0.009	57	0.011	57	0.012	57	0.012	57	0.014	57								
Chemical Impurities	B	0.032	∞	0.012	∞	0.079	∞	0.027	∞	0.175	∞	0.312	∞								
Hydrostatic head	B	0.032	∞	0.071	∞	0.012	∞	0.033	∞	0.022	∞	0.027	∞								
SPRT self-heating...	B	0.004	∞	0.001	∞	0.001	∞	0.003	∞	0.003	∞	0.003	∞								
SPRT self-heating...	B	0.002	29	0.027	29	0.027	29	0.029	29	0.029	29	0.029	29	0.031	29						
Standard resistor	B	0.007	49	0.023	49	0.031	49	0.047	49	0.056	49	0.081	49								
Resistance ratio...	B	0.001	29	0.016	29	0.016	29	0.016	29	0.017	29	0.018	29								
TPW propagation	B	0.009	74	0.038	74	0.052	74	0.078	74	0.094	74	0.135	74								
Gas pressure	B	0	∞	0.004	∞	0.040	∞	0.049	∞	0.033	∞	0.043	∞								
Heat flux...	B	0.100	∞	0.040	3	0.057	4	0.083	3	0.159	5	0.558	3								
Total type A	A	0.03	2	0.02	3	0.10	4	0.10	4	0.11	3	0.18	5								
Total type B	B	0.11	1081893	0.10	103	0.13	90	0.14	25	0.27	39	0.66	6								
Combined standard...																					
Expanded...																					

Table C.44: Uncertainty budget at VSL for SPRT 2 Ante-NIST.

	Type	Ar	Hg	Ga	In	Sn	Zn		
	mK	dof	mK	dof	mK	dof	mK	dof	
Realization...	A	0.057	2	0.016	2	0.038	4	0.080	4
SPRT resistance...	A	0.005	57	0.007	57	0.021	57	0.028	57
Chemical Impurities	B	0.032	∞	0.012	∞	0.079	∞	0.027	∞
Hydrostatic head	B	0.032	∞	0.071	∞	0.012	∞	0.033	∞
SPRT self-heating...	B	0.004	∞	0.001	∞	0.001	∞	0.003	∞
SPRT self-heating...	B	0.020	29	0.021	29	0.086	29	0.089	29
Standard resistor	B	0.005	49	0.021	49	0.028	49	0.042	49
Resistance ratio...	B	0.011	29	0.012	29	0.050	29	0.051	29
TPW propagation	B	0.009	74	0.038	74	0.052	74	0.078	74
Gas pressure	B	0	∞	0.004	∞	0.040	∞	0.049	∞
Heat flux...	B	0.100	∞	0.040	3	0.057	4	0.083	3
Total type A	A	0.06	2	0.02	3	0.04	7	0.08	5
Total type B	B	0.11	28396	0.10	95	0.16	124	0.17	46
Combined standard...	0.1.3	49	0.10	97	0.16	130	0.19	46	0.32
Expanded...	0.25	-	0.20	-	0.33	-	0.38	-	0.65
									1.47

Table C.45: Uncertainty budget at VSL for SPRT 2 Post-NIST.

Appendix D

Temperature shifts during SPRT transfer, by NMI

The following data display the difference between ante-NIST and post-NIST measurements for each SPRT at each fixed-, organized by NMI. They are identical to the data displayed in Chapter 4, but displayed in a different light. In the graphs that follow, error bars represent $k = 2$ coverage for the uncertainty in $W^{\text{Post}} - W^{\text{Ante}}$. When all random contributions to uncertainty have been quantified, we expect $W^{\text{Post}} - W^{\text{Ante}} = 0$ within uncertainty (i.e. cutoff criterion #1 is true), unless an adverse event occurred. We see many shifts in excess of the reported random uncertainties, suggesting the presence of an unaccounted source of error.

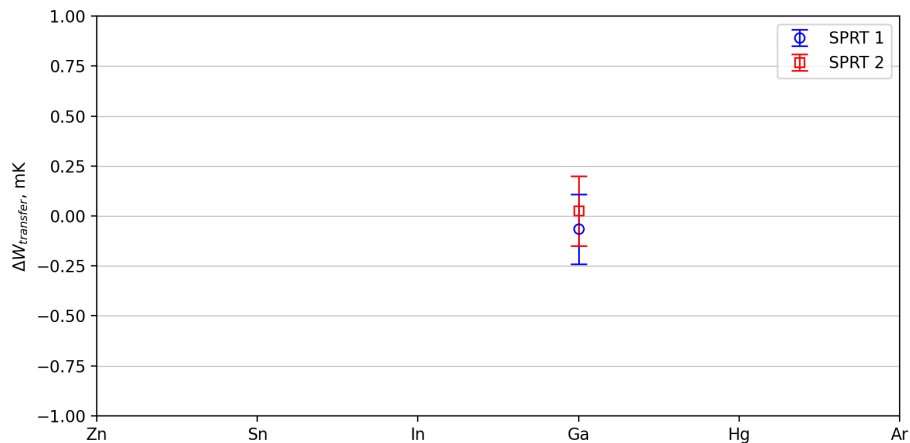


Figure D.1: Shift in measured W upon recalibration for each SPRT measured at BIPM.

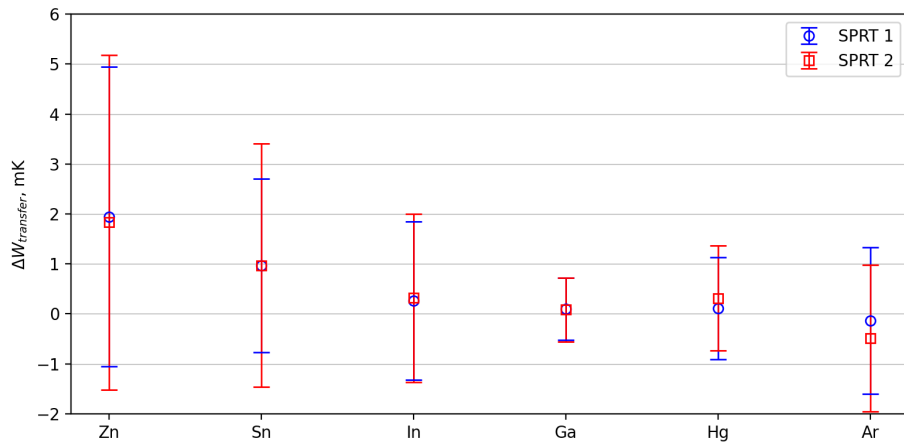


Figure D.2: Shift in measured W upon recalibration for each SPRT measured at INMETRO.

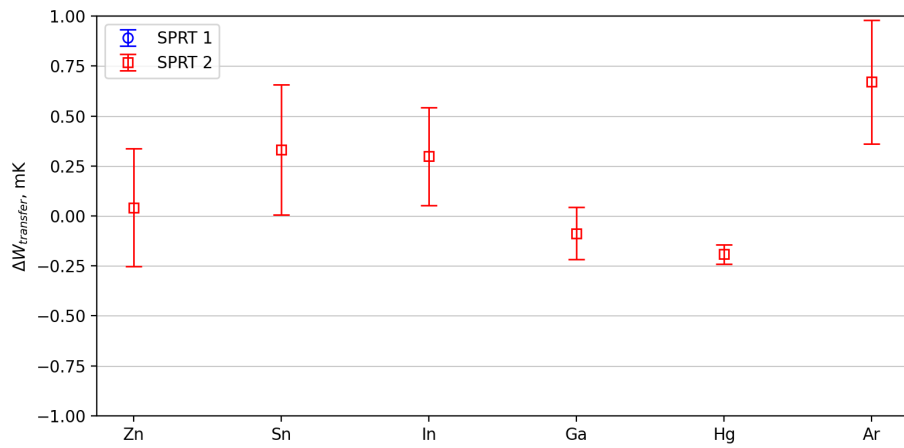


Figure D.3: Shift in measured W upon recalibration for each SPRT measured at INRIM.

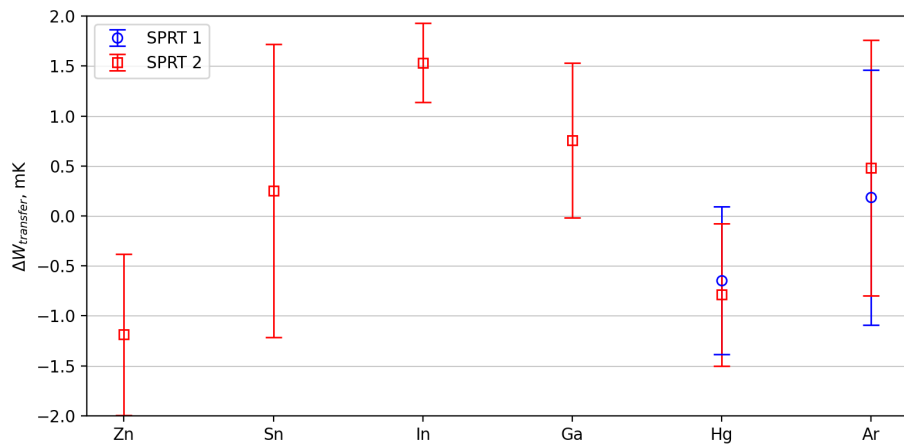


Figure D.4: Shift in measured W upon recalibration for each SPRT measured at INTI.

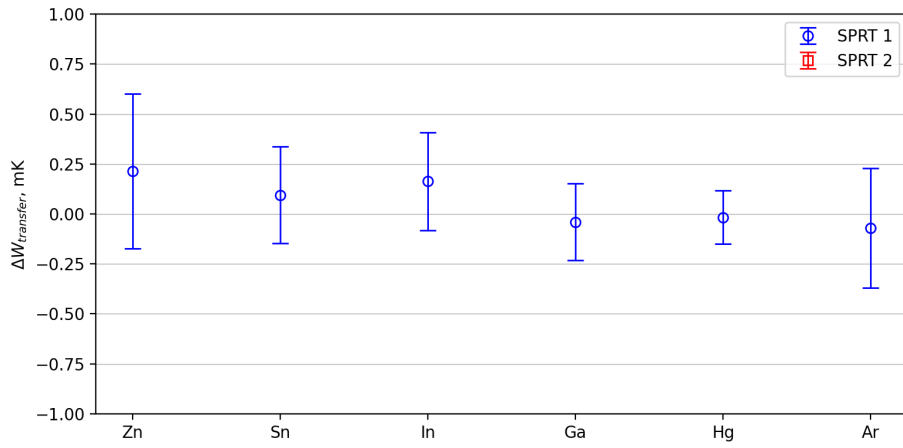


Figure D.5: Shift in measured W upon recalibration for each SPRT measured at KRISS.

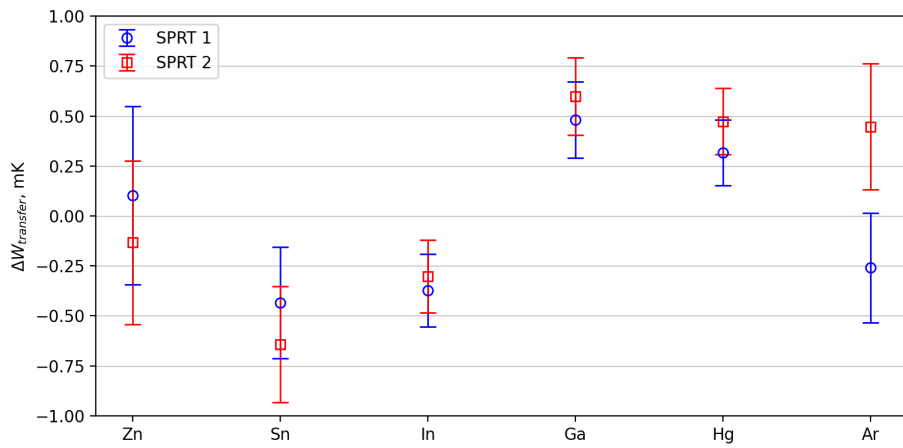


Figure D.6: Shift in measured W upon recalibration for each SPRT measured at LNE-CNAM.

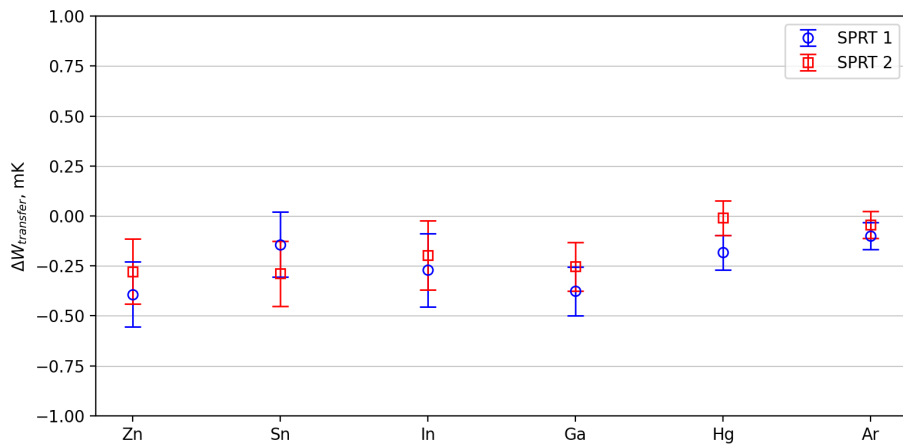


Figure D.7: Shift in measured W upon recalibration for each SPRT measured at NIM.

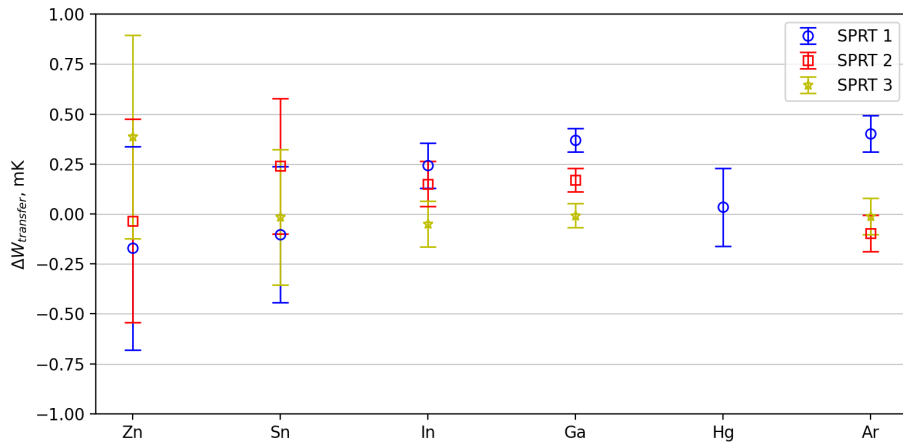


Figure D.8: Shift in measured W upon recalibration for each SPRT measured at NIST.

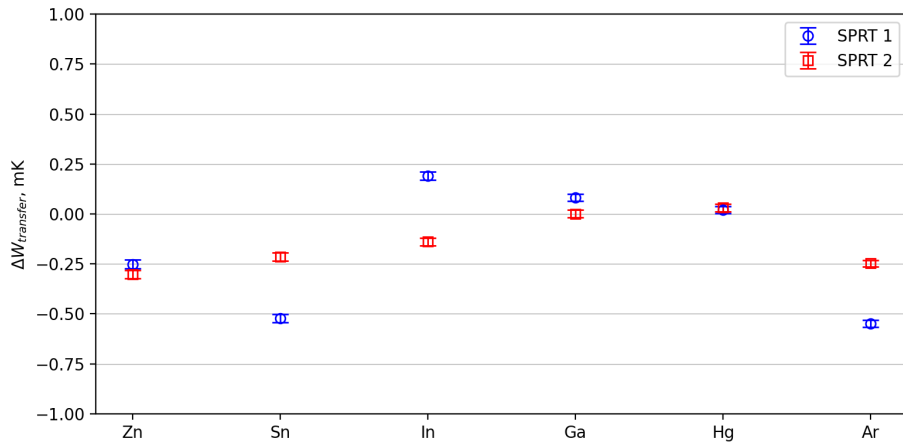


Figure D.9: Shift in measured W upon recalibration for each SPRT measured at NMIA.

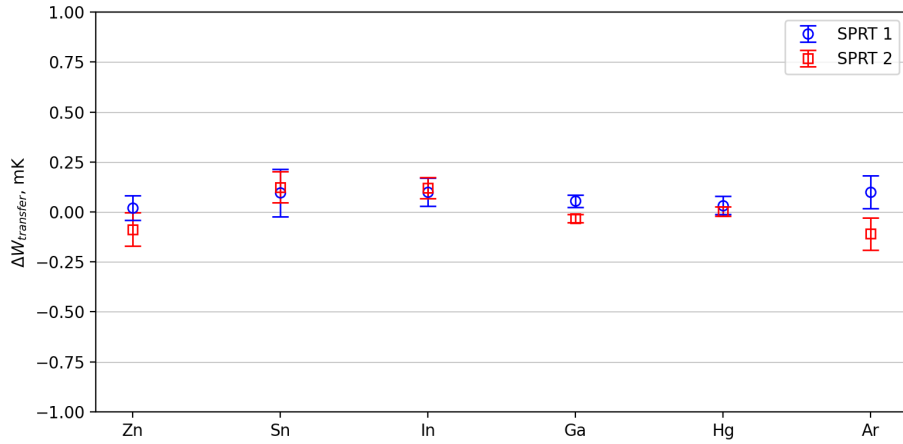


Figure D.10: Shift in measured W upon recalibration for each SPRT measured at NMIJ/AIST.

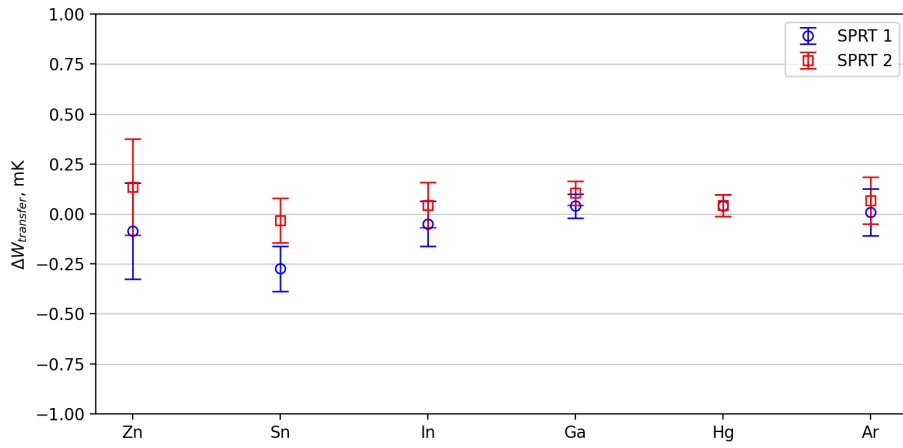


Figure D.11: Shift in measured W upon recalibration for each SPRT measured at NPL.

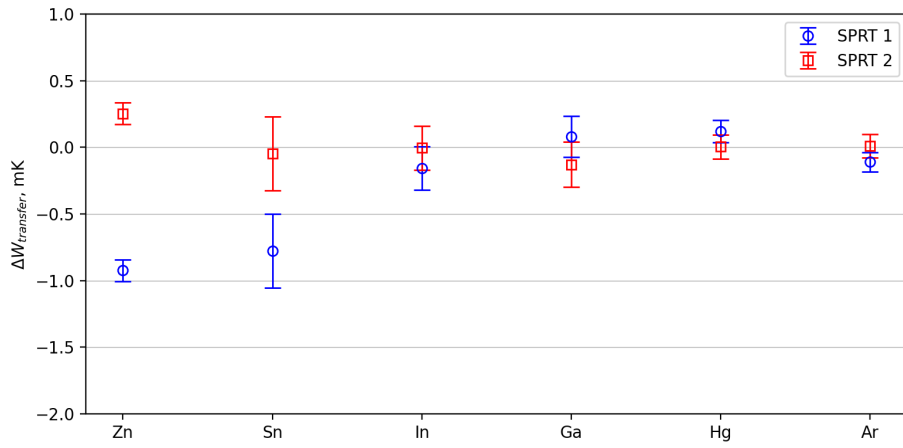


Figure D.12: Shift in measured W upon recalibration for each SPRT measured at NRC.

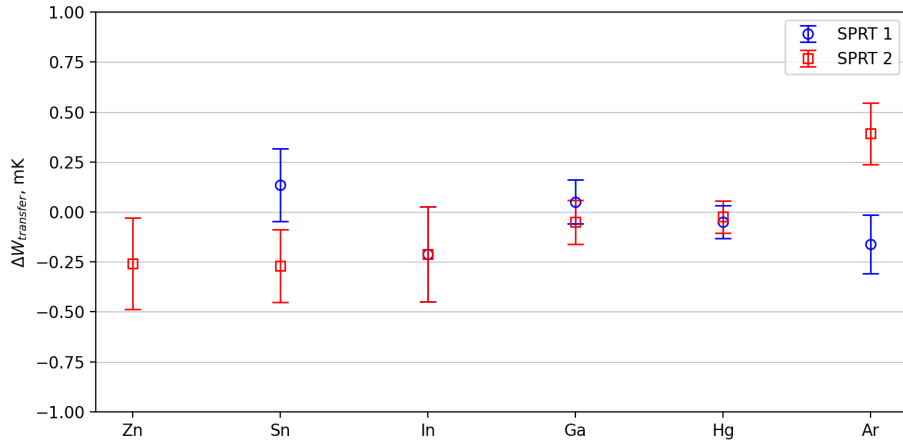


Figure D.13: Shift in measured W upon recalibration for each SPRT measured at PTB.

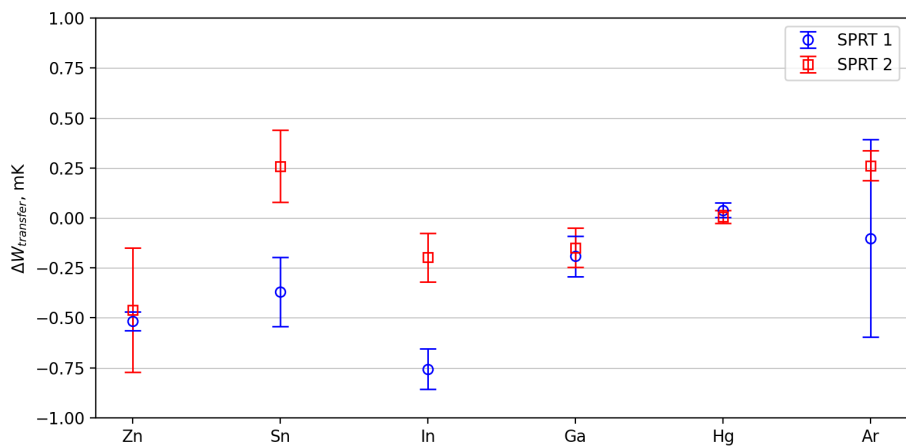


Figure D.14: Shift in measured W upon recalibration for each SPRT measured at VSL.

Appendix E

Variations on the calculation of $\overline{\Delta T}$

Here we present some alternative approaches to calculating the KCRV ($\overline{\Delta T}$) and the corresponding NMI results. None of these alternatives are used anywhere else in this report. These alternative derivations are presented here for two reasons:

1. To illustrate the sensitivity of the results to changes in the definition of $\overline{\Delta T}$
2. To present results for the comparison calculated without incorporating greater-than-expected scatter in measurements (that is, adhering strictly to the definition of ΔT in the original proposal)

E.1 $\overline{\Delta T}$ as a weighted average

During the exploratory analysis phase of our work on CCT-K9, we considered the alternatives below, but neither approach seemed more appropriate than the simple mean specified in the protocol. These alternative approaches – included here for completeness – are summarized in Table E.1.

E.1.1 Weighted by SPRT failures

During analysis, we became concerned that some SPRTs failed the cutoff criteria at multiple points, but were still used to calculate $\overline{\Delta T}$ at points where they passed the criteria. To minimize this effect, we weighted each SPRT by a factor ‘ X ’:

$$X = \frac{\#\text{fixed points passed}}{\#\text{fixed points measured}}$$

For example, an SPRT that passed the cutoff criteria at all six fixed points would contribute twice as much weight to $\Delta T_{\text{NMI}}^{\dagger}$ as one that passed the cutoff criteria at only three fixed points.

This approach introduced a very small effect (changes of $\overline{\Delta T}$ were 50 μK or less, changes in $U(\overline{\Delta T})$ were 20 μK or less), so we don’t believe this weighting is necessary.

E.1.2 Weighted by uncertainty budget

We also calculated $\overline{\Delta T}$ using a weighting factor equal to the inverse of the uncertainty of ΔT_{NMI} for each lab. The results of this calculation were significantly different than the simple mean. However, given the additional scatter/transfer uncertainty discussed earlier, it seems unwise to weight the results based exclusively on the uncertainty budgets as submitted. Nonetheless, the interested reader can find the results in Table E.1.

	Unweighted		Weighted by SPRT		Weighted by uncertainty	
	$\bar{\Delta T}$ (mK)	U (mK)	$\bar{\Delta T}$ (mK)	U (mK)	$\bar{\Delta T}$ (mK)	U (mK)
Zn	-0.196	0.220	-0.146	0.236	-0.544	0.015
Sn	0.058	0.156	0.045	0.169	0.298	0.010
In	-0.077	0.094	-0.079	0.098	-0.112	0.004
Ga	0.231	0.067	0.221	0.071	0.215	0.003
Hg	0.282	0.076	0.284	0.076	0.301	0.003
Ar	0.801	0.167	0.797	0.167	0.651	0.017

Table E.1: Values of $\bar{\Delta T}$ at each fixed point calculated as calculated in the main text, and using two alternative formulations.

E.2 Ignoring the additional variation seen in the at-NIST measurements

Following the calculation steps exactly as laid out in the protocol, without including an additional term in the uncertainty due to the observed variation in the NIST measurements, leads to a different set of SPRTs passing the cutoff criteria and thus to slightly different KCRVs and different combined uncertainties in those KCRVs.

Furthermore, the protocol did not unambiguously define the role of ante- and post-NIST measurements. While they are clearly used to assess a transfer uncertainty due to travel, and that uncertainty is clearly used to calculate cutoff criteria for calculating $\bar{\Delta T}$, it is not clearly stated whether \bar{W}_i should be taken as W_i^{Ante} , W_i^{Post} or an average of the two.

The definition of $u(C_i)$ in Eq. 2.10 assumes that C_i has a rectangular distribution with a width of $W_i^{\text{Post}} - W_i^{\text{Ante}}$ centered about $\frac{1}{2}(W_i^{\text{Ante}} + W_i^{\text{Post}})$, implying that \bar{W} denotes the mean value but it is not explicitly stated.

The contrasting interpretations:

1. $\bar{W}_i = \frac{1}{2}(W_i^{\text{Ante}} + W_i^{\text{Post}})$
2. $\bar{W}_i = W_i^{\text{Ante}}$
3. $\bar{W}_i = W_i^{\text{Post}}$

lead to slightly different values of $\bar{\Delta T}$ and values of $\Delta T_{\text{NMI-KCRV}}$ for each NMI/fixed point.

As unanimously agreed by the participants, the body of this work uses the first interpretation (Table 5.1), with additional uncertainty included to account for the observed scatter of the NIST measurements. This section presents results calculated using each of the three interpretations (Tables E.2, E.4 and E.5).

E.2.1 Average of ante-NIST and post-NIST data used

Without the additional uncertainty from the scatter in the NIST measurements the cutoff criteria can result in fewer SPRTs (Table E.3) contributing to some KCRVs (Table E.2). Despite this, shifts in KCRV are small, as are changes in the uncertainty of the KCRVs.

	$\overline{\Delta T}$ (mK)	U (mK)	#NMIs contributing
Zn	-0.20	0.22	12
Sn	0.06	0.16	10
In	-0.09	0.09	11
Ga	0.21	0.06	11
Hg	0.28	0.07	10
Ar	0.81	0.14	11

Table E.2: Values for $\overline{\Delta T}$ at each fixed point, without incorporating an increased NIST uncertainty due to scatter at the pilot lab.

NMI		Zn	Sn	In	Ga	Hg	Ar
BIPM	SPRT1	–	–	–	✓	–	–
	SPRT2	–	–	–	✓	–	–
INMETRO	SPRT1	✓	✓	✓	✓	✓	✓
	SPRT2	✓	✓	✓	✓	✓	✓
INRIM	SPRT1	–	–	–	–	–	–
	SPRT2	✓	✓	✓	✓	✗	✗
INTI	SPRT1	–	–	–	–	✓	✓
	SPRT2	✓	✓	✗	✓	✗	✓
KRISS	SPRT1	✓	✓	✓	✓	✓	✓
	SPRT2	–	–	–	–	–	–
LNE-CNAM	SPRT1	✓	✗	✗	✗	–	✓
	SPRT2	✓	✗	✓	✗	✗	✗
NIM	SPRT1	✓	✓	✗	✗	–	✓
	SPRT2	✓	✓	✓	✗	✓	✓
NIST	SPRT1	–	–	–	–	–	–
	SPRT2	–	–	–	–	–	–
	SPRT3	–	–	–	–	–	–
NMIA	SPRT1	✓	✗	✓	✓	✓	✓
	SPRT2	✓	✓	✓	✓	✓	✓
NMIJ/AIST	SPRT1	✓	✓	✓	✓	✓	✓
	SPRT2	✓	✓	✓	✓	✓	✓
NPL	SPRT1	✓	✗	✓	✓	✓	✓
	SPRT2	✓	–	✓	✗	✓	✓
NRC	SPRT1	✗	✗	✓	✓	✓	✓
	SPRT2	✓	✓	✓	✓	✓	✓
PTB	SPRT1	–	✓	✓	✓	✓	✓
	SPRT2	✓	✓	✓	✓	✓	✗
VSL	SPRT1	✗	✗	✗	✗	✓	✓
	SPRT2	✓	✓	✓	✓	✓	✗

Table E.3: Results of tests against the cutoff criteria. A checkmark (✓) indicates an SPRT that was used in the calculation of the KCRV, an X (✗) represents an SPRT that was excluded since it failed the cutoff criteria and ‘–’ indicates an SPRT that did not include a measurement at that fixed point, or was marked as unstable

E.2.2 Only ante-NIST data used

In some other comparisons the difference between participant and pilot lab values is computed using only the initial two sets of measurements. A third set of measurements, performed upon the return of the transfer standard to its home laboratory, is solely for the assessment of drift. In this case the third set of measurements for each SPRT serves solely as a method of calculating the transfer uncertainty, $u(C_{\text{SPRT}_i})$, while the first two sets of measurements are used when computing $\overline{\Delta T}$ (Table E.4).

	$\overline{\Delta T}$ (mK)	U (mK)	#NMIs
Zn	-0.19	0.23	12
Sn	-0.01	0.17	9
In	-0.07	0.10	11
Ga	0.22	0.07	12
Hg	0.30	0.08	10
Ar	0.81	0.17	11

Table E.4: Values for $\overline{\Delta T}$ at each fixed point, calculated using only ante-NIST data from each NMI.

E.2.3 Only post-NIST data used

Similar to the previous section, here one set of measurements is used solely to assess a transfer uncertainty while the other two are also used when computing $\overline{\Delta T}$ (Table E.5). Since measurements in this comparison were spaced over a long period, the post-NIST measurements used in this section may be much more recent than the ante-NIST measurement and may better represent the current state of affairs at each NMI.

	$\overline{\Delta T}$ (mK)	U (mK)	#NMIs
Zn	-0.20	0.22	12
Sn	0.13	0.16	10
In	-0.08	0.09	11
Ga	0.25	0.07	12
Hg	0.27	0.08	10
Ar	0.79	0.17	11

Table E.5: Values for $\overline{\Delta T}$ at each fixed point, calculated using only post-NIST data.

Appendix F

Bilateral comparisons

These tables display bilateral comparisons between participating NMIs. There are two presentation formats: 1) bilateral comparisons bewteen all NMIs at a single fixed point, and 2) bilateral comparisons between a single NMI and all other NMIs at each of the six fixed points. In each case the data are presented in millikelvin and include the uncertainty enclosed in parentheses.

F.1 Bilateral comparisons organized by fixed point

					NIST	NMIA	NMIJ/AIST	NPL	NRC	P ^{TB}	VSL
		KRISS	LNE-CNAM	INRIM	INTI	NIM	NIST	NMIA	NMIJ/AIST	P ^{TB}	VSL
BIPM	—	—	—	—	—	—	—	—	—	—	—
INMETRO	—	—	0.07 (1.82)	0.88 (4.30)	1.30 (1.88)	1.69 (1.86)	0.81 (1.71)	0.70 (1.63)	0.39 (1.65)	0.88 (1.73)	1.10 (1.65)
INRIM	—	—	0.95 (4.12)	1.23 (1.43)	1.62 (1.40)	0.74 (1.19)	0.63 (1.08)	0.46 (1.11)	0.80 (1.22)	1.17 (1.11)	0.91 (1.20)
INTI	—	—	—	2.18 (4.15)	2.57 (4.14)	1.69 (4.07)	1.58 (4.04)	0.49 (4.05)	1.75 (4.08)	0.22 (4.05)	1.86 (4.05)
KRISS	—	—	—	—	0.40 (1.48)	0.49 (1.28)	0.60 (1.18)	1.69 (1.20)	0.42 (1.31)	2.40 (1.20)	0.31 (1.29)
LNE-CNAM	—	—	—	—	—	0.88 (1.25)	0.99 (1.14)	2.08 (1.16)	0.82 (1.28)	2.79 (1.17)	0.71 (1.26)
NIM	—	—	—	—	—	0.11 (0.87)	1.20 (0.90)	0.06 (1.05)	1.91 (0.91)	0.17 (1.02)	1.08 (1.74)
NIST	—	—	—	—	—	—	1.09 (0.75)	0.17 (0.92)	1.80 (0.76)	0.28 (0.88)	1.56 (1.46)
NMIA	—	—	—	—	—	—	—	1.26 (0.95)	0.71 (0.79)	1.37 (0.92)	2.76 (1.48)
NMIJ/AIST	—	—	—	—	—	—	—	—	1.97 (0.95)	0.11 (1.06)	1.50 (1.57)
NPL	—	—	—	—	—	—	—	—	—	2.08 (0.92)	3.48 (1.48)
NRC	—	—	—	—	—	—	—	—	—	—	—
P ^{TB}	—	—	—	—	—	—	—	—	—	—	0.84
VSL	—	—	—	—	—	—	—	—	—	—	(1.78)

Table F.1: Bilateral comparison of measurements at the Zn point. Numerical results are displayed in millikelvin and uncertainty ($k = 2$) is included in parentheses.

					NIST	NMIA	NMIJ/AIST	NPL	NRC	P ^{TB}	VSL
		KRISS	LNE-CNAM	INRIM	INTI	NIM	NIST	NMIA	NMIJ/AIST	P ^{TB}	VSL
BIPM	-	-	-	-	-	-	-	-	-	-	-
INMETRO	-	-	0.99 (1.17)	0.19 (2.52)	1.12 (1.30)	1.20 (1.13)	1.24 (1.12)	0.69 (1.01)	0.88 (1.07)	0.99 (1.12)	1.55 (1.06)
INRIM	-	-	-	1.18 (2.40)	0.13 (1.06)	0.21 (0.84)	0.25 (0.83)	0.30 (0.76)	0.11 (0.83)	0.00 (0.74)	0.56 (0.77)
INTI	-	-	-	-	1.31 (2.47)	1.39 (2.38)	1.43 (2.38)	0.98 (2.33)	0.88 (2.36)	1.07 (2.35)	1.18 (2.35)
KRISS	-	-	-	-	0.07 (1.02)	0.12 (1.01)	0.33 (0.89)	0.43 (0.95)	0.24 (1.01)	0.13 (0.94)	0.43 (0.96)
LNE-CNAM	-	-	-	-	-	0.04 (0.78)	0.40 (0.61)	0.50 (0.70)	0.32 (0.77)	0.21 (0.68)	0.36 (0.71)
NIM	-	-	-	-	-	-	0.44 (0.60)	0.55 (0.69)	0.36 (0.76)	0.25 (0.67)	0.32 (0.70)
NIST	-	-	-	-	-	-	-	0.10 (0.49)	0.08 (0.59)	0.20 (0.46)	0.76 (0.51)
NMIA	-	-	-	-	-	-	-	-	0.19 (0.68)	0.30 (0.57)	0.86 (0.61)
NMIJ/AIST	-	-	-	-	-	-	-	-	0.11 (0.66)	0.68 (0.69)	0.31 (1.05)
NPL	-	-	-	-	-	-	-	-	-	0.56 (0.59)	0.20 (0.98)
NRC	-	-	-	-	-	-	-	-	-	0.36 (1.01)	0.11 (0.73)
P ^{TB}	-	-	-	-	-	-	-	-	-	-	0.26 (1.07)
VSL	-	-	-	-	-	-	-	-	-	-	-

Table F.2: Bilateral comparison of measurements at the Sn point. Numerical results are displayed in millikelvin and uncertainty ($k = 2$) is included in parentheses.

					NIST	NMIA	NMIJ/AIST	NPL	NRC	P ^T B	VSL
			KRIS	LNE-CNAM							
			INTI	INRIM							
BIPM	—	—	—	—	—	—	—	—	—	—	—
INMETRO	—	—	0.63 (0.98)	1.10 (2.45)	0.92 (1.36)	1.29 (0.90)	0.78 (0.86)	0.61 (0.74)	0.81 (0.83)	0.35 (0.80)	0.77 (0.76)
INRIM	—	—	—	0.46 (2.44)	0.29 (1.34)	0.65 (0.87)	0.15 (0.82)	0.14 (0.70)	0.02 (0.79)	0.17 (0.76)	0.28 (0.72)
INTI	—	—	—	—	0.17 (2.61)	0.19 (2.41)	0.31 (2.39)	0.32 (2.35)	0.49 (2.38)	0.29 (2.37)	0.74 (2.36)
KRISS	—	—	—	—	0.36 (1.28)	0.14 (1.25)	0.15 (1.18)	0.31 (1.23)	0.11 (1.22)	0.57 (1.19)	0.15 (1.19)
LNE-CNAM	—	—	—	—	—	0.50 (0.73)	0.51 (0.59)	0.68 (0.69)	0.48 (0.66)	0.93 (0.66)	0.51 (0.61)
NIM	—	—	—	—	—	0.01 (0.52)	0.17 (0.63)	0.03 (0.60)	0.43 (0.54)	0.43 (0.54)	0.01 (0.54)
NIST	—	—	—	—	—	—	0.17 (0.46)	0.03 (0.43)	0.42 (0.34)	0.00 (0.34)	0.07 (0.91)
NMIA	—	—	—	—	—	—	—	0.20 (0.56)	0.26 (0.49)	0.16 (0.49)	0.10 (0.98)
NMIJ/AIST	—	—	—	—	—	—	—	—	0.45 (0.46)	0.03 (0.46)	0.10 (0.96)
NPL	—	—	—	—	—	—	—	—	—	0.42 (0.38)	0.36 (0.93)
NRC	—	—	—	—	—	—	—	—	—	0.06 (0.93)	0.15 (0.51)
P ^T B	—	—	—	—	—	—	—	—	—	—	0.09 (0.99)
VSL	—	—	—	—	—	—	—	—	—	—	—

Table F.3: Bilateral comparison of measurements at the In point. Numerical results are displayed in millikelvin and uncertainty ($k = 2$) is included in parentheses.

	INMELTRO										NMIIJ/AIST																																												
	INRIM					INTI					LNE-CNAM					KRISS					NIM					NIST					NMIA					NPL					NRC					PTB					VSL				
BIPM	-	0.18 (0.51)	0.07 (0.52)	0.04 (1.09)	0.20 (0.58)	0.47 (0.50)	0.15 (0.55)	0.34 (0.41)	0.44 (0.52)	0.35 (0.47)	0.17 (0.44)	0.01 (0.45)	0.16 (0.45)	0.25 (0.53)																																									
INMETRO	-	-	0.25 (0.54)	0.14 (1.10)	0.38 (0.60)	0.65 (0.52)	0.03 (0.57)	0.51 (0.43)	0.62 (0.54)	0.53 (0.49)	0.35 (0.46)	0.17 (0.47)	0.34 (0.47)	0.43 (0.54)																																									
INRIM	-	-	-	0.11 (1.11)	0.13 (0.61)	0.41 (0.53)	0.21 (0.58)	0.27 (0.45)	0.37 (0.55)	0.28 (0.51)	0.10 (0.48)	0.08 (0.48)	0.10 (0.51)	0.19 (0.56)																																									
INTI	-	-	-	-	0.24 (1.14)	0.51 (1.10)	0.11 (1.12)	0.37 (1.06)	0.48 (1.11)	0.39 (1.08)	0.21 (1.07)	0.03 (1.08)	0.20 (1.09)	0.29 (1.11)																																									
KRISS	-	-	-	-	-	0.28 (0.59)	0.34 (0.63)	0.14 (0.51)	0.24 (0.60)	0.15 (0.56)	0.03 (0.54)	0.21 (0.54)	0.03 (0.54)	0.06 (0.57)																																									
LNE-CNAM	-	-	-	-	-	-	0.62 (0.56)	0.14 (0.42)	0.03 (0.53)	0.12 (0.48)	0.30 (0.45)	0.48 (0.46)	0.31 (0.48)	0.22 (0.53)																																									
NIM	-	-	-	-	-	-	-	0.48 (0.48)	0.59 (0.58)	0.50 (0.53)	0.32 (0.51)	0.14 (0.52)	0.31 (0.54)	0.40 (0.59)																																									
NIST	-	-	-	-	-	-	-	-	0.11 (0.44)	0.02 (0.38)	0.16 (0.35)	0.34 (0.36)	0.17 (0.39)	0.08 (0.45)																																									
NMIA	-	-	-	-	-	-	-	-	-	0.09 (0.50)	0.27 (0.47)	0.45 (0.48)	0.28 (0.50)	0.19 (0.55)																																									
NMIIJ/AIST	-	-	-	-	-	-	-	-	-	-	0.18 (0.42)	0.36 (0.42)	0.19 (0.45)	0.10 (0.51)																																									
NPL	-	-	-	-	-	-	-	-	-	-	-	0.18 (0.39)	0.36 (0.42)	0.19 (0.45)	0.08 (0.51)																																								
NRC	-	-	-	-	-	-	-	-	-	-	-	-	0.17 (0.43)	0.26 (0.49)	-																																								
PTB	-	-	-	-	-	-	-	-	-	-	-	-	-	-																																									
VSL	-	-	-	-	-	-	-	-	-	-	-	-	-	-																																									

Table F.4: Bilateral comparison of measurements at the Ga point. Numerical results are displayed in millikelvin and uncertainty ($k = 2$) is included in parentheses.

					NIST	NMIA	NMIJ/AIST	NPL	NRC	P ^T B	VSL
			KRIS	LNE-CNAM	INRIM	INTI	INRIM	INMETRO	BIPM		
BIPM	—	—	—	—	—	—	—	—	—	—	—
INMETRO	—	—	0.29 (0.54)	0.03 (0.93)	0.08 (0.66)	0.88 (0.78)	0.35 (0.59)	0.21 (0.53)	0.07 (0.56)	0.29 (0.85)	0.17 (0.53)
INRIM	—	—	—	0.26 (0.84)	0.37 (0.53)	0.59 (0.67)	0.06 (0.43)	0.49 (0.35)	0.22 (0.39)	0.00 (0.75)	0.11 (0.34)
INTI	—	—	—	—	0.10 (0.93)	0.85 (1.01)	0.32 (0.87)	0.23 (0.84)	0.04 (0.86)	0.27 (1.07)	0.15 (0.84)
KRIS	—	—	—	—	0.95 (0.77)	0.42 (0.58)	0.13 (0.52)	0.15 (0.55)	0.37 (0.85)	0.25 (0.52)	0.20 (0.52)
LNE-CNAM	—	—	—	—	—	0.53 (0.71)	1.08 (0.66)	0.80 (0.69)	0.58 (0.94)	0.70 (0.66)	0.76 (0.66)
NIM	—	—	—	—	—	—	0.55 (0.42)	0.28 (0.46)	0.06 (0.79)	0.17 (0.41)	0.23 (0.41)
NIST	—	—	—	—	—	—	—	0.28 (0.39)	0.50 (0.75)	0.38 (0.33)	0.33 (0.33)
NMIA	—	—	—	—	—	—	—	—	0.22 (0.77)	0.10 (0.38)	0.05 (0.38)
NMIJ/AIST	—	—	—	—	—	—	—	—	—	0.12 (0.74)	0.17 (0.74)
NPL	—	—	—	—	—	—	—	—	—	0.05 (0.32)	0.06 (0.39)
NRC	—	—	—	—	—	—	—	—	—	0.11 (0.39)	0.08 (0.33)
P ^T B	—	—	—	—	—	—	—	—	—	—	0.20 (0.40)
VSL	—	—	—	—	—	—	—	—	—	—	—

Table F.5: Bilateral comparison of measurements at the Hg point. Numerical results are displayed in millikelvin and uncertainty ($k = 2$) is included in parentheses.

					NIST	NMIA	NMIJ/AIST	NPL	NRC	P ^{TB}	VSL
		KRIS	INTI	LNE-CNAM							
BIPM	-	-	-	-	-	-	-	-	-	-	-
INMETRO	-	-	0.01 (1.34)	0.74 (2.26)	0.07 (1.48)	0.38 (1.24)	0.88 (1.11)	1.62 (1.01)	0.57 (1.44)	0.01 (1.76)	0.14 (1.11)
INRIM	-	-	-	0.73 (2.32)	0.07 (1.57)	0.39 (1.35)	0.89 (1.24)	1.63 (1.15)	0.58 (1.53)	0.02 (1.84)	0.13 (1.23)
INTI	-	-	-	0.66 (2.40)	1.12 (2.26)	1.62 (2.20)	2.36 (2.15)	1.31 (2.38)	0.75 (2.58)	0.60 (2.19)	1.00 (2.19)
KRISS	-	-	-	-	0.46 (1.49)	0.96 (1.38)	1.69 (1.30)	0.65 (1.65)	0.09 (1.94)	0.06 (1.38)	0.34 (1.37)
LNE-CNAM	-	-	-	-	-	0.50 (1.13)	1.24 (1.03)	0.19 (1.45)	0.37 (1.77)	0.52 (1.12)	0.12 (1.12)
NIM	-	-	-	-	-	0.74 (0.87)	0.31 (1.34)	0.87 (1.68)	1.02 (0.98)	0.62 (0.97)	0.19 (1.19)
NIST	-	-	-	-	-	-	1.04 (1.25)	1.60 (1.62)	1.76 (0.86)	1.35 (0.86)	0.62 (0.94)
NMIA	-	-	-	-	-	-	-	0.56 (1.91)	0.71 (1.33)	0.31 (1.33)	0.46 (1.39)
NMIJ/AIST	-	-	-	-	-	-	-	-	0.15 (1.68)	0.25 (1.67)	0.10 (1.72)
NPL	-	-	-	-	-	-	-	-	-	0.40 (0.97)	0.25 (1.05)
NRC	-	-	-	-	-	-	-	-	-	0.15 (1.04)	0.76 (0.95)
P ^{TB}	-	-	-	-	-	-	-	-	-	-	0.92 (1.03)
VSL	-	-	-	-	-	-	-	-	-	-	-

Table F.6: Bilateral comparison of measurements at the Ar point. Numerical results are displayed in millikelvin and uncertainty ($k = 2$) is included in parentheses.

F.2 Bilateral comparisons organized by NMI

	Zn	Sn	In	Ga	Hg	Ar
BIPM	—	—	—	—	—	—
INMETRO	—	—	—	0.18 (0.51)	—	—
INRIM	—	—	—	0.07 (0.52)	—	—
INTI	—	—	—	0.04 (1.09)	—	—
KRISS	—	—	—	0.20 (0.58)	—	—
LNE-CNAM	—	—	—	0.47 (0.50)	—	—
NIM	—	—	—	0.15 (0.55)	—	—
NIST	—	—	—	0.34 (0.41)	—	—
NMIA	—	—	—	0.44 (0.52)	—	—
NMIJ/AIST	—	—	—	0.35 (0.47)	—	—
NPL	—	—	—	0.17 (0.44)	—	—
NRC	—	—	—	0.01 (0.45)	—	—
PTB	—	—	—	0.16 (0.47)	—	—
VSL	—	—	—	0.25 (0.53)	—	—

Table F.7: Bilateral comparison of measurements at BIPM. Numerical results are displayed in millikelvin and uncertainty ($k = 2$) is included in parentheses.

	Zn	Sn	In	Ga	Hg	Ar
BIPM	—	—	—	0.18 (0.51)	—	—
INMETRO	—	—	—	—	—	—
INRIM	0.07 (1.82)	0.99 (1.17)	0.63 (0.98)	0.25 (0.54)	0.29 (0.54)	0.01 (1.34)
INTI	0.88 (4.30)	0.19 (2.52)	1.10 (2.45)	0.14 (1.10)	0.03 (0.93)	0.74 (2.26)
KRISS	1.30 (1.88)	1.12 (1.30)	0.92 (1.36)	0.38 (0.60)	0.08 (0.66)	0.07 (1.48)
LNE-CNAM	1.69 (1.86)	1.20 (1.13)	1.29 (0.90)	0.65 (0.52)	0.88 (0.78)	0.38 (1.24)
NIM	0.81 (1.71)	1.24 (1.12)	0.78 (0.86)	0.03 (0.57)	0.35 (0.59)	0.88 (1.11)
NIST	0.70 (1.63)	0.79 (1.01)	0.78 (0.74)	0.51 (0.43)	0.21 (0.53)	1.62 (1.01)
NMIA	0.39 (1.65)	0.69 (1.07)	0.61 (0.83)	0.62 (0.54)	0.07 (0.56)	0.57 (1.44)
NMIJ/AIST	0.88 (1.73)	0.88 (1.12)	0.81 (0.80)	0.53 (0.49)	0.29 (0.85)	0.01 (1.76)
NPL	1.10 (1.65)	0.99 (1.06)	0.35 (0.76)	0.35 (0.46)	0.17 (0.53)	0.14 (1.11)
NRC	0.99 (1.72)	1.55 (1.08)	0.77 (0.76)	0.17 (0.47)	0.12 (0.53)	0.27 (1.11)
PTB	2.38 (2.07)	1.19 (1.33)	0.71 (1.14)	0.34 (0.49)	0.23 (0.57)	0.11 (1.18)
VSL	3.21 (1.92)	1.45 (1.14)	0.62 (0.84)	0.43 (0.54)	0.04 (0.53)	1.03 (1.09)

Table F.8: Bilateral comparison of measurements at INMETRO. Numerical results are displayed in millikelvin and uncertainty ($k = 2$) is included in parentheses.

	Zn	Sn	In	Ga	Hg	Ar
BIPM	—	—	—	0.07 (0.52)	—	—
INMETRO	0.07 (1.82)	0.99 (1.17)	0.63 (0.98)	0.25 (0.54)	0.29 (0.54)	0.01 (1.34)
INRIM	—	—	—	—	—	—
INTI	0.95 (4.12)	1.18 (2.40)	0.46 (2.44)	0.11 (1.11)	0.26 (0.84)	0.73 (2.32)
KRISS	1.23 (1.43)	0.13 (1.06)	0.29 (1.34)	0.13 (0.61)	0.37 (0.53)	0.07 (1.57)
LNE-CNAM	1.62 (1.40)	0.21 (0.84)	0.65 (0.87)	0.41 (0.53)	0.59 (0.67)	0.39 (1.35)
NIM	0.74 (1.19)	0.25 (0.83)	0.15 (0.82)	0.21 (0.58)	0.06 (0.43)	0.89 (1.24)
NIST	0.63 (1.08)	0.20 (0.68)	0.14 (0.70)	0.27 (0.45)	0.49 (0.35)	1.63 (1.15)
NMIA	0.46 (1.11)	0.30 (0.76)	0.02 (0.79)	0.37 (0.55)	0.22 (0.39)	0.58 (1.53)
NMIJ/AIST	0.80 (1.22)	0.11 (0.83)	0.17 (0.76)	0.28 (0.51)	0.00 (0.75)	0.02 (1.84)
NPL	1.17 (1.11)	0.00 (0.74)	0.28 (0.72)	0.10 (0.48)	0.11 (0.34)	0.13 (1.23)
NRC	0.91 (1.20)	0.56 (0.77)	0.14 (0.72)	0.08 (0.48)	0.17 (0.34)	0.27 (1.23)
PTB	2.31 (1.67)	0.20 (1.10)	0.08 (1.11)	0.10 (0.51)	0.05 (0.40)	0.12 (1.29)
VSL	3.14 (1.48)	0.46 (0.85)	0.01 (0.80)	0.19 (0.56)	0.25 (0.35)	1.04 (1.21)

Table F.9: Bilateral comparison of measurements at INRIM. Numerical results are displayed in millikelvin and uncertainty ($k = 2$) is included in parentheses.

	Zn	Sn	In	Ga	Hg	Ar
BIPM	—	—	—	0.04 (1.09)	—	—
INMETRO	0.88 (4.30)	0.19 (2.52)	1.10 (2.45)	0.14 (1.10)	0.03 (0.93)	0.74 (2.26)
INRIM	0.95 (4.12)	1.18 (2.40)	0.46 (2.44)	0.11 (1.11)	0.26 (0.84)	0.73 (2.32)
INTI	—	—	—	—	—	—
KRISS	2.18 (4.15)	1.31 (2.47)	0.17 (2.61)	0.24 (1.14)	0.10 (0.93)	0.66 (2.40)
LNE-CNAM	2.57 (4.14)	1.39 (2.38)	0.19 (2.41)	0.51 (1.10)	0.85 (1.01)	1.12 (2.26)
NIM	1.69 (4.07)	1.43 (2.38)	0.31 (2.39)	0.11 (1.12)	0.32 (0.87)	1.62 (2.20)
NIST	1.58 (4.04)	0.98 (2.33)	0.32 (2.35)	0.37 (1.06)	0.23 (0.84)	2.36 (2.15)
NMIA	0.49 (4.05)	0.88 (2.36)	0.49 (2.38)	0.48 (1.11)	0.04 (0.86)	1.31 (2.38)
NMIJ/AIST	1.75 (4.08)	1.07 (2.38)	0.29 (2.37)	0.39 (1.08)	0.27 (1.07)	0.75 (2.58)
NPL	0.22 (4.05)	1.18 (2.35)	0.74 (2.36)	0.21 (1.07)	0.15 (0.84)	0.60 (2.19)
NRC	1.86 (4.07)	1.74 (2.36)	0.32 (2.36)	0.03 (1.08)	0.09 (0.84)	1.00 (2.19)
PTB	3.25 (4.24)	1.38 (2.49)	0.39 (2.51)	0.20 (1.09)	0.21 (0.86)	0.85 (2.23)
VSL	4.09 (4.16)	1.64 (2.39)	0.47 (2.38)	0.29 (1.11)	0.01 (0.84)	1.77 (2.18)

Table F.10: Bilateral comparison of measurements at INTI. Numerical results are displayed in millikelvin and uncertainty ($k = 2$) is included in parentheses.

	Zn	Sn	In	Ga	Hg	Ar
BIPM	—	—	—	0.20 (0.58)	—	—
INMETRO	1.30 (1.88)	1.12 (1.30)	0.92 (1.36)	0.38 (0.60)	0.08 (0.66)	0.07 (1.48)
INRIM	1.23 (1.43)	0.13 (1.06)	0.29 (1.34)	0.13 (0.61)	0.37 (0.53)	0.07 (1.57)
INTI	2.18 (4.15)	1.31 (2.47)	0.17 (2.61)	0.24 (1.14)	0.10 (0.93)	0.66 (2.40)
KRISS	—	—	—	—	—	—
LNE-CNAM	0.40 (1.48)	0.07 (1.02)	0.36 (1.28)	0.28 (0.59)	0.95 (0.77)	0.46 (1.49)
NIM	0.49 (1.28)	0.12 (1.01)	0.14 (1.25)	0.34 (0.63)	0.42 (0.58)	0.96 (1.38)
NIST	0.60 (1.18)	0.33 (0.89)	0.15 (1.18)	0.14 (0.51)	0.13 (0.52)	1.69 (1.30)
NMIA	1.69 (1.20)	0.43 (0.95)	0.31 (1.23)	0.24 (0.60)	0.15 (0.55)	0.65 (1.65)
NMIJ/AIST	0.42 (1.31)	0.24 (1.01)	0.11 (1.22)	0.15 (0.56)	0.37 (0.85)	0.09 (1.94)
NPL	2.40 (1.20)	0.13 (0.94)	0.57 (1.19)	0.03 (0.54)	0.25 (0.52)	0.06 (1.38)
NRC	0.31 (1.29)	0.43 (0.96)	0.15 (1.19)	0.21 (0.54)	0.20 (0.52)	0.34 (1.37)
PTB	1.08 (1.74)	0.07 (1.24)	0.21 (1.46)	0.03 (0.57)	0.31 (0.56)	0.19 (1.43)
VSL	1.91 (1.55)	0.33 (1.03)	0.30 (1.24)	0.06 (0.61)	0.12 (0.53)	1.10 (1.36)

Table F.11: Bilateral comparison of measurements at KRISS. Numerical results are displayed in millikelvin and uncertainty ($k = 2$) is included in parentheses.

	Zn	Sn	In	Ga	Hg	Ar
BIPM	—	—	—	0.47 (0.50)	—	—
INMETRO	1.69 (1.86)	1.20 (1.13)	1.29 (0.90)	0.65 (0.52)	0.88 (0.78)	0.38 (1.24)
INRIM	1.62 (1.40)	0.21 (0.84)	0.65 (0.87)	0.41 (0.53)	0.59 (0.67)	0.39 (1.35)
INTI	2.57 (4.14)	1.39 (2.38)	0.19 (2.41)	0.51 (1.10)	0.85 (1.01)	1.12 (2.26)
KRISS	0.40 (1.48)	0.07 (1.02)	0.36 (1.28)	0.28 (0.59)	0.95 (0.77)	0.46 (1.49)
LNE-CNAM	—	—	—	—	—	—
NIM	0.88 (1.25)	0.04 (0.78)	0.50 (0.73)	0.62 (0.56)	0.53 (0.71)	0.50 (1.13)
NIST	0.99 (1.14)	0.40 (0.61)	0.51 (0.59)	0.14 (0.42)	1.08 (0.66)	1.24 (1.03)
NMIA	2.08 (1.16)	0.50 (0.70)	0.68 (0.69)	0.03 (0.53)	0.80 (0.69)	0.19 (1.45)
NMIJ/AIST	0.82 (1.28)	0.32 (0.77)	0.48 (0.66)	0.12 (0.48)	0.58 (0.94)	0.37 (1.77)
NPL	2.79 (1.17)	0.21 (0.68)	0.93 (0.61)	0.30 (0.45)	0.70 (0.66)	0.52 (1.12)
NRC	0.71 (1.26)	0.36 (0.71)	0.51 (0.61)	0.48 (0.46)	0.76 (0.66)	0.12 (1.12)
PTB	0.68 (1.71)	0.01 (1.06)	0.58 (1.04)	0.31 (0.48)	0.64 (0.69)	0.27 (1.19)
VSL	1.52 (1.52)	0.25 (0.80)	0.66 (0.70)	0.22 (0.53)	0.84 (0.66)	0.65 (1.10)

Table F.12: Bilateral comparison of measurements at LNE-CNAM. Numerical results are displayed in millikelvin and uncertainty ($k = 2$) is included in parentheses.

	Zn	Sn	In	Ga	Hg	Ar
BIPM	—	—	—	0.15 (0.55)	—	—
INMETRO	0.81 (1.71)	1.24 (1.12)	0.78 (0.86)	0.03 (0.57)	0.35 (0.59)	0.88 (1.11)
INRIM	0.74 (1.19)	0.25 (0.83)	0.15 (0.82)	0.21 (0.58)	0.06 (0.43)	0.89 (1.24)
INTI	1.69 (4.07)	1.43 (2.38)	0.31 (2.39)	0.11 (1.12)	0.32 (0.87)	1.62 (2.20)
KRISS	0.49 (1.28)	0.12 (1.01)	0.14 (1.25)	0.34 (0.63)	0.42 (0.58)	0.96 (1.38)
LNE-CNAM	0.88 (1.25)	0.04 (0.78)	0.50 (0.73)	0.62 (0.56)	0.53 (0.71)	0.50 (1.13)
NIM	—	—	—	—	—	—
NIST	0.11 (0.87)	0.44 (0.60)	0.01 (0.52)	0.48 (0.48)	0.55 (0.42)	0.74 (0.87)
NMIA	1.20 (0.90)	0.55 (0.69)	0.17 (0.63)	0.59 (0.58)	0.28 (0.46)	0.31 (1.34)
NMIJ/AIST	0.06 (1.05)	0.36 (0.76)	0.03 (0.60)	0.50 (0.53)	0.06 (0.79)	0.87 (1.68)
NPL	1.91 (0.91)	0.25 (0.67)	0.43 (0.54)	0.32 (0.51)	0.17 (0.41)	1.02 (0.98)
NRC	0.17 (1.02)	0.32 (0.70)	0.01 (0.54)	0.14 (0.52)	0.23 (0.41)	0.62 (0.97)
PTB	1.56 (1.55)	0.05 (1.06)	0.07 (1.01)	0.31 (0.54)	0.11 (0.47)	0.77 (1.05)
VSL	2.40 (1.33)	0.21 (0.79)	0.16 (0.64)	0.40 (0.59)	0.31 (0.42)	0.15 (0.96)

Table F.13: Bilateral comparison of measurements at NIM. Numerical results are displayed in millikelvin and uncertainty ($k = 2$) is included in parentheses.

	Zn	Sn	In	Ga	Hg	Ar
BIPM	—	—	—	0.34 (0.41)	—	—
INMETRO	0.70 (1.63)	0.79 (1.01)	0.78 (0.74)	0.51 (0.43)	0.21 (0.53)	1.62 (1.01)
INRIM	0.63 (1.08)	0.20 (0.68)	0.14 (0.70)	0.27 (0.45)	0.49 (0.35)	1.63 (1.15)
INTI	1.58 (4.04)	0.98 (2.33)	0.32 (2.35)	0.37 (1.06)	0.23 (0.84)	2.36 (2.15)
KRISS	0.60 (1.18)	0.33 (0.89)	0.15 (1.18)	0.14 (0.51)	0.13 (0.52)	1.69 (1.30)
LNE-CNAM	0.99 (1.14)	0.40 (0.61)	0.51 (0.59)	0.14 (0.42)	1.08 (0.66)	1.24 (1.03)
NIM	0.11 (0.87)	0.44 (0.60)	0.01 (0.52)	0.48 (0.48)	0.55 (0.42)	0.74 (0.87)
NIST	—	—	—	—	—	—
NMIA	1.09 (0.75)	0.10 (0.49)	0.17 (0.46)	0.11 (0.44)	0.28 (0.39)	1.04 (1.25)
NMIJ/AIST	0.17 (0.92)	0.08 (0.59)	0.03 (0.43)	0.02 (0.38)	0.50 (0.75)	1.60 (1.62)
NPL	1.80 (0.76)	0.20 (0.46)	0.42 (0.34)	0.16 (0.35)	0.38 (0.33)	1.76 (0.86)
NRC	0.28 (0.88)	0.76 (0.51)	0.00 (0.34)	0.34 (0.36)	0.33 (0.33)	1.35 (0.86)
PTB	1.68 (1.46)	0.39 (0.94)	0.07 (0.91)	0.17 (0.39)	0.44 (0.40)	1.50 (0.94)
VSL	2.51 (1.23)	0.65 (0.63)	0.15 (0.48)	0.08 (0.45)	0.25 (0.35)	0.59 (0.84)

Table F.14: Bilateral comparison of measurements at NIST. Numerical results are displayed in millikelvin and uncertainty ($k = 2$) is included in parentheses.

	Zn	Sn	In	Ga	Hg	Ar
BIPM	—	—	—	0.44 (0.52)	—	—
INMETRO	0.39 (1.65)	0.69 (1.07)	0.61 (0.83)	0.62 (0.54)	0.07 (0.56)	0.57 (1.44)
INRIM	0.46 (1.11)	0.30 (0.76)	0.02 (0.79)	0.37 (0.55)	0.22 (0.39)	0.58 (1.53)
INTI	0.49 (4.05)	0.88 (2.36)	0.49 (2.38)	0.48 (1.11)	0.04 (0.86)	1.31 (2.38)
KRISS	1.69 (1.20)	0.43 (0.95)	0.31 (1.23)	0.24 (0.60)	0.15 (0.55)	0.65 (1.65)
LNE-CNAM	2.08 (1.16)	0.50 (0.70)	0.68 (0.69)	0.03 (0.53)	0.80 (0.69)	0.19 (1.45)
NIM	1.20 (0.90)	0.55 (0.69)	0.17 (0.63)	0.59 (0.58)	0.28 (0.46)	0.31 (1.34)
NIST	1.09 (0.75)	0.10 (0.49)	0.17 (0.46)	0.11 (0.44)	0.28 (0.39)	1.04 (1.25)
NMIA	—	—	—	—	—	—
NMIJ/AIST	1.26 (0.95)	0.19 (0.68)	0.20 (0.56)	0.09 (0.50)	0.22 (0.77)	0.56 (1.91)
NPL	0.71 (0.79)	0.30 (0.57)	0.26 (0.49)	0.27 (0.47)	0.10 (0.38)	0.71 (1.33)
NRC	1.37 (0.92)	0.86 (0.61)	0.16 (0.49)	0.45 (0.48)	0.05 (0.38)	0.31 (1.33)
PTB	2.76 (1.48)	0.50 (1.00)	0.10 (0.98)	0.28 (0.50)	0.16 (0.44)	0.46 (1.39)
VSL	3.60 (1.26)	0.76 (0.71)	0.01 (0.60)	0.19 (0.55)	0.03 (0.39)	0.46 (1.32)

Table F.15: Bilateral comparison of measurements at NMIA. Numerical results are displayed in millikelvin and uncertainty ($k = 2$) is included in parentheses.

	Zn	Sn	In	Ga	Hg	Ar
BIPM	—	—	—	0.35 (0.47)	—	—
INMETRO	0.88 (1.73)	0.88 (1.12)	0.81 (0.80)	0.53 (0.49)	0.29 (0.85)	0.01 (1.76)
INRIM	0.80 (1.22)	0.11 (0.83)	0.17 (0.76)	0.28 (0.51)	0.00 (0.75)	0.02 (1.84)
INTI	1.75 (4.08)	1.07 (2.38)	0.29 (2.37)	0.39 (1.08)	0.27 (1.07)	0.75 (2.58)
KRISS	0.42 (1.31)	0.24 (1.01)	0.11 (1.22)	0.15 (0.56)	0.37 (0.85)	0.09 (1.94)
LNE-CNAM	0.82 (1.28)	0.32 (0.77)	0.48 (0.66)	0.12 (0.48)	0.58 (0.94)	0.37 (1.77)
NIM	0.06 (1.05)	0.36 (0.76)	0.03 (0.60)	0.50 (0.53)	0.06 (0.79)	0.87 (1.68)
NIST	0.17 (0.92)	0.08 (0.59)	0.03 (0.43)	0.02 (0.38)	0.50 (0.75)	1.60 (1.62)
NMIA	1.26 (0.95)	0.19 (0.68)	0.20 (0.56)	0.09 (0.50)	0.22 (0.77)	0.56 (1.91)
NMIJ/AIST	—	—	—	—	—	—
NPL	1.97 (0.95)	0.11 (0.66)	0.45 (0.46)	0.18 (0.42)	0.12 (0.74)	0.15 (1.68)
NRC	0.11 (1.06)	0.68 (0.69)	0.03 (0.46)	0.36 (0.42)	0.17 (0.74)	0.25 (1.67)
PTB	1.50 (1.57)	0.31 (1.05)	0.10 (0.96)	0.19 (0.45)	0.06 (0.77)	0.10 (1.72)
VSL	2.34 (1.36)	0.57 (0.78)	0.18 (0.57)	0.10 (0.51)	0.25 (0.75)	1.01 (1.67)

Table F.16: Bilateral comparison of measurements at NMIJ/AIST. Numerical results are displayed in millikelvin and uncertainty ($k = 2$) is included in parentheses.

	Zn	Sn	In	Ga	Hg	Ar
BIPM	—	—	—	0.17 (0.44)	—	—
INMETRO	1.10 (1.65)	0.99 (1.06)	0.35 (0.76)	0.35 (0.46)	0.17 (0.53)	0.14 (1.11)
INRIM	1.17 (1.11)	0.00 (0.74)	0.28 (0.72)	0.10 (0.48)	0.11 (0.34)	0.13 (1.23)
INTI	0.22 (4.05)	1.18 (2.35)	0.74 (2.36)	0.21 (1.07)	0.15 (0.84)	0.60 (2.19)
KRISS	2.40 (1.20)	0.13 (0.94)	0.57 (1.19)	0.03 (0.54)	0.25 (0.52)	0.06 (1.38)
LNE-CNAM	2.79 (1.17)	0.21 (0.68)	0.93 (0.61)	0.30 (0.45)	0.70 (0.66)	0.52 (1.12)
NIM	1.91 (0.91)	0.25 (0.67)	0.43 (0.54)	0.32 (0.51)	0.17 (0.41)	1.02 (0.98)
NIST	1.80 (0.76)	0.20 (0.46)	0.42 (0.34)	0.16 (0.35)	0.38 (0.33)	1.76 (0.86)
NMIA	0.71 (0.79)	0.30 (0.57)	0.26 (0.49)	0.27 (0.47)	0.10 (0.38)	0.71 (1.33)
NMIJ/AIST	1.97 (0.95)	0.11 (0.66)	0.45 (0.46)	0.18 (0.42)	0.12 (0.74)	0.15 (1.68)
NPL	—	—	—	—	—	—
NRC	2.08 (0.92)	0.56 (0.59)	0.42 (0.38)	0.18 (0.39)	0.05 (0.32)	0.40 (0.97)
PTB	3.48 (1.48)	0.20 (0.98)	0.36 (0.93)	0.01 (0.42)	0.06 (0.39)	0.25 (1.05)
VSL	4.31 (1.26)	0.46 (0.69)	0.27 (0.51)	0.08 (0.48)	0.14 (0.33)	1.17 (0.95)

Table F.17: Bilateral comparison of measurements at NPL. Numerical results are displayed in millikelvin and uncertainty ($k = 2$) is included in parentheses.

	Zn	Sn	In	Ga	Hg	Ar
BIPM	—	—	—	0.01 (0.45)	—	—
INMETRO	0.99 (1.72)	1.55 (1.08)	0.77 (0.76)	0.17 (0.47)	0.12 (0.53)	0.27 (1.11)
INRIM	0.91 (1.20)	0.56 (0.77)	0.14 (0.72)	0.08 (0.48)	0.17 (0.34)	0.27 (1.23)
INTI	1.86 (4.07)	1.74 (2.36)	0.32 (2.36)	0.03 (1.08)	0.09 (0.84)	1.00 (2.19)
KRISS	0.31 (1.29)	0.43 (0.96)	0.15 (1.19)	0.21 (0.54)	0.20 (0.52)	0.34 (1.37)
LNE-CNAM	0.71 (1.26)	0.36 (0.71)	0.51 (0.61)	0.48 (0.46)	0.76 (0.66)	0.12 (1.12)
NIM	0.17 (1.02)	0.32 (0.70)	0.01 (0.54)	0.14 (0.52)	0.23 (0.41)	0.62 (0.97)
NIST	0.28 (0.88)	0.76 (0.51)	0.00 (0.34)	0.34 (0.36)	0.33 (0.33)	1.35 (0.86)
NMIA	1.37 (0.92)	0.86 (0.61)	0.16 (0.49)	0.45 (0.48)	0.05 (0.38)	0.31 (1.33)
NMIJ/AIST	0.11 (1.06)	0.68 (0.69)	0.03 (0.46)	0.36 (0.42)	0.17 (0.74)	0.25 (1.67)
NPL	2.08 (0.92)	0.56 (0.59)	0.42 (0.38)	0.18 (0.39)	0.05 (0.32)	0.40 (0.97)
NRC	—	—	—	—	—	—
PTB	1.39 (1.55)	0.36 (1.01)	0.06 (0.93)	0.17 (0.43)	0.11 (0.39)	0.15 (1.04)
VSL	2.23 (1.34)	0.11 (0.73)	0.15 (0.51)	0.26 (0.49)	0.08 (0.33)	0.76 (0.95)

Table F.18: Bilateral comparison of measurements at NRC. Numerical results are displayed in millikelvin and uncertainty ($k = 2$) is included in parentheses.

	Zn	Sn	In	Ga	Hg	Ar
BIPM	—	—	—	0.16 (0.47)	—	—
INMETRO	2.38 (2.07)	1.19 (1.33)	0.71 (1.14)	0.34 (0.49)	0.23 (0.57)	0.11 (1.18)
INRIM	2.31 (1.67)	0.20 (1.10)	0.08 (1.11)	0.10 (0.51)	0.05 (0.40)	0.12 (1.29)
INTI	3.25 (4.24)	1.38 (2.49)	0.39 (2.51)	0.20 (1.09)	0.21 (0.86)	0.85 (2.23)
KRISS	1.08 (1.74)	0.07 (1.24)	0.21 (1.46)	0.03 (0.57)	0.31 (0.56)	0.19 (1.43)
LNE-CNAM	0.68 (1.71)	0.01 (1.06)	0.58 (1.04)	0.31 (0.48)	0.64 (0.69)	0.27 (1.19)
NIM	1.56 (1.55)	0.05 (1.06)	0.07 (1.01)	0.31 (0.54)	0.11 (0.47)	0.77 (1.05)
NIST	1.68 (1.46)	0.39 (0.94)	0.07 (0.91)	0.17 (0.39)	0.44 (0.40)	1.50 (0.94)
NMIA	2.76 (1.48)	0.50 (1.00)	0.10 (0.98)	0.28 (0.50)	0.16 (0.44)	0.46 (1.39)
NMIJ/AIST	1.50 (1.57)	0.31 (1.05)	0.10 (0.96)	0.19 (0.45)	0.06 (0.77)	0.10 (1.72)
NPL	3.48 (1.48)	0.20 (0.98)	0.36 (0.93)	0.01 (0.42)	0.06 (0.39)	0.25 (1.05)
NRC	1.39 (1.55)	0.36 (1.01)	0.06 (0.93)	0.17 (0.43)	0.11 (0.39)	0.15 (1.04)
PTB	—	—	—	—	—	—
VSL	0.84 (1.78)	0.26 (1.07)	0.09 (0.99)	0.09 (0.51)	0.20 (0.40)	0.92 (1.03)

Table F.19: Bilateral comparison of measurements at PTB. Numerical results are displayed in millikelvin and uncertainty ($k = 2$) is included in parentheses.

	Zn	Sn	In	Ga	Hg	Ar
BIPM	—	—	—	0.25 (0.53)	—	—
INMETRO	3.21 (1.92)	1.45 (1.14)	0.62 (0.84)	0.43 (0.54)	0.04 (0.53)	1.03 (1.09)
INRIM	3.14 (1.48)	0.46 (0.85)	0.01 (0.80)	0.19 (0.56)	0.25 (0.35)	1.04 (1.21)
INTI	4.09 (4.16)	1.64 (2.39)	0.47 (2.38)	0.29 (1.11)	0.01 (0.84)	1.77 (2.18)
KRISS	1.91 (1.55)	0.33 (1.03)	0.30 (1.24)	0.06 (0.61)	0.12 (0.53)	1.10 (1.36)
LNE-CNAM	1.52 (1.52)	0.25 (0.80)	0.66 (0.70)	0.22 (0.53)	0.84 (0.66)	0.65 (1.10)
NIM	2.40 (1.33)	0.21 (0.79)	0.16 (0.64)	0.40 (0.59)	0.31 (0.42)	0.15 (0.96)
NIST	2.51 (1.23)	0.65 (0.63)	0.15 (0.48)	0.08 (0.45)	0.25 (0.35)	0.59 (0.84)
NMIA	3.60 (1.26)	0.76 (0.71)	0.01 (0.60)	0.19 (0.55)	0.03 (0.39)	0.46 (1.32)
NMIJ/AIST	2.34 (1.36)	0.57 (0.78)	0.18 (0.57)	0.10 (0.51)	0.25 (0.75)	1.01 (1.67)
NPL	4.31 (1.26)	0.46 (0.69)	0.27 (0.51)	0.08 (0.48)	0.14 (0.33)	1.17 (0.95)
NRC	2.23 (1.34)	0.11 (0.73)	0.15 (0.51)	0.26 (0.49)	0.08 (0.33)	0.76 (0.95)
PTB	0.84 (1.78)	0.26 (1.07)	0.09 (0.99)	0.09 (0.51)	0.20 (0.40)	0.92 (1.03)
VSL	—	—	—	—	—	—

Table F.20: Bilateral comparison of measurements at VSL. Numerical results are displayed in millikelvin and uncertainty ($k = 2$) is included in parentheses.

References

- [1] H. Preston-Thomas. “The International Temperature Scale of 1990 (ITS-90)”. In: Metrologia 27 (1990), pp. 3–10.
- [2] JCGM 100:2008: Evaluation of measurement data – Guide to the expression of uncertainty in measurement. 2008.
- [3] Any mention of commercial products is for information only; it does not imply recommendation or endorsement by NIST.
- [4] Gregory F. Strouse. Standard Platinum Resistance Thermometer Calibrations from the Ar TP to the Ag FP Special Publication (NIST SP) - 250-81.
- [5] Accessed March 2017. URL: kcdb.bipm.org.
- [6] A. I. Pokhodun et al. Guide to the Realization of the ITS-90; Part 5 - Platinum Resistance Thermometry.